Enhanced Molybdate Conversion Coatings

By

Dane Elliot Walker

A Doctoral Thesis

Submitted in partial fulfilment of the requirements

for the award of

the degree of Doctor of Philosophy of Loughborough University

July 2012

Department of Materials

Supervisor: Dr G.D. Wilcox *Department of Materials*

Dedication

This thesis is dedicated to the memory of my dear friend Craig 'Jonesy' Jones.

Acknowledgements

Firstly I would like to express my immense gratitude to Dr Geoff Wilcox for his invaluable support and guidance throughout. His tireless enthusiasm and encouragement has been first class.

A thank you must go to all of the staff at Department of Materials who helped with characterisation: Dr Gary Critchlow, Mr John Bates, Mr Frank Page and Dr Geoff West. Their expertise was greatly appreciated.

I also wish to thank my colleagues Dr Oliver Lewis, Dr Roshan Chapaneri, Paul Cantwell and Dr Keith Yendall for their assistance and support throughout.

I must also thank my fiancée Louise Whittaker for all her support and kindness.

I also thank my parents for their support.

Acknowledgement is also given to Loughborough University for the receipt of a studentship.

Abstract

The replacement of chromate conversion coatings for zinc coated components has been necessitated by the materials finishing industries due to the inherent toxicity issues with Cr(VI) and the legislative enforcement of 'WEEE' and 'ELV' Directives by the European Union. Current replacements are based on 'non-chromate', Cr(III) systems, these may be perceived by some to be problematic as they still contain 'chromium'.

Molybdate based conversion coatings have long been viewed by many researchers to be a viable 'non-chromium' alternative due to their low toxicity. An extensive literature review of the research carried out in the last 20 years was carried out, highlighting areas of interest for improving the corrosion resistance of the coatings studied. These were, primarily, the synergesis that exists with molybdate and phosphate compounds for corrosion resistance and the incorporation of nanoparticle silica into treatment solution. Also discovered was the importance of the acid used to adjust treatment solution pH, immersion time, oxidising agent additions and the incorporation of rare earth metal species. Silicate sealant layers were also highlighted as a post treatment.

Molybdate-based coatings were formed on commercial electrodeposited acid zinc surfaces. Many treatment conditions were investigated, and initially performance analysed using DC Linear Polarisation Resistance (LPR) trials. Subsequently, the highest performing coatings were subjected to the more aggressive, industry standard, ASTM B 117 Neutral Salt Spray (NSS) corrosion test. The highest performing molybdate coatings were found to have an average LPR of ~ 9 000 Ω. cm^2, in contrast to ~ 12 000 Ω. cm^2 for the Cr(VI) based reference. NSS results were amongst the highest performing for molybdate based coatings documented, at 24 h until 5% white rust, however remained inferior to Cr(VI) coatings, which lasted 120 h.

The highest performing coatings were characterised using FEG-SEM, Cryofracture EDXA and site specific AES. These techniques revealed that the enhanced molybdate coatings had a columnar structure that was around 300 nm thick, with pores that appeared to expose the substrate. AES showed this type of coating to have a mixed Mo, P and Zn oxide surface.

Corrosion initiation was also studied; this can be thought of as an investigation to determine the point(s) of weakness or the mechanism that causes coating failure. Coatings were immersed in 5 % wt/ vol $NaCl_{(aq)}$ until they showed any surface change. Initial signs of corrosion were deemed to be any appearance of pitting or discolouration of the film, not a voluminous corrosion product. Untreated Zn, Cr(VI) and simple molybdate coatings were studied as well as enhanced molybdate coatings. There were clear differences in the way the coatings behaved at the onset of corrosion. Cr(VI) coatings delaminated, leaving an area of decreased Cr concentration. The enhanced molybdate coatings failed by the appearance of localised pores of ~ 70 µm in diameter. Substrate exposure was indisputably the reason for coating failure in chloride environments.

In light of the work carried out in the present thesis the outlook for the use of molybdate as a potential replacement for chromate for the conversion coating of electrodeposited zinc surfaces is a positive one.

Key Words

Molybdate, Conversion Coatings, Corrosion Control, Chromate Replacement, Mixed Metal Oxide Films, Surface Characterisation.

Used Acronyms / Abbreviations

AES	Auger Electron Spectroscopy
DC	Direct Current
EDXA	Energy Dispersive X-ray Analysis
FEG-SEM	Field Emission Gun Scanning Electron Microscope/ Microscopy
FIB	Focussed Ion Beam
LPR	Linear Polarisation Resistance
NSS	Neutral Salt Spray Corrosion (Testing)
REM	Rare Earth Metal
SEM	Scanning Electron Microscope/ Microscopy
XPS	X-ray Photoelectron Spectroscopy

Contents

List of Figures

List of Tables

List of Equations

$Na_2MoO_4 + 2H^+ \rightarrow H_2MoO_4 + 2Na^+$ .....Equation 18

$H_2MoO_4 + Zn^{2+} \rightarrow ZnMoO_4 + 2H^+$ .....Equation 19

$Zn^{2+} + HMoO_4^- \rightarrow ZnMoO_4 + H^+$ (at lower pH).....Equation 20

$3(Mo_7O_{24})^{6-} + 14\ Zn^{2+} + 32H^+ + 42e^- \rightarrow 7Zn_2Mo_3O_8 + 16H_2O$.....Equation 21

$m = (MQ) / (F/z)$.....Equation 22

$i_{app} = i_{corr}\ (\ exp\ [\ 2.3\ (E - E_{corr}) / \beta_a\ ] – exp\ [\ -2.3\ (E - E_{corr}) / \beta_c]\ )$.....Equation 23

$R_p\ (\Omega.cm^2) = [\ \Delta E / \Delta i_{app}]\ (E – E_{corr}) > 0$.....Equation 24

$PO_4^{3-} + 12MoO_4^{2-} + 16H^+ \rightarrow [H^+\ 25°C] \rightarrow PMo_{12}O_{40}^{3-} + 8H_2O$.....Equation 25

$PMo_{12}O_{40}^{3-} + 24Zn^{2+} + 11PO_4^{3-} + 176H^+ + 164e^- \rightarrow 12Zn_2PMoO_7 + 88H_2O$.....Equation 26

$MoO_4^{2-} + PO_4^{3-} + 2Zn^{2+} + 2H^+ + 2e^- \rightarrow Zn_2PMoO_7 + H_2O$.....Equation 27

$Zn^{2+} + PO_4^{3-} + H^+ \rightarrow ZnHPO_4$.....Equation 28

1 Introduction

1.1 Corrosion Prevention

It is very important for every engineer and designer who uses metals in an engineering context to carefully and thoroughly consider the effect of corrosion on their product in its desired service lifetime.

From an environmental as well as an economic standpoint, the prevention of corrosion is critical. A pertinent example being mild steel, which is an important engineering material, due to the fact that it is relatively cheap and has good mechanical properties. However, with the inherent poor corrosion resistance of mild steel in ambient atmospheres, it is necessary that in order to be a viable engineering material steel needs to be protected from corrosion.

When metals corrode, they form oxides on their surface, some oxides, such as aluminium oxide, Al_2O_3, provide protection from further corrosion by forming a thin, homogeneous physical barrier, thus preventing further oxidation. In contrast, when steel is exposed to ambient environments, corrosion products such as porous iron oxides and hydroxides, Fe_2O_3 and $Fe(OH)_3$, form, which are not only undesirable aesthetically, but also have far inferior mechanical properties to the bulk steel and will potentially lead to failure of the material in service.

1.2 Corrosion Preventative Coatings

It is important to distinguish the difference between paint and coatings. For the purpose of this report, paints can be considered to be primarily for decorative use and as such are not considered a corrosion preventative coating. Whereas coatings add

additional function to the substrate material in terms of corrosion resistance, paint adhesion, increased hardness and abrasion resistance.

Corrosion preventative coatings can be further divided into two varieties, non-metallic and metallic. Non-metallic coatings do not offer any enhancement of electrochemical corrosion resistance to a metal surface, but instead provide a physical 'barrier' to corrosion. Typical non-metallic coatings are organic paints and lacquers as well as other polymer based finishes. They can be applied by aerosol or compressed air spraying or in the case of epoxy resins, applied in a two part process with the resin and a cross linking agent.

Metallic coatings are applied to metal surfaces in a variety of applications; with the most common being for corrosion resistance, where an economical base metal, such as mild steel, is coated with another metal to form a barrier to corrosion. The resulting part will then maintain the bulk properties of the substrate, with the surface enhancements that the coating can provide to it. Metallic coatings can also be applied for aesthetic reasons such as when chromium is electrodeposited onto mild steel bath fittings to give a shiny metallic finish.

There are many ways in which metallic coatings can be applied to a substrate. These techniques are: electrodeposition, electroless deposition, thermal spraying, hot dipping, cladding, electrophoresis, vacuum deposition, vapour decomposition oxide reduction and cementation (Gabe 1978).

1.3 Zinc Coatings

Zinc coatings are widely used to protect steels from corrosion in outdoor environments. They protect the steel substrate in two ways: Firstly by providing a physical barrier to corrosion, therefore preventing the steel from being exposed to the ambient atmosphere. Secondly, the zinc coating adds sacrificial protection to the steel, zinc has a lower (more negative) corrosion potential than steel (see Table 1-1) and will therefore corrode preferentially to steel in a corrosive environment. When zinc is exposed to an unpolluted atmosphere it corrodes to form zinc oxide, ZnO. With a longer exposure time it will react further to form zinc hydroxide, $Zn(OH)_2$. This can then react with the carbon dioxide that is present in the air to form 'white rust', a complex hydrated mixture of zinc carbonate and hydroxide (Slunder 1971). White rust forms a barrier to further corrosion of the coating and substrate and is also alkaline, with a pH of around 10, and so can 'neutralise' the surface in slightly acidic aqueous environments. The corrosion products are also voluminous and so act to 'heal' any discontinuities in the coating thus preventing any further corrosion in the area of damage.

Table 1-1: Table of standard electrode potentials of selected metals at 25°C against a Saturated Calomel Electrode after Gabe (1978).

Metal	Standard Electrode Potential at 25°C vs SCE/ v
Aluminium	-1.66
Zinc	-0.76
Iron	-0.44
(Hydrogen)	0
Copper	0.34
Gold	1.68

1.3.1 Electrodeposition of Zinc

Zinc can be deposited onto steel in a variety of ways. With the most common of these being hot-dip-galvanising (HDG) and electrodeposition. The steel samples used in this investigation will be electrodeposited with zinc, therefore this technique will be discussed further. During electrodeposition, the zinc forms the anode and is oxidised to Zn^{2+} and dissolved into the aqueous electrolyte, it is then transported to the cathode, where it is reduced to zinc metal and deposited onto the surface [(Gabe, 1978)], Figure 1-1 shows this process schematically.

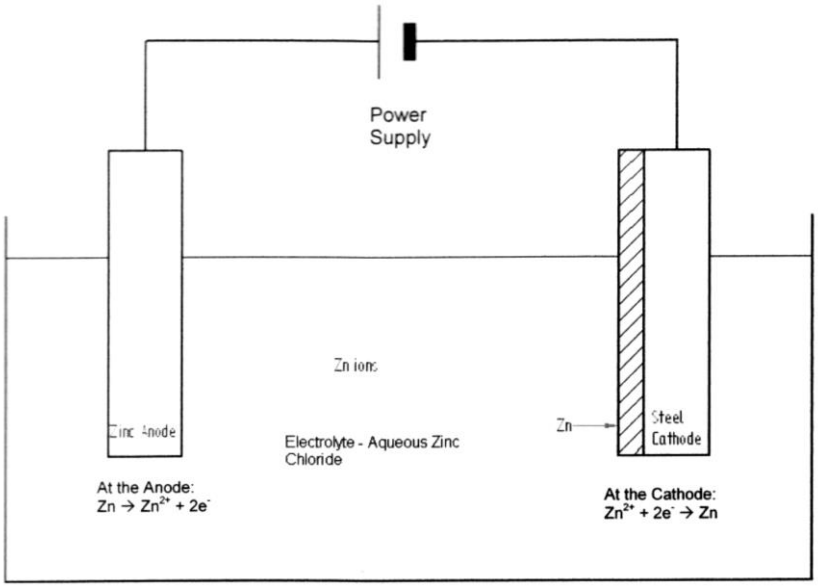

Figure 1-1: ***Diagram to show a typical zinc electrodeposition process.***

1.4 Conversion Coatings

1.4.1 Definition

Conversion coatings are a means of converting a metal surface from an electrochemically active to passive state by the formation of a mixed metal oxide layer. The base metal and species from the treatment solution form a layer which enhances the properties of the substrate. These enhancements can be in the form of increased corrosion resistance, adhesion of subsequent organic finishes, wear resistance, hardness and durability. Colouration can also be enhanced and this can increase aesthetics, promoting marketability and functionality.

1.4.2 Historical

The next section is a brief history of the development of conversion coatings. Key milestones are highlighted as well as the current situation for chromate conversion coatings.

1.4.3 Conversion Coating Development Timeline

- 1869 first phosphate type coating patented by W. A. Ross, UK patent no. 3,119 (Ross 1869).
- Phosphate coatings further developed in 1906 by W.T. Coslett with the tradename 'Coslettizing', UK patent no. 8,663 (Coslett 1906).
- Cr(VI) coatings – First documented instance in 1926 as corrosion preventative coating, US Patent no. 1574289 (Keeler 1926).

- 1980s – Cr(III) based coatings suggested as Cr(VI) replacements for use on Zn coated parts in the automotive industry (Bishop *et al.*, 1979, Barnes *et al.*. 1982, Bibber 2007).
- 2003 – European Union (EU) directives 'Waste Electronic and Electrical Equipment' (WEEE) (2003), 'Restriction of Hazardous Substances' (RoHS) (2008) and 'End-of Life Vehicle' (ELV) (2000) to outlaw the use of Cr(VI) in coatings for consumer electronics and automotive industries.
- Present – Cr(VI) still in limited use in the aerospace industry due to lack of suitable replacement for Al-based surfaces for safety critical components (Eichenger *et al.* 1997).
- Present – Cr(III) has become the widespread replacement conversion coating technique for Zn surfaces and to a lesser extent Al surfaces (Zaki 2007, Bibber 2008, Chautatqua Metal Finishing Supply 2008, Dingwerth and Bishop 2008[)].

1.4.4 Key Applications of Conversion Coatings

This section describes some key applications of conversion coatings. Conversion coatings have a wide spectrum of applications in many industries, from ranging from electronics to aerospace. Table 1-2 is by no means an exhaustive list, but focuses on some key applications.

Table 1-2: Table showing typical applications and industries for named conversion coatings

Industry	Substrate	Coating	Application
Automotive	Zn (EG), HDG, Al	Cr(VI), Cr(III), Phosphate	Fasteners, corrosion protection, paint adhesion
	Fe	Nitride, Carbonitride, Sulphide	Piston Rings, bearings, hardness, wear resistance, lubricant retention
Aerospace	Al 2xxx, 6xxx, 7xxx, Mg and alloys, Ti and alloys	Cr(VI), Phosphate, Permanganate	Fasteners, adhesive joints, corrosion protection
Electronics/ Electrical	Zn (EG)	Cr(III), Phosphate	Fasteners, corrosion protection, paint adhesion

Note: EG = Electrogalvanised, HDG = Hot-Dip Galvanised

In conclusion, it can be seen that conversion coatings are added to a metal surface to increase functionality, adding value to the base metal. The flexibility of conversion coatings means that they are adaptable to their application. An increase in corrosion resistance by a factor of five hundred times or more can be seen. Surface hardness of soft materials, such as aluminium can be increased by 10 times or more with the addition of a conversion coating, leading to very functional increases in wear resistance. Coatings can also be added to decrease the hardness of a surface, allowing for easy 'wearing in' of pistons and other engine components. Coatings can be porous, to allow for excellent adhesion or lubrication retention, or non-porous barriers, protecting the substrate from corrosion or wear.

1.4.5 Coating Types

1.4.5.1 Oxide Films on Iron

Oxide films can be formed on ferrous substrates using a process known as chemical blackening. The substrate is immersed in a strongly alkaline bath in the presence of an

oxidising agent. A typical solution contains oxidising agents such as sodium nitrate and nitrite (Biestek and Weber 1976).

Films attained from this process give slightly enhanced corrosion resistance as well as improved aesthetics, with low light reflectivity being an advantage in certain applications. Geometry tolerances are generally maintained as the film has a thickness of only ~0.75 µm (Biestek and Weber 1976).

1.4.5.2 Nitriding and Carbonitriding

Nitride coatings see use in many industries, particularly in sliding contact applications such as engine components and bearings. When used in bearing applications, they offer significant advantages such as good lubricant retention, low 'running-in' time and increased wear resistance (Wiederholt 1965).

Nitride coatings are applied to steels to give greatly enhanced hardness, wear and fatigue resistance. The coating consists of a pseudo-ceramic layer of iron-nitride under compression, which prevents crack propagation on the substrate surface, leading to enhanced mechanical properties and greater resistance to fatigue failure.

Coatings are generally formed under a nitrogen rich environment at temperatures in excess of 500 °C. Nitriding treatments can be generally divided into two types, soft nitriding and gas nitriding (Biestek and Weber 1976, Wiederholt 1965).

Soft nitriding is an immersion process where the substrate is treated in a bath containing cyanide or cyanate salts. Treatment times of 60 – 90 minutes are common to give a compact, < 10 µm film of iron nitride and carbide. Iron carbide is also formed due

to the presence of carbon in cyanide, producing further enhancements in hardness and wear resistance.

Gas nitriding is carried out at temperatures of 495-565 °C in an ammonia rich atmosphere. The films obtained from this technique are generally thicker, at 70 – 600 µm. The addition of carbon, obtained from propane or natural gas, leads to the formation of carbides. Typical applications for coatings of this type are for gear teeth and tool steels.

1.4.5.3 Sulphidising

Suplhidising is similar to nitriding, but with the addition of sulphide to the treatment solution. The coating produced has enhanced lubricity, which is important for applications such as piston rings, where it is difficult to retain an external lubricant because of the high temperatures involved. Coating morphology is similar to nitrided coatings, with a hard inner layer of nitride needles, but with the addition of a more loosely adherent, softer outer layer of sulphide. Coating thickness is typically in the region of 3 – 10 µm (Biestek and Weber 1976, Wiederholt 1965).

1.4.5.4 Oxalate Coatings

Oxalate coatings are formed on alloy steel substrates to facilitate cold working due to the lower coefficient of friction of the coating. Improvements in paint adhesion and corrosion resistance are also gained with this treatment. Typical oxalate coatings are 15 – 25 µm thick (Matsushima 1972) and have a grey-black finely crystalline morphology. Treatment conditions are similar to conventional phosphate treatments, with a major advantage being that high alloy steels, such as those with > 10 % Cr can be treated

(whereas they cannot be phosphated). A typical treatment solution consists of oxalic acid, oxalate salts, phosphate and chloride. Oxalate allows Fe^{3+} ions to be complexed in solution, where they will not form a sludge and interfere with coating uniformity as can occur with phosphate coatings on steel.

Chromic acid can also be used as a post treatment to improve the corrosion resistance further, giving an even finer crystalline morphology and a surface composition of Fe_2O_3 / Cr_2O_3 (similar to stainless steel) (Biestek and Weber 1976, Wiederholt 1965). For ferritic and austenitic stainless steels, activating and accelerating compounds need to be used, these allow breakdown of the natural passive layer on the surface. Accelerators are generally sulphur based and form an initial sulphide film on which the oxalate layer can be formed, this further increases coating lubricity. Activators are generally fluoride or bromide based. Coating formation occurs when the surface reaches its breakdown potential (after ~ 60 s) it is then re-passivated by the oxalate solution, forming a mixed metal (due to the alloying metals) oxalate coating.

1.4.5.5 Phosphate Coatings

Phosphate conversion coatings are based on the reaction of a metal substrate (usually Fe, Zn or Al) with aqueous phosphate (PO_4^{3-}) ions, which leads to the local deposition of Fe, Zn or Mn phosphates. Coatings are generally crystalline and porous, with the porosity leading to the poor corrosion resistance that is typical of this type of coating. Phosphate coatings continue to be used in many industries to provide excellent paint adhesion, wear resistance, lubricant retention and electrical insulation.

1. Introduction

Phosphating is a mature technique, with the first documented use being as early as 1869 by W. A. Ross (1869). The technique was further developed by T. W. Coslett and patented in 1906 in the UK (1906) and 1907 in the US (1907). 'Coslettizing' was a process based on an aqueous phosphoric acid treatment bath and primarily used to delay the onset of corrosion on ferrous surfaces.

Substrates are generally ferrous, but phosphate coatings can be applied to Zn, Al and their alloys to provide low to moderate increases in corrosion and wear resistance as well as increased adhesion for subsequent organic finishes. Due to the amphoteric nature of Zn and Al, treatments can be acid or alkaline, with Zn, Fe and Mn salts being used to form the coatings.

For Al treatments, the addition of fluoride is necessary to allow the dissolved Al to react with the substrate. 'Bonderite' is a typical process for Al and its alloys and is based on zinc or zinc-calcium phosphates and can be applied by spray or immersion, with treatment times of up to 5 minutes. Although first developed in the early 1930s (Montagu and Nicholson 1953), Bonderite has continued to see use in many sheet metal industries; latterly utilising proprietary additions such as nano-ceramics and Zr oxides (Sienkowski 1999).

Whilst phosphating is a very important conversion coating technique, its original primary use as an anti-corrosion coating has been superseded initially by chromate conversion coatings and more recently by their replacements, however, it continues to be used for its excellent adhesion for subsequent organic finishes.

1.4.5.6 Phosphate Conversion Coating Mechanism (Wiederholt 1965)

The following reactions are thought to occur on the substrate surface. Where Me represents the metal, typically Zn, Mn or Fe. This leads to the precipitation of insoluble metal phosphates on the substrate surface. The formation mechanism can be found in Equations 1 and 2, where the formation of iron phosphate can be seen. Equation 2 shows the incorporation of the solution cation into the iron phosphate coating.

$Fe + Me(H_2PO_4)_2 \rightarrow MeHPO_4 + FeHPO_4 + H_2$.....Equation 1

$Fe + Me(H_2PO_4)_2 \rightarrow MeFe(HPO_4)_2 + H_2$.....Equation 2

1.4.5.7 Chromate Coatings

Chromate conversion coatings have been the most widely used conversion coatings. With the earliest documented use being in 1926, when a process was patented in the US, for corrosion prevention of Mg (Keeler 1926). Subsequent coatings have been applied to a range of metallic substrates such as Al, Cu, Zn, Sn and Ag, where coating thicknesses of ~0.1-10 µm can be attained. Whilst coated surfaces have enhanced corrosion resistance in relatively mild environments, chromate films can often act as a precursor to subsequent organic finishes (Gabe 1978).

Corrosion is reduced by the formation of a mixed metal-chromium oxide film. There is uncertainty about the actual chemical composition of the coating, but it can be thought to be similar to $Cr_2O_3.H_2O$ and/or $Cr(OH)_3.CrO_4$ (Biestek and Weber 1976). Coating formation is initiated by substrate dissolution due to the low pH of the treatment solution. This is usually accelerated by the presence of sulphate anions or activating halogen compounds. The substrate reacts with hexavalent chromium compounds in the

solution leading to coating precipitation in a gelatinous, hydrated form. The gelatinous layer will stabilise and become hydrophobic with prolonged drying for a period of around 24 h or heat treatment at temperatures of less than 70 °C.

Chromate coatings typically show a cracked microstructure when viewed using SEM, this is thought to be due to volume contraction due to water loss from the hydrated coating in a vacuum environment. Figure 1-2 shows a typical 'dried riverbed' crack structure, commonly exhibited by chromate conversion coatings (author's own image).

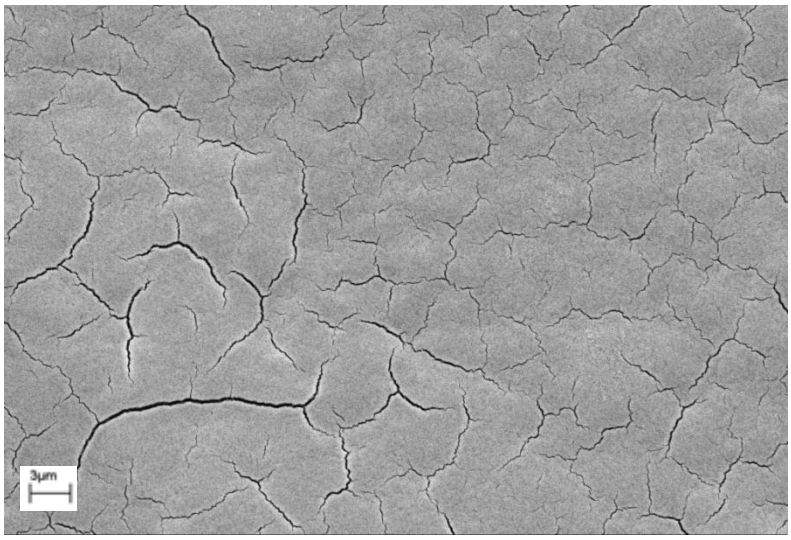

Figure 1-2: *SEM micrograph showing a typical 'dried riverbed' crack structure exhibited by a chromate conversion coating on a zinc electroplated surface, treatment conditions:10 s immersion in 200 g dm^{-3} $Na_2Cr_2O_7$, 200 ml H_2SO_4 pH 1.2 adjusted with HNO_3.*

Chromate finishes are generally characterised in terms of their colour, which is also usually indicative of coating thickness, therefore corrosion resistance on zinc surfaces can be indicated by colour as Table 1-3 shows (Biestek and Weber 1976, Hulser 1999):

Table 1-3: Time to 5% white rust of various chromate conversion coatings on zinc surfaces, exposed to ASTM B117 Neutral Salt Spray (NSS) corrosion tests adapted from Hulser 1999.

Coating Type	Time to 5% WR in ASTM B117 NSS Test	Approximate Thickness (nm)
Blue Chromate	14-24 h	80
Iridescent/ Yellow Chromate	120 - 300 h	200 – 300
Olive Drab Chromate	300 - 400 + h	1000 – 1500
Black Chromate	150 – 300 h	250 – 1000

The thinnest coatings have a documented Cr(VI) content of around 7%, with thicker coatings containing up to 12% (Biestek and Weber 1976). Chromate conversion coatings prevent substrate corrosion in two ways, firstly, barrier protection is provided by the relatively insoluble Cr(III) oxides. Secondly, at sites of damage on the coating, 'self-repair' can occur as Cr(VI) is leached out from the gelatinous layer and re-passivates the coating through the formation of Cr(III) oxides (Biestek and Weber 1976).

1.4.5.8 Chromate Conversion Coating Formation Mechanism

Anodic Reactions

$Zn \rightarrow Zn^{2+} + 2e^-$.....***Equation 3***

Substrate oxidation and dissolution due to the presence of acid. In the case of Equation 3, zinc is oxidised, leading to the loss of electrons from the surface. These then react with the hydrogen ions in solution, from the acid (Equation 4).

Cathodic Reactions

$2H^+ + 2e^- \rightarrow H_2$.....***Equation 4***

Simultaneous hydrogen evolution then ensues at the substrate surface. Hydrogen then reacts with chromate ions from solution, close to the substrate surface (Equation 5).

$CrO_4^{2-} + 2½H_2 \rightarrow Cr(OH)_3 + H_2O$.....***Equation 5***

The reaction causes reduction of the chromate ion, with chromium in the Cr(VI) state, to a chromium hydroxide ion in the Cr(III) oxidation state (Equation 5). The coating can then be thought of as a precipitation of gelatinous chromium hydroxide on substrate surface (Biestek and Weber 1976).

The following reaction (Equation 6) is also thought to occur (Abd El Aal *et al.* 1994). Where chromate ions from solution are reduced close to the substrate surface, as in Equation 5, leading to the formation of chromium oxide:

$2CrO_4^{2-} + 10H^+ \rightarrow Cr_2O_3 + 5H_2O$.....***Equation 6***

1.4.6 Conversion Coatings Replacing Chromates

It is well documented that hexavalent chromium poses a significant risk to human and animal health (Page and Loar 2004, Stiefel 2001). It is known to be mutagenic and carcinogenic to animals and is a class A carcinogen for humans (Page and Loar 2004). Because of this toxicity, legislation was brought in by the European Union (EU) in the form of the directives 2002/95/EC (2008): Restriction of Hazardous Substances in Electrical and Electronic equipment, 2002/96/EC (2000): Waste Electrical and Electronic Equipment and 2003/53/EC (2003): End of Life Vehicle and termed 'RoHS', 'WEEE' and 'ELV' respectively. Annex II of 2003/53/EC was amended later with the date for the total replacement of Cr(VI) in corrosion preventative coatings was moved back to 1st July 2007 from the original date of 1st July 2003 due to the perceived lack of a suitable replacement for hexavalent chromium based coatings. Chromium in its hexavalent form

has thus been significantly restricted for use in the automotive, electronics and electrical industries; this has included its use in corrosion preventative coatings.

1.4.6.1 Trivalent Chromium Conversion Coatings

At present, industry has chosen trivalent chromium, Cr(III), based coatings as chromate replacements for Zn based surfaces. The main advantages of this system is the enhanced corrosion resistance that it affords the substrate, with in excess of 300 h to 5% white rust in NSS tests performed on treatments on Zn surfaces (Zaki 2007).

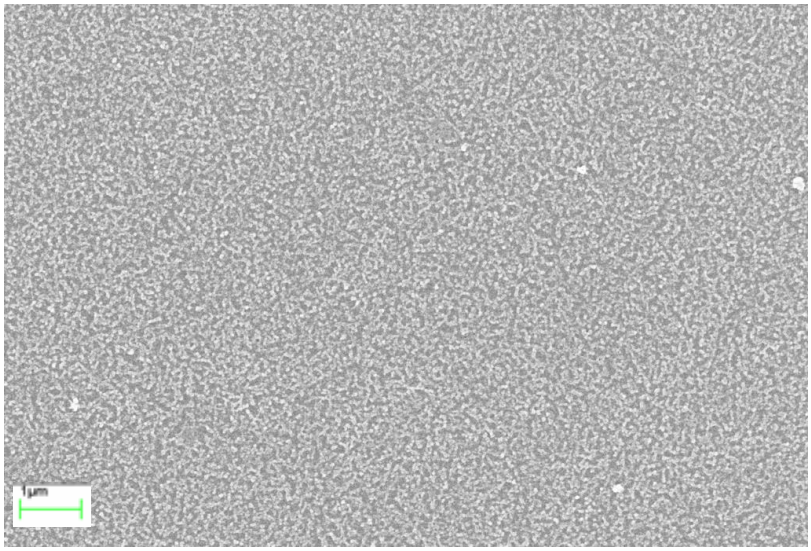

Figure 1-3: *SEM micrograph showing the typical morphology of a trivalent chromium conversion coating on a zinc electroplated surface (Chapaneri 2009).*

Protection from Cr(III) coatings is afforded by a compact, insoluble, non-porous layer of Cr_2O_3 and $ZnCr_2O_4$, which gives barrier protection, Figure 1-3 shows an example of a typical coating. Coating formation occurs with the Cr(III) compounds directly reacting with the substrate, this means that additives such as accelerators and complexants are needed to facilitate substrate dissolution. Typical early 'blue' treatments were ~60 nm thick, whilst newer, more corrosion resistant coatings are in excess of 300 nm thick.

Early coatings were only able to offer comparable resistance to industry standard 'yellow' chromate coatings with the addition of an organic sealant layer and were marketed as such. Second generation coatings significantly outperform their chromate counterparts in chloride corrosion tests. Cr(III) passive coatings do not exhibit 'self-repair' unlike Cr(VI) coatings and therefore areas of damage cannot be re-passivated by a reservoir of Cr(VI) in the coating (Eichinger *et al.* 1997, Zaki 2007, Bibber 2008, Dingwerth and Bishop, 2008).

1.4.7 Trivalent Chromium Conversion Coating Mechanism (Martyak 1996)

$Zn^{2+} + 2OH^- \rightarrow Zn(OH)_2$ ***Equation 7***

$Cr^{3+} + 3OH^- \rightarrow Cr(OH)_3$ ***Equation 8***

The oxidation of the zinc substrate and simultaneous hydrogen evolution occur due to the presence of acidic media (Equations 3 and 4). The coating is then formed by the reaction of the dissolved zinc and trivalent chromium species with hydroxyl groups at the substrate surface (Equations 7 and 8).

1.5 Other Non-Chromate Conversion Coatings

1.5.1 Rare Earth Metal Conversion Coatings

Interest in the use of rare earth metals (REM), particularly cerium and lanthanum, has been accelerated because of the possibility of their use as an alternative to Cr(VI) process for protection of Zn, Mg and Al surfaces (Mansfeld *et al.* 1992). Work by Hinton and Wilson (1989) showed promising results for cerium based treatments for Al

surfaces, while there has been less fruitful progress for the treatment of Zn surfaces to date.

REM coatings are an attractive candidate for chromate replacement conversion coatings because of their low toxicity and ability to form thin, non-porous coatings on Al, Mg and Zn surfaces. Coatings are usually formed by simple immersion in a low concentration, typically 5 x 10^{-3} mol dm^{-3}, solution of REM chloride or nitrate. Coatings are made up of REM (and substrate) oxides and hydroxides (Rudd *et al.* 2000, Aramaki 2005, Conde *et al.* 2008), with the REMs in the +3 and +4 oxidation states. It is also hypothesised that coatings may be capable of 'self-repair' in a similar way to chromate coatings (Trabelsi *et al.* 2005). Table 1-4 gives a brief summary of treatment conditions favoured by the named authors.

Table 1-4: Data showing the treatment conditions for REM coatings from the named authors.

Author	Year	REM Species	Conc.	Treatment
Mansfeld	1992	$Ce(NO_3)_3$	5 x10^{-3} M	2 h
Aramaki	2005	$Ce(NO_3)_3$	1 x10^{-3} M	30 min
Hosseini	2007	$Ce(NO_3)_3$	50 x10^{-3} M	3-7 min
Mansfeld	2000	$Ce(NO_3)_3$, $La(NO_3)_3$, $Pr(NO_3)_3$	50 x10^{-3} M	5 min to 3 h
Yu	2002	$Ce(NO_3)_3$, H_2O_2	5 g/l, 0.5 g/l	n/a
Davo	2004	$CeCl_3$, $LaCl_3$	1000 ppm $RECl_3$	n/a
Ferreira	2004	$Ce(NO_3)_3$, $La(NO_3)_3$	0.01 M	10 s imm, 40 min cure
Takenaka	2007	$Ce(NO_3)_3$, $La(NO_3)_3$, $Nd(NO_3)_3$	1 x10^{-3} M	1 day
Conde	2008	0.6 M NaCl, $CeCl_3$, 0.3% H_2O_2	10000 ppm	3-60 min

1.5.2 Permanganate Coatings

Permanganate coatings have been proposed as possible chromate replacements since the late 1980s, when a treatment system was patented for the use on Al surfaces (Bibber 1987). Permanganate coatings have poorer corrosion resistance than their chromate counterparts and so have not really been a widespread replacement. Their main advantage over chromate coatings is the ability to be used in higher temperature applications because they are not damaged by the dehydration effects and remain uncracked. They are also able to accept a cured sealant coating without damage (Bibber 2007, Bibber 2008).

Coatings are formed by immersion in a solution containing MnO_4^- ions where Mn(VII) is reduced to Mn(IV) on the substrate surface (Kulinich *et al.* 2007). The coating formed is a mixture of MnO_2 and substrate hydroxide. Films are thin and non-porous, with thicknesses quoted of 50 - 70 nm on Al surfaces after 60 s immersion (Hughes *et al.* 2006).

1.5.2.1 Permanganate Conversion Coating Mechanism (Kulinich et al. 2007)

The following reaction is thought to occur (Equation 9), leading to the precipitation of substrate hydroxide and manganese oxide on the metal surface.

$$Al + MnO_4^- + 2H_2O \rightarrow Al(OH)_4^- + MnO_2 \quad \text{.....Equation 9}$$

1.5.3 Tungstate Conversion Coatings

Coatings based on the tungstate anion have been suggested by authors to be of interest as chromate replacements because of their low toxicity and ability to form mixed metal oxide coatings on ferrous and Zn surfaces. Original research was carried out into

tungstates for use as corrosion inhibitors in cooling water systems (Robertson 1951). More recently, research has focussed on producing conversion coatings for Zn based surfaces (Da Silva *et al.* 2005). Da Silva and co-workers produced a tungstate-phosphate conversion coating system, which they found to be similar to a chromate coating in terms of coating formation, but far inferior in corrosion resistance.

2 Literature Review

2.1 Molybdate Conversion Coatings

Molybdates have been seen by industry as a possible replacement for chromates in a variety of corrosion prevention applications. This is because not only is molybdenum in the same periodic group as chromium and so should produce a similar chemistry, its compounds are far less toxic, negating the carcinogenic and toxicity risks associated with hexavalent chromium.

2.1.1 Scope

This literature review sets out to examine the variables that determine the performance of molybdate conversion coatings on zinc-based metal surfaces. There has been a significant amount of research undertaken in this area since 1986 when a comprehensive review was written by Wilcox and Gabe (1986). This section serves as an update to that work.

Although the previous review examined the effectiveness of molybdates as corrosion inhibitors and conversion coatings, as well as their use as paint pigments; this section primarily focuses on molybdate's role in forming conversion coatings on metallic surfaces and as a possible replacement for chromate on zinc-based surfaces.

2.1.2 Historical

In 1986 Wilcox and Gabe (1986) reported that molybdates had not been widely utilised as promoters of conversion coatings. Nonetheless, their ability to form these coatings

has been well known since the 1940s, when a process based on sodium molybdate, molybdic acid and nickel sulphate was patented (Schweikher 1944). 1986 saw a treatment patented by Kobe Steel in Japan (1986) for use as a conversion coating for zinc-based surfaces which used a molybdate with orthophosphoric acid as an additive, the effectiveness of this was proven in corrosion tests in salt water in comparison to chromate coatings.

Even at the time of the previous review, the toxicological problems of hexavalent chromium were well documented and there were signs that legislation to limit its use was imminent. Since then, researchers have tried to produce a formulated system that will perform as well as chromium (VI) based systems and can be used on a variety of substrates, however, whilst niche treatments have been suggested, there is no single system that can offer a level of protection similar to chromates for zinc-based surfaces. At present, trivalent chromium based processes are the most widely used (Wilcox 2003), but are thought to be incapable of 'self-repair', from the local reduction of hexavalent chromium to trivalent chromium, in the form of Cr_2O_3 at sites of localised damage. 'Self-repair' is known to enhance the performance of hexavalent chromium based coatings. It remains to be seen whether these coatings are due to suffer from legislative threats due to their perceived 'chromium' content (although not a hexavalent-chromium containing process) in the near future.

At the time of publication of the research carried out by Wilcox and Gabe (1986), the widest use of molybdates was as a corrosion inhibitor for a variety of metal surfaces, including ferrous and aluminium alloys. This is because of its corrosion inhibition

efficiency in aerated conditions and relatively low toxicity. Since 1986, research into molybdates as replacements for chromates for use in conversion coatings has increased, steadily at first and then, with imminent legislative threats to Cr(VI), investigation has increased apace.

2.1.3 Toxicity of Molybdenum and Chromium Compounds

Molybdenum is known to be an essential trace element for plant, animals and bacteria and can be found in over 20 different enzymes. In fact, the lack of sufficient molybdenum or molybdenum-containing compounds for humans will eventually lead to death (Stiefel 2001). Molybdate, however, is known to have an inhibiting effect on the enzyme adenosine triphosphate (ATP), which is integral in energy production in animals (it substitutes with the sulphate ion which leads to a loss of function of the enzyme) (Stiefel 2001).

Sodium molybdate, the most commonly used form of molybdate for the formation of conversion coatings, is classed as an irritant by the EU in directive 67/548/EEC (1967). Whereas sodium dichromate, a common hexavalent chromium compound used to produce conversion coatings is classed in the same directive by the EU as a carcinogen and is known to be highly toxic (1967). The toxicities of sodium and ammonium molybdates as well as sodium dichromate can be seen in Table 2-1.

Table 2-1*: The comparative toxicities of molybdate and chromate compounds (LD_{50} is the concentration of a compound required to kill 50% of a test population)* ***(Stiefel 2001, Page and Loar 2004.).***

Compound	Molecular Formula	LD_{50} mg/kg (Rat, Oral)
Sodium molybdate	Na_2MoO_4	4000
Ammonium heptamolybdate	$(NH_4)_6Mo_7O_44H_2O$	333
Sodium dichromate	$Na_2Cr_2O_7$	50

It can be seen in the context that this data was measured that sodium dichromate is 80 times more toxic than sodium molybdate. Excessive exposure to hexavalent chromium compounds, for humans, can cause skin sensitisation as well as nasal ulcers which in severe cases, can penetrate the nasal septum and lead to a condition called 'chrome holes' (Page and Loar 2004). Hexavalent chromium is known to be mutagenic and carcinogenic to animals and is a class A carcinogen for humans, a compound known to cause cancer (Page and Loar 2004).

Chromium, in its trivalent form, is known to be an essential trace element for human consumption. Cr(III) deficiency has been attributed to a higher risk of heart disease, increased cholesterol and a higher risk of type 2 diabetes (Page and Loar 2004.).

2.1.4 Molybdate Chemistry

2.1.4.1 Mo(IV) Compounds

The most common Mo(IV) compound is molybdenum dioxide, MoO_2, which is a brown-violet solid with a coppery lustre (Stiefel 2001). MoO_2 is insoluble in non-oxidising acids, but is soluble in oxidising acids such as nitric acid, where it is oxidised to Mo(VI).

There are a many non-stoichiometric oxides that can be formed between MoO_2 and MoO_3 these take the form of blue or purple solids, typically known as 'molybdenum blue' (Staufer 1983, Wilcox and Gabe 1984, Jahan *et al.* 1997, Stiefel 2001).

2.1.4.2 Simple Molybdates

It is important to discuss the compounds that molybdenum can produce in solution under various conditions. The simplest molybdate anion, MoO_4^{2-}, is a tetrahedral arrangement consisting of a central molybdenum ion bonded to four oxygen ions. Sodium molybdate is a simple molybdate containing solution when aqueous. It is formed when molybdenum trioxide, MoO_3, reacts with sodium hydroxide, NaOH, in an acid-base reaction (Equation 10) (Stiefel 2001).

$$\mathbf{MoO_3 + 2NaOH \rightarrow 2Na^+ + MoO_4^{2-} + H_2O} \quad \textbf{\textit{Equation 10}}$$

When the pH is lowered, sodium molybdate forms polymolybdates. When other atoms are present during this acidification, this can lead to the formation of heteropolymolybdates. For example, Cobalt cations, Co^{2+}, will go into the complex to form $H_6CoMo_6O_{24}^{4-}$. Phosphate anions, Po_4^{3-}, will form $PMo_{12}O_{40}^{3-}$ in acidic solutions (Steifel 2001). When strongly acidified, sodium molybdate forms molybdic acid and at room temperature yellow $MoO_3.2H_2O$ crystallises (Cotton *et al.* 1999).

The more complex $Mo_2O_7^{2-}$ anion is analogous to the dichromate anion (Cotton *et al.* 1999) and can be obtained by the addition of $[Bu_4N]OH$ to a solution of $[Bu_{4n}N]_4Mo_8O_{26}$ in CH_3CN. $Mo_2O_7^{2-}$ is able to retain its structure in organic solvents, but with the addition of small cations, it is converted to the 'paramolybdate' anion (Greenwood and

Earnshaw, 1998), $[Mo_7O_{24}]^{6-}$. An example of this is ammonium molybdate, $(NH_4)_2Mo_2O_{24}$.

2.1.4.3 Iso and Hetero-poly Acids and Salts

When in solution with a number of oxo-ligands molybdenum is known to form many different poly anions. These poly anions can be split into two types, Isopolymolybdates and Heteropolymolybdates. Isopoly acids contain only molybdenum, with oxygen and hydrogen. Heteropoly acids and anions contain one or two atoms of another element in addition to molybdenum, oxygen and hydrogen. It is important to note that whilst tungsten and molybdenum are able to form poly anions in solution, chromium is not. Molybdenum poly anions are primarily made up of octahedral MoO_6 and are formed from tetrahedral MoO_4^{2-} ions (Stiefel 2001).

2.1.4.4 Formation of Isopolymolybdates

When strongly basic, Mo(IV) is present in solution only as MoO_4^{2-}, when this is acidified, protonation occurs and the equilibria shown in Equations 11 and 12 occur (Stiefel 2001):

$MoO_4^{2-} + H^+ \leftrightarrow HMoO_4^-$.....*Equation 11*

$HMo_4^- + H^+ (+ 2H_2O) \leftrightarrow Mo(OH)_6$.....*Equation 12*

The second reaction has a very negative enthalpy change because of the formation of two new Mo-O, whilst the number of O-H bonds is unchanged. Because of this very negative enthalpy change, the reaction in Equation 13 is <u>not</u> known to occur, which would be analogous to an important reaction that occurs in Cr(VI) chemistry:

$2HMoO_4^+ \leftrightarrow Mo_2O_7^{2-} + H_2O$.....*Equation 13*

The absence of this reaction in Mo(VI) chemistry is likely to be an important reason for the inferiority of the conversion coatings from molybdate solutions to their chromate counterparts. Mo(VI) forms no polynuclear species with less than 7 Mo atoms in solution, Equations 14 and 15 are known to take place in solution:

$$7MoO_4^- + 8H^+ \leftrightarrow Mo_7O_{24}^{6-} + 4H_2O \quad \textit{Equation 14}$$

At lower pHs

$$Mo_7O_{24}^{6-} + 3H^+ + HMoO_4^- \leftrightarrow Mo_8O_{26}^{4-} + 4H_2O \quad \textit{Equation 15}$$

2.1.4.5 Heteropolymolybdates

Heteropolymolybdates can be formed in solution with acidification in the presence of a simple anion such as phosphate, HPO_4^-, this can also be added after the solution has been acidified. Mechanisms for the formation of common heteropolymolybdates containing phosphorous and cobalt are detailed in Equations 16 and 17 (Stiefel 2001):

$$HPO_4^- + MoO_4^{2-} + 23\ H^+ \rightarrow [H^+\ 25°C] \rightarrow PMo_{12}O_{40}^{3-} + 12H_2O \quad \textit{Equation 16}$$

$$6MoO_4^{2-} + Co^{2+} + 6H^+ \rightarrow [pH < 6] \rightarrow CoMo_6O_{24}H_6^{4-} \quad \textit{Equation 17}$$

Similar compounds to $PMo_{12}O_{40}^{3-}$ are known to form in the presence of Si(IV), Ge(IV), As(IV), Ti(IV) and Zr(IV). Similar compounds to $CoMo_6O_{24}H_6^{4-}$ are known to form in the presence of Al(III), Cr(III), Fe(III), Ga(III), Mn(III), Rh(III), Co(II), Ni(II), Cu(II) and Zn(II) species (Stiefel 2001, Cotton *et al.* 1999).

2.1.5 Molybdates on Zinc Surfaces

Molybdates are well known for their ability to form attractive coatings on zinc surfaces (Wilcox *et al.* 1986, Wilcox 2003, Stiefel 2001, Gabe and Gould 1988, Wilcox and Gabe 1988, Wilcox 1989, Tang *et al.* 1994, Jahan *et al.* 1997, Wharton *et al.* 1996, Han *et al.* 1996, Treacy *et al.* 1999, Wharton *et al.* 1999, Boose *et al.* 2001, Lu *et al.* 2001, Konno *et al.* 2002, Lee *et al.* 2002a, Wharton *et al.* 2003, Magalhães *et al.* 2003, Lewis *et al.* 2006, Rout *et al.* 2007). These coatings, however, are also renowned for their poor performance in corrosion tests, especially the ASTM B117 neutral salt spray (NSS) test (Wilcox and Gabe 1988, Han *et al.* 1996, Wilcox 2003, Lewis *et al.* 2006) and other chloride based corrosion tests. This is possibly because of the formation of soluble chloride corrosion products (Wharton *et al.* 1999), defects in the film and lack of a strong 'self-repair' mechanism, due to molybdate being a weaker oxidising agent than chromate.

2.1.6 Characteristics of Molybdate Passivated Zinc Surfaces

Prior to the 1986 review by Wilcox *et al.* (1986), molybdate coatings had not yet been fully characterised. Subsequent authors have worked to characterise the coatings, debate remains over the species present in the coating and with certain aspects of the coating morphology. There now exists more comprehensive information on these characteristics and these will be discussed in detail in this section.

2.1.6.1 Visual Appearance

The visual appearance of molybdate coatings has been reported by many authors (Gabe and Gould 1988, Wilcox and Gabe 1988, Jahan *et al.* 1997, Han *et al.* 1996, Lewis *et al.* 2006, Rout and Bandyopadhyay 2007) with the thinnest coatings appearing iridescent due to an interference effect, and thicker coatings producing a dark brown or matt black finish (Gabe and Gould 1988, Wilcox and Gabe 1988, Wilcox 1989, Wilcox 2003, Magalhães *et al.* 2003, Lewis *et al.* 2006) possibly attributable to the cracked nature of the coatings. Because of these properties black coatings have been suggested to be of use as solar absorbers on zinc, tin and aluminium alloy coatings (Gabe and Gould 1988, Jahan *et al.* 1997). The adherent dark black coatings have been cited by some authors to give the highest corrosion resistance (Wilcox 1989) whereas, other authors have suggested that the thinner and possibly more compact iridescent surfaces, show the best corrosion resistance (Han *et al.* 1996, Konno *et al.* 2002, Magalhães *et al.* 2003, Lee *et al.* 2002).

2.1.6.2 Coating Morphology

The cracked 'dried riverbed' morphology that is characteristic of molybdate conversion coatings has been reported by a number of authors (Wilcox 2003, Gabe and Gould 1988, Wilcox and Gabe 1988, Jahan *et al.* 1997, Wharton *et al.* 1996, Wharton *et al.* 1999, Lu *et al.* 2001, Magalhães *et al.* 2003, Lewis *et al.* 2006, Almeida *et al.* 1998). This appearance is similar to that of chromate conversion coatings (Figure 2-1a). It remains to be seen whether the cracks are a product of volume contraction due to atmospheric drying of the hydrated coating or caused by water removal in the high vacuum of the

Scanning Electron Microscope (SEM) as the cracks are not thought to be visible by optical microscopy. It has also been suggested that the cracks may be due to the relief of residual internal stresses in the coating that build up as the thickness increases (Gabe and Gould 1988, Wilcox and Gabe 1988, Heavens 1970).

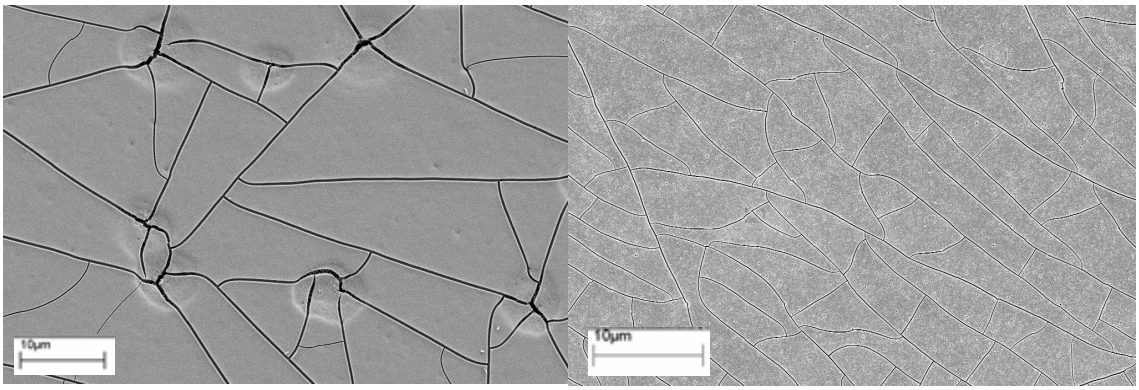

a b

Figure 2-1 : *a: SEM micrograph showing the typical cracked morphology of a molybdate conversion coating on a zinc electroplated surface. b: Typical coating morphology of a chromate conversion coating on a zinc electroplated surface after Chapaneri et al.. (2009).*

A typical chromate conversion coated surface is shown in Figure 2-1a, included for comparison with the molybdate coating in Figure 2-1b. Chromate conversion coatings tend to be similar in thickness to their molybdate counterparts, with Biestek and Weber (1976) reporting thicknesses of 0.01 to 1.5 µm. Molybdate coatings have thicknesses reported of 0.06 µm - ~2 µm (Gabe and Gould 1988, Han *et al.* 1996, Almeida *et al.* 1998, Lu *et al.* 2003). This illustrates that there is a very large difference between thicknesses in simple molybdate conversion coatings and these depend strongly, as chromate conversion coatings do, on the passivation conditions such as concentration, immersion time, pH and acid used to adjust the pH (Biestek and Weber 1976). These factors will be discussed in detail later in the relevant sections. It can be deduced, though, that coating thickness is not always a reliable indicator of corrosion resistance,

as even some of the thickest coatings have not generally performed well in corrosion tests. This is thought to be due to the cracked surface of the coating leading to porosity and allowing corrosive species to react directly with the zinc substrate (Treacy *et al.* 1999).

Lu *et al.* (2003) noted that the width of the surface cracks depend strongly on the treatment time for the coating, with longer treatment times giving a much more cracked surface. The thinnest surfaces and the thicker, highly cracked surfaces gave poor results in the NSS corrosion tests with similar results obtained for treatment times of 20 and 120 s. This suggests that there is a trade-off between the barrier properties gained from a thick coating and the ability of the corrosive chloride ions to penetrate the cracked surfaces and lead to poor corrosion resistance as cited by Treacy *et al.* (1999).

It is also important to note that Lu *et al.* (2003) subjected these coatings to an acetic acid spray test according to ASTM B368 (2009) and in these tests; the thicker coatings significantly outperformed the thinner coatings in terms of time to white rust. The results from this test are not comparable to those from ASTM B117 because of the differences in corrosion mechanisms that exist between the two tests. Both of these tests also did not report the time until 5% white rust, instead showing corrosion at 24 h, and because of this, comparison with other reported data is difficult. Iridescent chromate conversion coatings are able to resist the formation of 5% white rust on a zinc surface for than 96 - 120 h (Biestek and Weber 1976) in an ASTM B117 NSS corrosion test, and any possible replacement for them would need to be tested for at least this duration to determine whether it is a viable replacement.

2.1.6.3 Surface Composition of Molybdate Treatments

As previously stated, there is debate as to the species present on the surface of the molybdate coating. Whether this can be attributed to the method used to detect the species present or from differences in the coatings remains conjecture. Authors have employed X-Ray Photoelectron Spectroscopy (XPS) and Extended X-Ray Absorption Fine Structure (EXAFS) techniques to detect the oxidation states of the species present. Table 2-2 summarises the data obtained by the named authors.

Table 2-2: *Oxidation states of molybdenum present in molybdate based conversion coatings on zinc surfaces produced by named investigators.*

Author	Year	Mo Species Found	Techniques Used
Wilcox *et al.*	1988	Mo(V) and Mo(IV) as MoO_2	XPS
Schrott *et al.*	1991	Mo(VI) in internal layers	XPS
Tang *et al.*	1994	Mo(II), Mo(V) and Mo(VI) as either MoO_3 or MoO_4^{2-}	XPS
Han *et al.*	1996	Mo(VI) as either MoO_3 or MoO_4^{2-}	XPS
Jahan *et al.*	1997	Mo_4O_{11} – a mixture of Mo(V) and Mo(IV)	XPS
Almeida *et al.*	1998	Mo(IV) and Mo(VI)	XPS
Treacy *et al.*	1999	Mo(V) and Mo(VI)	XPS
Konno *et al.*	2002	Mo(V) and (VI)	XPS
Wharton *et al.*	2003	30-40% as Mo(VI) and Mo(IV)	EXAFS

The appearance of hexavalent molybdenum Mo(VI), noted by many investigators, is encouraging and suggests that this could possibly be reduced to a lower valence molybdenum oxide and hence potentially re-passivate the surface. This occurs in chromate conversion coatings where hexavalent chromium is reduced to trivalent chromium (as Cr_2O_3) on sites of damage on the substrate surface (Biestek and Weber

1976). Re-passivation has been investigated by using the Scanning Vibrating Electrode Technique (SVET) by Lewis *et al.* (2006). Through selective surface mapping around a freshly scratched surface, the authors found that, contrary to previous beliefs, molybdate coatings were capable of some degree of self-repair due possibly to the reduction of Mo(VI) but this does not happen as readily (or effectively) as with chromates.

Hexavalent molybdenum has been found on the surface as molybdenum trioxide, MoO_3 (Han *et al.* 1996) which has a complex layered structure where each Mo atom shares the face of an octahedron with another Mo atom (Stiefel 2001). The presence of this is also encouraging as this could be reduced to form Mo(IV) compounds on the coating surface (Stiefel 2001).

The presence of pentavalent and tetravalent molybdenum detected on the surface (Wilcox and Gabe 1988, Tang *et al.* 1994, Jahan *et al.* 1997, Treacy *et al.* 1999, Konno *et al.* 2002) could be due to the formation of 'molybdenum blue' which is a complex molybdenum oxide with the formula Mo_4O_{11} and is a non-stoichiometric compound consisting of a mixture of Mo(IV) and Mo(V) (Wilcox *et al.* 1984, Jahan *et al.* 1997) .

Trivalent molybdenum chloride species have been found on coating surfaces but only after 24 h corrosion in a NSS environment (Treacy *et al.* 1999), but were found to be in a soluble chloride form ($MoCl_3$). This is not analogous to chromate conversion coatings, as 25-30% of the coating is thought to be present as Cr(III) (Biestek and Weber 1976) in the relatively insoluble form of Cr_2O_3.

Divalent molybdenum, possibly as MoO, or as part of a more complex molybdenum-phosphate containing compound such as a heteropolymolybdate, has been found in molybdate-phosphate 'molyphos' coatings by Tang *et al.* (1994). This is possibly a unique find for a molybdate conversion coating surface on zinc. The authors claim much increased corrosion performance over conventional simple molybdate systems. The synergistic influence of the phosphate compound and electrochemical reduction from a heteropolymolybdate may have led to this low valence state of molybdenum and this may be a factor in the increased performance of these coatings.

All of the molybdenum compounds, apart from MoO_3 discussed above are soluble in water (Stiefel 2001), this may contribute to their poor performance in neutral salt spray tests and other tests in aqueous chloride based media.

2.1.7 Molybdate Coating Formation Mechanisms

A number of authors have suggested possible coating formation mechanisms for molybdate conversion coatings on zinc surfaces which can be seen in Section 2.1.7.1.

2.1.7.1 Possible Molybdate Conversion Coating Formation Mechanisms

After Rout and Bandyopadhyay (2007)

$Na_2MoO_4 + 2H^+ \rightarrow H_2MoO_4 + 2Na^+$.....***Equation 18***

Acidification of Na_2MoO_4

$H_2MoO_4 + Zn^{2+} \rightarrow ZnMoO_4 + 2H^+$.....***Equation 19***

$Zn^{2+} + HMoO_4^- \rightarrow ZnMoO_4 + H^+$ (at lower pH).....***Equation 20***

2. After Wharton et al. (2003)

$3(Mo_7O_{24})^{6-} + 14\ Zn^{2+} + 32H^+ + 42e^- \rightarrow 7Zn_2Mo_3O_8 + 16H_2O$.....*Equation 21*

The anodic formation of zinc ions (Equation 3) is due to zinc being an amphoteric metal which dissolves at pHs lower than 6 and higher than 12 (Biestek and Weber 1976, Slunder *et al.* 1971). This is followed by the cathodic evolution of hydrogen (Equation 4). When sodium molybdate is acidified, the simplest complex formed is hydrogen molybdate/ molybdic acid, where the sodium is displaced by hydrogen (Equation 18). This can then react with the zinc ions that are present in the substrate vicinity due to substrate dissolution, to form zinc molybdate (Equations 19 and 20) which precipitates onto the surface of the substrate to form the coating (Pourbaix 1966). This is analogous to the formation of iron molybdate reported at acidic pHs by Kurosawa *et al.* (1989) (Equations 1 and 2).

This mechanism is dissimilar to the one suggested for chromate conversion coatings (Equations 5 and 6). This may be due to molybdate being a weaker oxidising agent than chromate which has already been cited as a reason by a number of authors (Wilcox 2003, Wharton *et al.* 2003, Lewis *et al.* 2006).

In the second mechanism for molybdate conversion coating formation (Equation 21), proposed by Wharton *et al.* (2003), it is assumed that the molybdate is in the form of the more complex polymolybdate (heptamolybdate) species, $MoO_7O_{24}^{6-}$. This reacts with the zinc ions present in solution and precipitates as a complex zinc-molybdenum-

oxygen compound, of the molybdenum contained in this, 30 – 40% is considered to be Mo(IV) (Wharton *et al.* 2003).

It is clear from the proposals made by the aforementioned researchers that although some debate still remains over the formation mechanisms, it can be deduced that the majority of coatings possibly contain molybdenum in the (IV), (V) and (VI) valences.

2.1.8 Factors Influencing the Properties of Molybdate Conversion Coatings

2.1.8.1 Coating Formation via Immersion or by Cathodic Potential

Early authors (Gabe and Gould 1988, Wilcox and Gabe 1988) investigated the use of simple immersion and applied cathodic potential as a means of forming molybdate based passive films on a variety of substrates such as zinc, tin and platinum. They noted that coatings could be formed much more quickly when using a cathodic potential. This may not necessarily be a desirable property as Wharton *et al.* (1996) found when investigating the performance of coatings on zinc-nickel alloys, the structure of the film formed with cathodic potential had a much more coarse and cracked structure when viewed using SEM.

Subsequent authors (Treacy *et al.* 1999, Almeida *et al.* 1998, Wharton *et al.* 1999, Magalhães *et al.* 2003, Lewis *et al.* 2006, Song *et al.* 2006, Rout *et al.* 2007) have favoured immersion treatments, although the rationale for this is seldom discussed, it could be assumed that these are chosen to mirror industrial chromate based processes and favoured on a cost basis as suitable for industrial use.

Han *et al.* in 1996 and later Boose *et al.* in 2001 favoured the use of cathodic potential, when passivating zinc and zinc iron alloy surfaces using an ammonium molybdate and sodium phosphate system. The results obtained from these systems were encouraging. These findings are discussed in the relevant section later in the review.

2.1.8.2 Immersion Time

Immersion time has been found by many authors to have a great effect on the characteristics of the coatings obtained from various treatments. Typical immersion times for chromate conversion coatings on zinc surfaces are around 10 s ('Cronak' system) (Biestek and Weber 1976). In general, immersion times for molybdate conversion coatings tend to be longer, with times of 10 - 600 s quoted; some authors quoting optimum times of 300 s (Almeida *et al.* 1998, Treacy *et al.* 1999, Wharton *et al.* 1999, Lee *et al.* 2002, Wharton *et al.* 2003) with a maximum time studied of 30 minutes (Konno *et al.* 2002). Such long immersion times are needed to produce a thick coating, which is thought by some to be the most corrosion resistant. Other authors cite the un-cracked nature, hence more effective barrier properties of the thinner coatings to be more effective. There is also a strong issue of industrial viability with the longer treatment times stated above. More recent systems, such as those by Lu *et al.* (2001), Song *et al.* (2006) and Rout *et al.* (2007) show an improvement in corrosion resistance over the substrate material, with much shorter immersion times, ranging from 10 s (Song *et al.* 2006) through to 60 s (Lu *et al.* 2003). These shorter immersion times, mirror those of the current industrially used systems. Table 2-3 shows the range of reported immersion times used by investigators.

Table 2-3: *Immersion time data for molybdate based immersion coatings.*

Authors	Year	Use	Immersion Time
Gabe *et al.*	1988	Solar absorbers	1.5 min @ 30 g/l 7 min @ 10 g/l
Tang *et al.*	1994	'Molyphos' '0.33' and '0.66' on Zn surfaces	0.33 → 80 – 130 s 0.66 → 100 – 180 s
Wharton *et al.*	1996	Conversion coatings on Zn-Ni alloy surfaces	10 min
Jahan *et al.*	1997	Solar absorbers	> 20 s
Almeida *et al.*	1998	Cr(VI) replacement conversion coatings on Zn surfaces	300 s
Treacy *et al.*	1999	Conversion coatings on Zn surfaces	300 s
Wharton *et al.*	1999	Cr(VI) replacement conversion coatings on Zn-Ni alloy surfaces	300 s
Lee *et al.*	2002	Conversion coatings on Zn surfaces with Al additions	Up to 300 s
Lu *et al.*	2003	Conversion coatings on hot dip galvanised steel	20 – 60 s optimum
Konno *et al.*	2002	Molybdate/ Al(III) conversion coatings on Fe and Zn surfaces	10 – 30 min (ultrasonic agitation)
Wharton *et al.*	2003	EXAFS investigation into Mo based conversion coatings on Zn	300 s
Magalhaes *et al.*	2004	Conversion coatings on Zn surfaces	Varies – 10 min optimum
Lewis *et al.*	2006	SVET analysis for molybdate coatings on Zn surfaces	30 s
Song *et al.*	2007	MPSS conversion coatings on Zn surfaces	10 s
Rout *et al.*	2007	Molybdate - phosphate conversion coatings on hot dip galvanised steel	15 s

2.1.8.3 Synergistic Properties with Molybdate Containing Coating Formulations

The synergistic properties of molybdate with phosphate have been previously discussed by a number of authors (Wilcox *et al.* 1986, Kurosawa *et al.* 1989, Tang *et al.* 1994, Han *et al.* 1996, Boose *et al.* 2001, Magalhães *et al.* 2003, Song *et al.* 2006). In the 1986 review by Wilcox and Gabe (Wilcox *et al.* 1986), the authors report that molybdate had

well documented synergistic properties with a variety of compounds such as phosphate, nitrate, citrate, 1-Hydroxyethylidene diphosphonic Acid (HEDP), Benzenthonium chloride (BZT), tolytriazole and zinc sulphate. From these compounds, the majority of subsequent work to form conversion coatings has focused on the synergistic properties of phosphates with molybdates (Kurosawa *et al.* 1989, Tang *et al.* 1994, Han *et al.* 1996, Boose *et al.* 2001).

Kurusawa *et al.* (1989) used a molybdate solution as a corrosion inhibitor on steel surfaces. Orthophosphoric acid was used as an additive and gave increased corrosion resistance; with passive films being formed in a neutral solution and conversion coatings at lower pHs.

In 1994 Tang *et al.* (1994) developed a passivation system for use on zinc surfaces which contained molybdate and phosphate species. The authors claimed that this system was capable of outperforming a chromate based system and this was proven in outdoor exposure and prohesion tests (a less aggressive cyclic corrosion test than ASTM B117, thought to have better correlation with in-service conditions). Conversely, the coating was inferior in the industry standard ASTM B117 NSS test.

Research into molybdate-phosphate based formulations has subsequently been carried out by Han *et al.* (1996) and Boose *et al.* (2001). The former studied the formation of molybdate-phosphate conversion coatings using a 300 mA dm^{-2} cathodic current at pH 6. Treatment times ranging from 40-540 s were investigated and performance was analysed in a 3% neutral salt spray test. After 24 h the samples had the amount of white rust present noted, the optimum treatment time was found to be 120 s which resulted

in a golden coloured coating which did not show any corrosion at this stage. None of the other treatments were uncorroded after 24 h.

Boose *et al.* (2001) investigated a molybdate-phosphate system which was based on the Han *et al.* (1996) system, at equivalent and higher constituent concentrations (40 – 60 g dm^{-3} ammonium molybdate, 80 – 100 g dm^{-3} $NaH_2PO_4.2H_2O$) and a higher pH of 6.5. Coating thicknesses were found to be 60 - 120 nm which compares with the 70 nm thick Han *et al.* (1996) coatings. The samples were subjected to 3 % neutral salt spray tests and with the addition of 40 g/l sodium gluconate gave consistent times of 96 h until 5% white rust with a maximum of 120 h on zinc-iron alloys. This was a promising result, albeit on more corrosion resistant zinc alloy surfaces.

In 2002 Konno *et al.* (2002) investigated the synergistic effects of molybdate and trivalent aluminium to form 'composite' coatings on mild, stainless steel and zinc electrodeposited steel surfaces. The coatings could be successfully formed on all of the substrates tested. With a 600 s immersion, a two layer coating was formed; this consisted of a molybdenum ion rich outer layer and trivalent aluminium rich inner layer. These coatings offered good corrosion resistance in aerated 0.5M NaCl + 0.15 M H_3BO_3 at pH 7. Even though the molybdate concentration was comparatively very low for the zinc electrodeposited steel, at 0.002 M, there was a significantly higher concentration of molybdenum compounds in the coating than trivalent aluminium compounds; this may be due to the coating being made up of an aluminium heteropolymolybdate compound similar to the cobalt heteropolymolybdate compound found in Equations 14 and 15.

Also in 2002, Lee *et al.* (2002) investigated the addition of aluminium sulphate to the molybdate passivating solution for a zinc substrate. The authors found that the addition of 0.05M $Al_2(SO_4)_3$ to 0.1M Na_2MoO_4, along with reduction of the pH of the solution from 5 to 3, significantly slowed the coating formation, with samples showing a metallic lustre after 300 s immersion with 0.39 x 10^{-7} mol cm^{-2} of molybdenum deposited. Without this addition samples showed iridescent films ranging from golden and blue to green with immersion times of less than 60 s with 7.2 x 10^{-7} mol cm^{-2} of molybdenum deposited. The addition of $Al_2(SO_4)_3$ gave improved corrosion resistance when the samples were immersed in 5% NaCl for 10 h, showing less than 10% white rust, whereas the equivalent simple molybdate system produced more than 50% corrosion. This improvement clearly shows a positive synergistic relationship between molybdate and trivalent aluminium compounds.

Magalhães *et al.* (2003) investigated the effect of a number of additives on a simple molybdate system including F^-, NO_2^- and NO_3^-. These additives generally had a negative effect on the corrosion resistance of the coatings obtained. The exception was fluoride when it was added to baths acidified with sulphuric and nitric acid. Fluoride additions were found not to have any effect on the coatings formed from baths containing orthophosphoric acid which showed the highest corrosion performance. The samples obtained from these baths did show improved corrosion resistance, which does correlate with findings of previous authors that molybdate based coatings can be improved with the addition of phosphate species (Kurosawa *et al.* 1989, Tang *et al.* 1994, Han *et al.* 1996, Boose *et al.* 2001, Rout and Bandyopadhyay 2007). The authors

also claimed that these coatings have corrosion resistance comparable to a chromate system. This was, however, tested in a sulphate (SO_4^{2-}) medium, not chloride in which molybdates are known to perform poorly (Treacy *et al.* 1999). The sulphate medium was possibly used to simulate an accelerated industrial environment, in contrast to the accelerated marine corrosion that the chloride medium represents.

In 2006 Song and Mansfeld proposed a molybdate system with the additions of phosphate, silane and silicate (2006) which the authors named 'MPSS'. The treatment solution was made up of 60 g dm^{-3} $Na_2MoO_4.2H_2O$, 90 g dm^{-3} $Na_3PO_4.12H_2O$, 50 g dm^{-3} $Na_2SiO_3.9H_2O$, 50 g dm^{-3} Glycidoxy propyltri mothoxy silane and 10 ml dm^{-3} HNO_3. The synergistic effects of molybdate and phosphate are well documented. Silane was added because of its ability to seal porous coatings. This is achieved by the reaction between silanol groups and metal surface to form a covalently bonded interface.

The coating needs to be cured at > 100 °C (the authors used 120 °C for 10 min) to allow the unreacted silanol groups to condense and form siloxane chains. The resulting cross linked structure is dense enough to give effective barrier protection to the substrate. Silica was added because it gives enhanced corrosion resistance because it is insoluble in aqueous media. Unusually for a molybdate based passivation treatment, the solution was highly alkaline, at pH 11.9 and this was used instead of the more widespread acid pH because of zinc's amphoteric nature (Biestek and Weber 1976, Slunder *et al.* 1971). Corrosion performance was investigated using 0.5 M NaCl. Corrosion potential, Electronic Impedance Spectroscopy (EIS) and potentiodynamic polarisation measurements were taken. The treated surfaces gave positive results in these

electrochemical tests as well as in ASTM B-117 neutral salt spray tests, where they were able to withstand 24 h exposure without the formation of white rust. After 1 h exposure to 0.5 M NaCl, the corrosion potential, E_{corr}, of the samples were measured, a MPSS treated surface had an open circuit rest potential of 40 mV higher than the untreated surface. The MPSS coating showed a calculated protection efficiency of 95.6 %. The treated samples showed a decrease in anodic current density, which the authors attributed to the coatings blocking parts of the substrate surface from attack by the corrosive test environment.

2.1.8.4 Colloidal Silica Coatings

Nano-sized silica has been added to coating formulations to increase the corrosion resistance of silane based coatings on Zn and Al surfaces (Dalbin *et al.* 2005, Hara *et al.* 2003, Jesionowski *et al.* 2001, Palanivel *et al.* 2003, Liu *et al.* 2006). Coatings investigated by Dalbin *et al.* (2005) appeared matt grey and homogeneous. They resisted the appearance of white rust on electrodeposited alkaline zinc surfaces for 216 h in 5 % NSS tests at 35 °C, the test was not the industry standard ASTM B117 test, but tested to an Association Française de Normalisation, AFNOR, standard (AFNOR XPA- 05-109), a test under similar conditions. On acid zinc surfaces, however, they showed voluminous white rust after 120 h. It is not clear whether the voluminous corrosion appeared before 120 h, it appears that this was the first time that the samples were checked and it is probable that 5 % white rust occurred well before this time. The coatings were around 500 nm thick and well adhered to the alkaline zinc substrates; adhesion was found to be poorer to the acid zinc substrate.

Silica based coatings have been suggested as chromate and trivalent chromium coatings in their own rights by Winn and Dalton (2008). The authors describe a commercially available coating, 'Elisha EMC (Electrolytic Mineral Coating)', derived from the addition of colloidal silica nano-particles to an undescribed coating system. The resultant coatings are a pseudo-ceramic type and 200 nm thick. They have been reported in corrosion resistance tests against three commercially available trivalent chromium conversion coatings on deformed fasteners. They were comparable to the second highest performing trivalent chromium system and about 50 % as good as the highest performing. This report is undoubtedly a marketing piece, as it was written by the manufacturer of these coatings. Therefore the results reported, although encouraging, should be viewed with caution as this was not a test that is directly comparable with the industry standard ASTM B117 NSS test reported on an undamaged surface.

From the work studied it appears that the main benefits to be gained from the addition of silica nano-particles give to conversion coatings are their lack of toxicity, ease of incorporation into aqueous conversion coatings and improvements in corrosion resistance. Corrosion resistance is improved because the resultant coating is thickened; dense and well adhered to the substrate (Jesionowski *et al.* 2001, Hara *et al.* 2003, Palanivel *et al.* 2003, Dalbin *et al.* 2005, Liu *et al.* 2006, Winn and Dalton 2008).

2.1.8.5 Cobalt Additives

The synergistic properties of cobalt with molybdenum was highlighted by Meyers *et al.* at the McClellan Air Force Base in California, USA (1994), the authors described the effectiveness of a cobalt and molybdenum based conversion coating as a chromate

replacement for Al surfaces. The study does not give specific details about the specific treatment conditions and coating characteristics. Cobalt has also been used as an additive for Cr(III) based systems, where it is thought to be a catalyst to the surface reactions producing thicker trivalent chromium coatings (Crotty 1981). Co(II) is also capable of forming heteropolymolybdates in solution (Stiefel 2001).

2.1.8.6 Solutions Based Solely on Molybdate

Most authors have used sodium molybdate at various concentrations as the basis for passivating systems. The reasoning for this, although seldom discussed, seems to mirror chromate based systems, which often use sodium dichromate. It is also worthy of note that, at laboratory scale levels, ammonium molybdate is considerably more expensive than sodium molybdate (Fisher.co.uk 2007).

Research by Almeida *et al.* (1998) has shown that coatings produced from ammonium molybdate solutions are inferior in terms of time to white rust in NSS exposure tests. Ammonium molybdate has been used by a number of authors in conjunction with phosphates or trivalent aluminium compounds (Han *et al.* 1996, Boose *et al.* 2001, Konno *et al.* 2002, Lee *et al.* 2002). The reasoning for this may be that compounds formed using ammonium molybdate may be more complex and are able to promote a larger number of other passivating species onto the treated surface.

2.1.8.7 Molybdate Treatment Concentration

Molybdate concentration varies between investigators, with some authors citing the use of a particular concentration to mirror the level of sodium dichromate in commercially available solutions (Magalhães *et al.* 2003, Lewis *et al.* 2006). The most common

concentration used is ~0.1 mol dm^{-3} (24.2 g dm^{-3}) (Gabe and Gould 1988, Wilcox 1989, Wharton *et al.* 1996, Treacy *et al.* 1999, Wharton *et al.* 1999, Lee *et al.* 2002, Wharton *et al.* 2003) but concentrations have ranged from 0.002 mol dm^{-3} ammonium molybdate (in a composite system with Al(III) (Konno *et al.* 2002) to 1.5 mol dm^{-3} (363 g dm^{-3}) (Almeida *et al.* 1998).

It is thought that increasing the molybdate concentration decreases coating formation time (Gabe and Gould 1988, Wilcox and Gabe 1988, Lewis *et al.* 2006), with higher concentrations producing darker, particularly black coatings more readily. It may be on the basis of cost that lower concentrations are selected or it may be that the faster coating formation time produces a more porous, heterogeneous coating. Although it has been suggested by some authors that this is a result of other factors used to increase the coating formation rate such as decreasing the pH, increasing the cathodic current used and increasing the temperature of the treatment solution (Gabe and Gould 1988, Tang *et al.* 1994, Jahan *et al.* 1997, Wharton *et al.* 1996, Kurosawa *et al.* 1989).

2.1.8.8 Solution pH and Acid used for pH Adjustment

The pH of the treatment solution has been linked to various properties of the coating such as thickness and morphology. Wilcox and Gabe (1988) investigated a range of pHs from 1 to 13 and found that black, adherent coatings were formed at pH 3 and 5, with dissolution of the zinc substrate at pH 1 and only slight staining at pH 9 and 13.

Subsequent investigations (Treacy *et al.* 1999, Wharton *et al.* 1999, Almeida *et al.* 1998) have found pH 5 to give the most corrosion resistant coating. Although solutions at pH 3 have been found to give thicker coatings because of the increased coating formation

rate. When examined using SEM they were shown to have a more cracked morphology which has been attributed to the poor performance of molybdate conversion coatings in chloride environments (Treacy *et al.* 1999).

Tang *et al.* (1994) noted that optimum pHs for the 'Molyphos' systems, 0.33 and 0.66 on zinc and zinc-alloy substrates, were 2.1 and 4.6 respectively. While higher pHs produced coatings, it was noted that they required a longer immersion time. This suggests that coating formation rate is highly dependent on pH, with lower pHs giving faster rates.

When investigating molybdate based coatings on electrodeposited Zn-Ni alloys, Wharton *et al.* (1996) noted that coatings formed at pH 3 and 6 had a much finer crack structure and pH 3 and 5.5 gave the best performance in NSS tests (giving a 300% improvement for the time to white rust over an unpassivated substrate).

Magalhães *et al.* (2003) considered pH when investigating molybdate passivation systems on zinc surfaces and also the acid used to adjust the pH and found both of these variables to have significant effects on the properties of the coatings. Orthophosphoric, nitric and sulphuric acids were examined. The authors found that coatings from baths acidified with orthophosphoric acid were very compact and showed little dissolution of the zinc substrate, the coatings formed from baths adjusted with nitric and sulphuric acids were much more voluminous, but more cracked and dissolved the zinc substrate to a higher extent. This is a study that has systematically investigated these variables, but does not contain neutral salt spray or linear polarisation data in chloride environments; all of the corrosion data was obtained using linear polarisation resistance in a sulphate medium. The work by Magalhães and co-workers (2003) highlighted the

importance of the acid used to adjust the pH on the characteristics of the coating achieved. Previous researchers have used a number of different acids to adjust the solution pH and these do seem to have had an effect on the nature of the coating attained. Sulphuric acid has been used by Wilcox and Gabe (1988) where the molybdate coatings were matt black after immersion or cathodic polarisation; it was also used by Wharton *et al.* (1996) to adjust the pH of solutions used to passivate zinc nickel alloys. Almeida *et al.* (1998) also acidified passivating solutions with sulphuric acid, and the molybdate coatings formed from these baths were thick and cracked, they performed poorly in corrosion tests. Lewis *et al.* (2006) also used sulphuric acid to adjust the pH of the molybdate solutions used and noted that the molybdate coatings obtained had the characteristic 'cracked dried riverbed' structure and performed very poorly in NSS corrosion tests.

Nitric acid has been utilised by Treacy *et al.* (1999), this gave an iridescent finish after a 300 s immersion, which suggests a much slower coating formation time than when sulphuric acid is used, iridescent coatings are typically formed within 30 – 120 s (Wilcox and Gabe 1988, Wilcox 1989, Lewis *et al.* 2006) . Treacy *et al.* (1999) observe that these coatings actually appear to *decrease* the time to the formation of white rust on zinc surfaces.

Nitric acid was used as an additive in the 'MPSS' system proposed in 2006 by Song *et al.*, whilst the treatment solution was alkaline, 10 ml dm^{-3} of nitric acid was added to accelerate substrate dissolution, reducing coating formation time. This seems to be

evident with this system, as the immersion time used is relatively short, at only 10 s which is indicative of an industrial system coating formation time.

Orthophosphoric acid has been used in to acidify molybdate baths for passivating steel surfaces by Kurusawa *et al.* (1989), the authors also investigated adjusting the pH with sulphuric and hydrochloric acids, and found that these systems produced coatings that were black and loosely adherent and offered poor corrosion resistance compared with orthophosphoric acid. Orthophosphoric acid was used in conjunction with boric acid in a recent investigation by Rout and Bandyopadhyay (2007) for use on hot-dip (zinc) galvanised (HDG) steel. The authors used a pH of 4-5 to maintain a level of zinc dissolution to enable coating formation. It is interesting to note that the level of phosphorous in the coating was nearly as high as the level of molybdenum measured using Energy Dispersive Spectroscopy (EDS), this shows that under these conditions it is possible to produce molybdenum and phosphorus compounds on the surface, these were found using Raman spectroscopy. A 2.3 times improvement in linear polarisation resistance was found over an untreated sample, which corroded rapidly in the 3.5% NaCl solution. A significant 5 times improvement was recorded in NSS corrosion resistance.

2.1.9 Neutral Salt Spray Corrosion Testing of Molybdate Conversion Coatings

Zinc performs particularly poorly in the NSS test, with galvanised surfaces showing times to white rust of as little as 1 hour (Almeida *et al.* 1998). This performance can be drastically increased by passivating the surface with a chromate based treatment which typically increases the time until 5% white rust to 100+ hours depending on the type/ thickness of the chromate film (Biestek and Weber 1976). Molybdate based treatments

for zinc have shown very little improvement to time to white rust over zinc alone, but some treatments have been shown to give comparable performance to chromates when subjected to outdoor exposure trials (Tang *et al.* 1994). An inherent problem with molybdate coatings is their poor performance in NSS corrosion tests. This has been attributed to the solubility of the molybdenum chloride corrosion products produced (Treacy *et al.* 1999).

Although there has been little success, to date, in formulating a molybdate based system for zinc surfaces comparable in terms of corrosion resistance to a chromate system in NSS tests, there has been a system that has been developed for use on zinc-nickel alloys by Wharton *et al.* (1996) which offers a time to white rust of 360h which is a 300% improvement over the substrate alone. This system is, however, still some way behind the chromate system. As previously stated in Section 2.1.8.1 Coating Formation via Immersion or Cathodic Potential, direct comparison cannot be made between the corrosion resistance of zinc and zinc alloy coatings.

Table 2-4 illustrates NSS corrosion test data for molybdate-based conversion coatings from selected authors.

Table 2-4: N*eutral salt spray test corrosion data cited from literature studied.*

Author	Year	Substrate	System	Time Until 5% White Rust	Test
Wharton *et al.*	1996	8 µm Zn-Ni alloy	Molybdate pH 5 immersion	360 h (145 h until white film)	ASTM B117
Han *et al.*	1996	Zinc	Molybdate – phosphate cathodic deposition	No change after 24 h for 'Golden' surface	3% NSS
Tang *et al.*	1997	Zn-Co alloy	'Molyphos 66'	24	ASTM B117
Almeida *et al.*	1998	Zinc	1 M Simple molybdate	7 h	ASTM B117
Treacy *et al.*	1999	8 µm Electroplated alkaline zinc	0.1 M Simple molybdate	21 h	ASTM B117
Boose *et al.*	2001	Zn-Fe Alloy	Molybdate – phosphate cathodic deposition	120 h	ASTM B117
Lee *et al.*	2002	Hot-dip galvanised steel	20-60s Immersions in molybdate – phosphate	2% at 24 h	ASTM B117
Lewis *et al.*	2006	8 µm electroplated zinc	Simple 10 g/l molybdate	<24 h	ASTM B117
Song *et al.*	2007	4 µm electroplated zinc	Molybdate phosphate silane silicate 'MPSS'	24 h with no corrosion	ASTM B117
Rout *et al.*	2007	Hot-dip galvanised steel	Simple molybdate with orthophosphoric/ boric acids to adjust pH	20 h until white film	3.5% NSS

On zinc surfaces, results from NSS corrosion tests are less promising; with some researchers noting that the molybdate coating actually increased the initial rate of corrosion (Treacy *et al.* 1999). Some authors quoted 7 h (Almeida *et al.* 1998) and 21 h (Treacy *et al.* 1999) until the appearance of white rust on an 8µm thick electrodeposited surface. Whereas a typical iridescent chromate conversion coating would show a 5% coverage of white rust in 72-120 h (Lewis *et al.* 2006, Biestek and Weber 1976).

The ‘golden’ coloured molybdate-phosphate based system proposed by Han *et al.* (1996) was able to resist a 3% NSS test for 24 h without surface change. The use of a less corrosive 3% NSS test instead of the industry standard ASTM B117 5% NSS test means that results are not directly comparable with data from the tests under the more concentrated conditions.

A similar system was used with zinc and zinc-iron alloys by Boose *et al.* (2001) in 2001, the authors increased the treatment temperature to >50 °C and added 40 g/l of sodium gluconate, treatment time was also increased to 600 s. The samples were subjected to an ASTM B117 NSS corrosion test and were able to resist the formation of white corrosion for up to 120 h. The authors do not refer as to whether this is on a zinc or zinc-iron alloy surface; it can therefore only be assumed that this ‘maximum’ result is for the more corrosion resistant zinc-iron alloy.

Song and Mansfeld’s (2006) Molybdate-Phosphate-Silane-Silicate (MPSS) system was able to produce a coating on 4 μm thick electroplated zinc which resisted corrosion for 24 h in an NSS test. This clearly shows an enhanced surface and this does pass the requirement for use in white goods. The test was, however, terminated after 24 h, which is not sufficient to demonstrate the treatment as a viable non-chromate option. Of the molybdate based systems reported so far in the literature, the MPSS system appears to have resisted corrosion for the longest time on a zinc surface in an ASTM B117 NSS test.

Rout and Bandyopadhyay (2007) proposed a simple molybdate system for use on HDG steel which used a mixture of orthophosphoric and boric acids to adjust the pH of the

solution. The surface of the material was reported to be a mixture of zinc molybdate and phosphate compounds. The authors claimed that it is able to resist the formation of white rust for 20 h compared to the unpassivated sample which lasted 4 h. The test used a 3.5% NaCl concentration, which is lower than the 5% NaCl utilised in ASTM B117. This prevents the results from being directly compared with those performed with a 5% NSS corrosion test.

2.2 Conclusions

It can be seen from the contents of this review, that molybdate based conversion coatings are not yet a viable direct replacement for chromate based conversion coatings on zinc surfaces. However, with the increasing environmental and legislative pressures serving as a major driving force, steady progress has been made by investigators in the field. Research has shown that the corrosion resistance of 'simple' molybdate formulations as promoters of conversion coatings is very poor. Limited and varied success has been made with the addition of synergistic chemical species, particularly phosphate, trivalent aluminium, cobalt, silica and silicate compounds, which promoted thinner, more compact coatings from solutions probably containing heteropolymolybdates.

It does appear, however, that the some of the more promising of the results obtained in the NSS corrosion tests are due, at least in part, to less severe corrosive conditions, such as a lower NaCl concentration of 3% instead of 5% in the ASTM B117 NSS test. There are apparent significant positive trends in reported research that are worthy of note. Synergistic formulations have shown improved results particularly with a phosphorous

(Wicox *et al.* 1986, Kurusawa 1989, Tang *et al.* 1994, Han *et al.* 1996, Boose *et al.* 2001, Magalhães *et al.* 2003, Song and Mansfeld 2006) or trivalent aluminium (Konno *et al.* 2002, Lee *et al.* 2002) containing compound and good results can be obtained using a sealing layer such as silane to produce a pore-free coating (Song and Mansfeld 2006).

Using a less 'aggressive' corrosion test does have advantages where molybdate conversion coatings are concerned, because easier differentiation between the performances of molybdate coatings under different conditions would allow for improvements to be more easily seen; thus a better performing coating may be discovered and subsequently investigated.

3 Justification of Experimental Work

From the scope of the discussed matter contained in the literature review it is clear that there is a need to further investigate the use of molybdate as a potential non-chromate conversion coating. Further to this, a molybdate based conversion coating system would be able to alleviate the growing perception that all 'chromium' is toxic by being a 'non-chromium' conversion coating. The author feels that, from the encouraging results shown by other authors researched, there the potential to enhance a molybdate conversion coating system so that could offer enough corrosion resistance for it to be commercially viable in the near future.

3.1 Focus of Experimental Work

Experimental work will focus on improving molybdate conversion coatings for use on acid zinc surfaces. Simple acid molybdate as well as Cr(VI) coatings will be investigated primarily to give a baseline to which subsequent improvement can be measured.

Primary corrosion testing will focus on Linear Polarisation Resistance (LPR) testing, as this is a less aggressive test than the industry standard ASTM B 117 NSS test which will allow small differences in the corrosion resistance between coatings to be more easily detected and thus, enhancements more easily seen. Improvements found using this technique, will lead to an enhanced coating system(s) and will subsequently be tested using ASTM B 117 NSS testing.

Corrosion results will be correlated with surface morphology data obtained from FEG-SEM investigations and compositional analyses from AES and EDXA techniques.

The investigation will focus on the effect of:

- Immersion time.
- Treatment temperature.
- Molybdate concentration.
- Polymerising additives, to form heteropolymolybdates.
- Oxidising additives, to increase coating rate by increased substrate dissolution.
- Particulate additives, to decrease coating solubility and thicken coating.
- Two-stage processes, to make a dual layer composite coating with enhanced properties.

It is hoped that the scope of the literature survey has highlighted areas of promise, where enhancements can be made, so that current molybdate conversion coating systems can be improved.

Work will also be focussed on determining how different molybdate systems fail in comparison to the substrate and Cr(VI) treatments, to test the hypotheses that have been made relating to ingress of corrosive species in the cracks and the dissolution of thin coatings.

4 Experimental

The main focus of the experimental work carried out was to produce a coating with enhanced corrosion resistance over previously studied 'simple' molybdate conversion coatings for electrodeposited zinc surfaces. The main quantitative corrosion analysis has been derived from linear polarisation resistance testing. This was a key technique in evaluating corrosion performance, as it is less aggressive than the industry standard ASTM B-117 neutral salt spray (NSS) test and therefore able to distinguish differences between samples more easily.

4.1 General Sample Preparation

Substrates selected for all experiments were polished mild steel, Hull cell sized panels (OSSIAN Hull J10) were supplied by McDermid plc, these were selected because of their compatibility with the electroplating system used. Substrates were received with a thin (flash) protective layer of Zn which gave a dull finish, attributable to the high surface roughness (See Figure 4-1a)

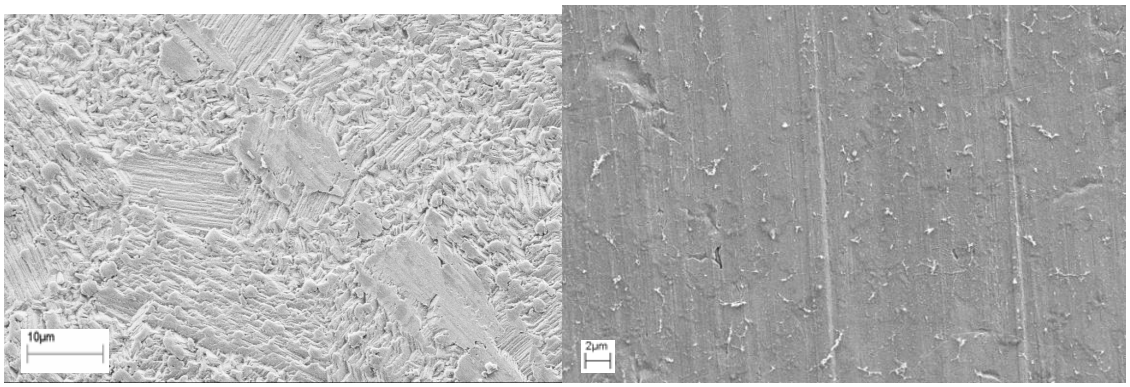

a b

Figure 4-1: *a: FEG-SEM image showing the surface of a substrate in the as received condition. b: FEG-SEM image showing the surface of a substrate after immersion in 50% HCl.*

After immersion in 50% HCl vol. /vol. (S.G 1.18), the protective layer of Zn was removed, exposing the polished mild steel surface, the rolling lines can be seen as well as a much smoother surface (see Figure 4-1b).

A lustrous Zn finish was achieved by cathodic electrodeposition in a proprietary acid Zn electroplating solution with the trade name 'Kenlevel', also supplied by McDermid plc.

The electrodeposition method was as follows:

- Substrate rinse with de-ionised water and immersion in 50% HCl vol. /vol. (S.G 1.18) to remove protective zinc from the surface then rinse again to remove residual acid.
- Electroplate at 2.25 mA for 567 s (9 min 27 s) to achieve a nominal 8 µm coating.
- Periodic agitation at 1 min intervals, to promote lustrous finish due to removal of local hydrogen evolution on the surface.
- Rinse with deionised water and dry with warm air.

4.1.1 Deposition Calculations

To determine the process parameters required to produce a nominal 8 µm thick electrodeposited Zn coating, on both sides of the polished mild steel substrates, the following calculations were utilised.

Surface Area of Substrate:

Area /mm^2 = (Area of one side /mm^2) x 2

= (100 x 75) x 2

= 15 000 mm^2

= 150 cm^2

= 1.5 dm^2

Volume of Zn Needed for 8 µm Coating:

Volume /mm^3 = Length /mm x width /mm x height /mm

= 100 x 75 x 8 x10^{-3}

= 60 mm^3 (for both sides x 2) = 120 mm^3

Mass of Zn Required:

Mass = Volume /mm^3 x Density /g mm^{-3}

= 120 x 7.1 x 10^{-3}

= 0.8592 g

Treatment Time Required (from Faraday's First Law)

m = (MQ) / (F/z).....Equation 22

Where:

m = Mass /g

M = Molar Mass /g mol^{-1}

Q = Charge /C

F = Faraday's Constant (96 500 C mol^{-1})

Therefore:

Mass /g = (Molar Mass /mol^{-1} x Time /s x Current /A) / (no. electrons per ion x Faraday's constant (F) / C mol^{-1})

Therefore:

Time = (Mass x no. electrons per ion x F) / (Molar Mass x Current)

= (0.8592 x 2 x 96500) / (65 x 2.25)

= 1134 s = 18.54 minutes (for a current of 2.25 A)

For a current of 4.5 A (factor of 2 increase)

T = 567 s = 9 minutes 27 s.

This calculation determined the treatment time required to deposit a nominal 8 µm thick electrodeposited Zn coating on the substrate. A current of 4.5 A was selected, because experiments with higher currents, although producing the required thickness of coating faster, showed dendritic growth on the surface. This was probably due to

them having localised areas of high current density causing dendritic growth. Dendrites are undesirable in electrodeposited coatings to be conversion coated, as they prevent a homogeneous coating forming.

Experiments were carried out to determine the thickness using FIB-SEM (Figure 4-2). These revealed the coating to indeed be approximately 8 µm (Figure was measured to be 7.95 µm).

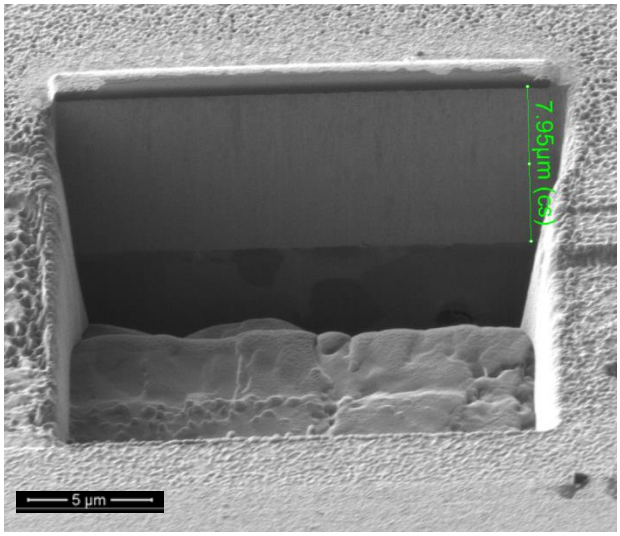

Figure 4-2: *FIB-SEM image showing approximate thickness of an electrodeposited Zn coating.*

4.1.2 Pre-treatment

It is important for the conversion coating process that the surface is free of contaminants and oxides. The prevention of contaminants was enabled by storage in a desiccator in the event that coating was not performed immediately subsequent to electrodeposition. Care was taken not to touch the surface of the samples at any time to eliminate finger staining.

Zn has a tendency to form surface oxides and hydroxides in ambient atmospheres that interfere with the conversion coating process; therefore the samples were immersed with slight agitation in 0.5% HNO_3 vol./ vol. for 30 s. This produced a homogeneous surface and removed any dried on organic contaminants from the proprietary electroplating solution. Figure 4-3, shows the effect of the HNO_3 etch on enhancing the homogeneity of the surface, light coloured organic staining can be seen to the left of the image in the 'un-etched' region. The 'etched' region, to the right of the image is absent of the staining.

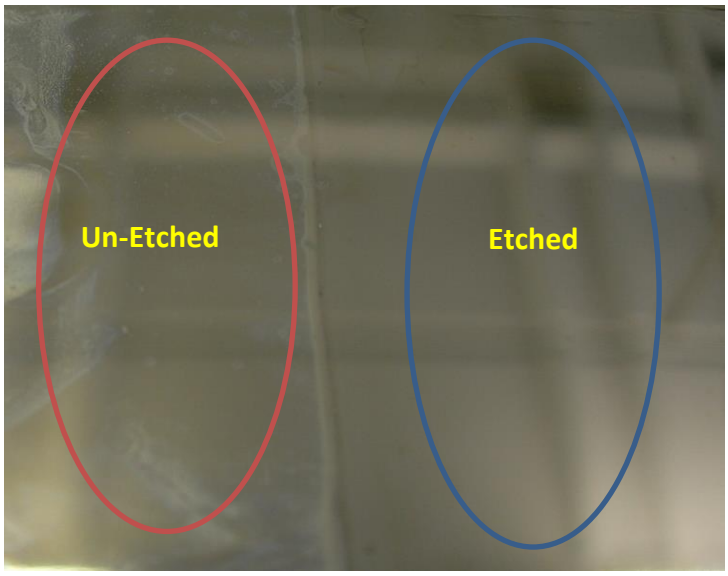

Figure 4-3: *Digital image showing the effect of HNO_3 pre-treatment on an electroplated Zn surface, where an un-etched area (right) and an etched area (left) can be seen.*

FEG-SEM investigations revealed that the acid etch had the effect of removing the larger areas of roughness from the surface, leaving a relatively flat surface, with a micro-roughness that the images (Figure 4-4) show.

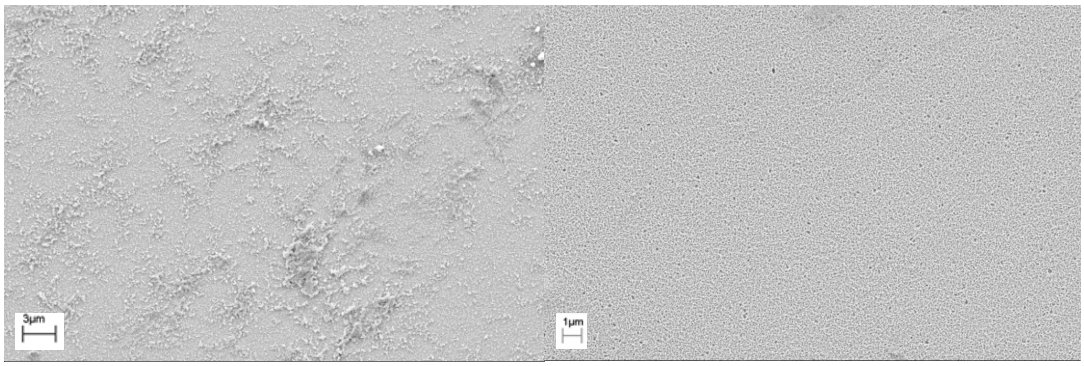

a b

Figure 4-4: *a: FEG-SEM image showing electrodeposited Zn surface before HNO_3 etch. b: FEG-SEM image showing electrodeposited Zn surface after HNO_3 etch.*

4.1.3 Conversion Coating Technique

Conversion coating was performed by simple immersion in the particular treatment solution. The latter were made up of chemicals at analytical reagent grade or above and high purity de-ionised water, with a resistivity of ~ 15 MΩ.cm. Various conversion coating systems were applied, the details of which can be viewed in the appropriate sections.

Early pilot experiments showed mild agitation by a magnetic stirrer at 200 rpm, with slight forward and backward movement by hand parallel to the direction of flow to be successful in creating a homogeneous conversion coating. After treatment for the appropriate time, the sample was carefully rinsed with de-ionised water and dried with an air dryer on a low heat setting before storage in a desiccator. The method of drying was selected because analogous coatings have been found to be gelatinous with a high water content. Rapid loss of this water has been found to lead to a highly cracked microstructure, compromising corrosion resistance to a certain extent.

4.1.4 Partially Corroded Sample Preparation for Corrosion Nucleation Experiments

Partially corroded samples were prepared with the intention of investigating the point of onset of corrosion and film breakdown using the techniques shown in subsequent sections. Samples were immersed in 5 % wt./ vol. NaCl (aq.), until they showed initial signs of corrosion, immersion times ranged from 20 minutes to 4 hours. Initial signs of corrosion were deemed to be any appearance of pitting or discolouration of the film, not voluminous corrosion product. Samples were rinsed thoroughly and carefully with de-ionised water to remove any NaCl present on the surface and taking care not to detach any of the coating. Samples were then air dried and stored in a desiccator for subsequent analysis.

4.2 Sample Corrosion Performance Analysis

4.2.1 Linear Polarisation Resistance Testing

Linear Polarisation Resistance (LPR) testing allows for the instantaneous corrosion rate and exchange current density to be found in one experiment. Because of this, it is a powerful tool in determining the corrosion resistance of metallic surfaces and gives a quantifiable means of comparing the corrosion resistance of coatings (Kelly *et al.* 2003).

The relationship between applied current density, i_{app}, and the current density of corrosion, i_{corr}, is seen experimentally in the corrosion cell in the absence of competing oxidation and reduction reactions, Equation 23 shows this: (Kelly *et al.* 2003).

$$i_{app} = i_{corr} (\exp [2.3 (E - E_{corr}) / \beta_a] - \exp [-2.3 (E - E_{corr}) / \beta_c]) \quad \textit{Equation 23}$$

Where β_a and β_c are the anodic and cathodic Tafel parameters respectively, which are given by the slopes of the respective anodic and cathodic polarisation curves. E is the applied potential whilst E_{corr} is the corrosion potential where $E - E_{corr} = \Delta E$ (Kelly *et al.* 2003). This relationship forms the basis of the polarisation resistance technique.

Theory suggests that applied current density has a linear relationship with applied potential close to the open circuit (rest) potential. Because of this linearity, the kinetic Equation (Equation 24) was simplified by Stern and Geary (1957) to:

$$R_p (\Omega.cm^2) = [\Delta E / \Delta i_{app}] (E - E_{corr}) > 0 \quad \textit{Equation 24}$$

Where R_p is the linear polarisation resistance. Coatings with higher polarisation resistances have higher corrosion resistance. It must be stressed however that, while R_p is a good indication of corrosion resistance, it does have its limitations. The corrosion current around the rest potential is influenced by redox reactions occurring on the surface, these may be due to corrosion, or localised re-passivation and because the test cannot distinguish between these two, results must be confirmed by NSS corrosion testing.

4.2.1.1 Sample Preparation and Testing

Samples were tested at least in triplicate so that a statistically viable result could be gained for each coating system. An area of 4 cm^2 was exposed, with the remainder of the sample being coated with 'Lacomit' lacquer, excluding an area to allow for an electrical connection to be made.

The corrosion cell consisted of:

- Working Electrode

  Sample to be tested.

- Reference Electrode:

  Saturated Calomel Electrode (SCE), the electrode was connected to a remote probe with a tube containing saturated KCl. The probe was positioned close to the surface of the sample without touching it and masking it as little as possible.

- Auxiliary Electrodes:

  Two platinum counter electrodes were used as platinum is fairly chemically inert.

- 5% wt./ vol. NaCl (aq.) electrolyte:

  The samples were immersed in the 5% wt./ vol. NaCl solution for a period of 1 hour before testing to enable them to stabilise.

Polarisation measurements were taken using an ACM instruments 'Autotafel' computer-controlled potentiostat, controlled by 'Tafanal' software See Figure 4-5.

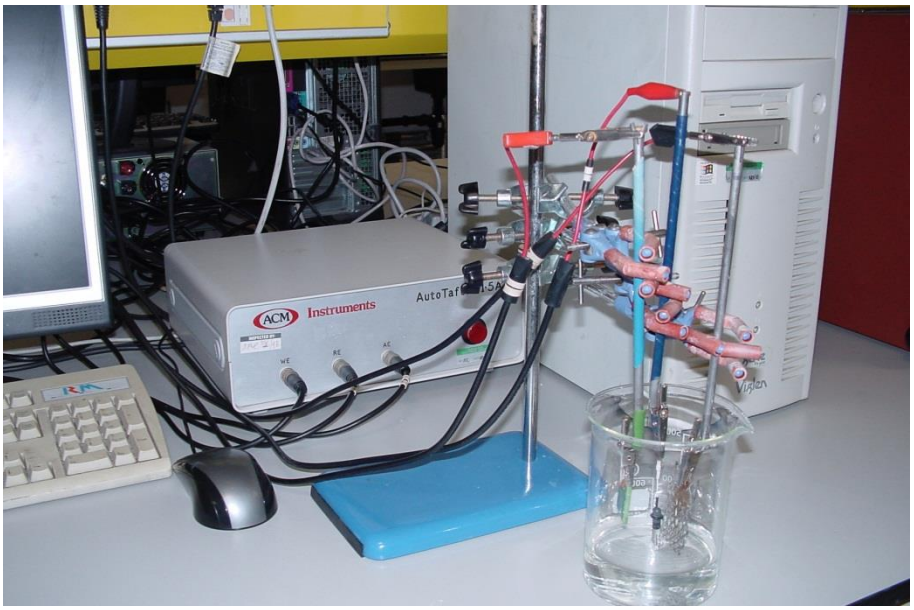

Figure 4-5: *Digital image showing the experimental setup used for the Linear Polarisation Resistance (LPR) technique.*

In all experiments the working electrode was immersed in the electrolyte for a period of 30 minutes at open circuit potential to allow it to reach an approximately steady-state value.

Open circuit potentials were measured versus a SCE, with all potentials quoted on this scale. A potential sweep was set to start at 20 mV cathodic and finish at 20 mV anodic of the open circuit potential, with a potentiodynamic scan rate of 6 mV.minute^{-1}. Data obtained was plotted in a graph of potential against current density using Microsoft Excel spreadsheet software, example data can be found in Figure 4-6. The inflection on the chart is the open circuit potential, with the anodic region above and cathodic region below.

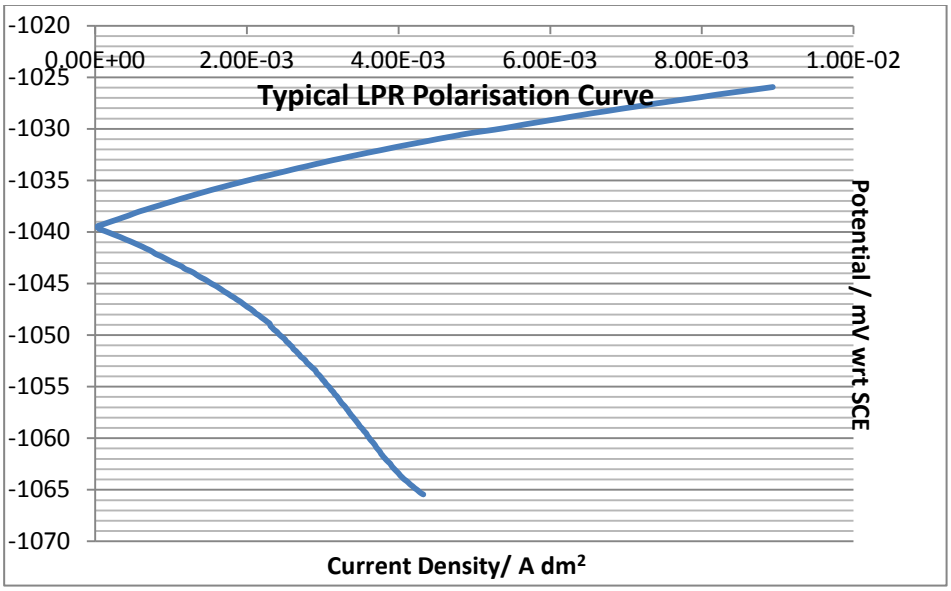

Figure 4-6: *Data showing a typical Polarisation Curve attained from LPR testing.*

R_p was obtained by the gradient of the linear region, made positive, within 3 mV of the rest potential, example experimental data can be found in Figure 4-7.

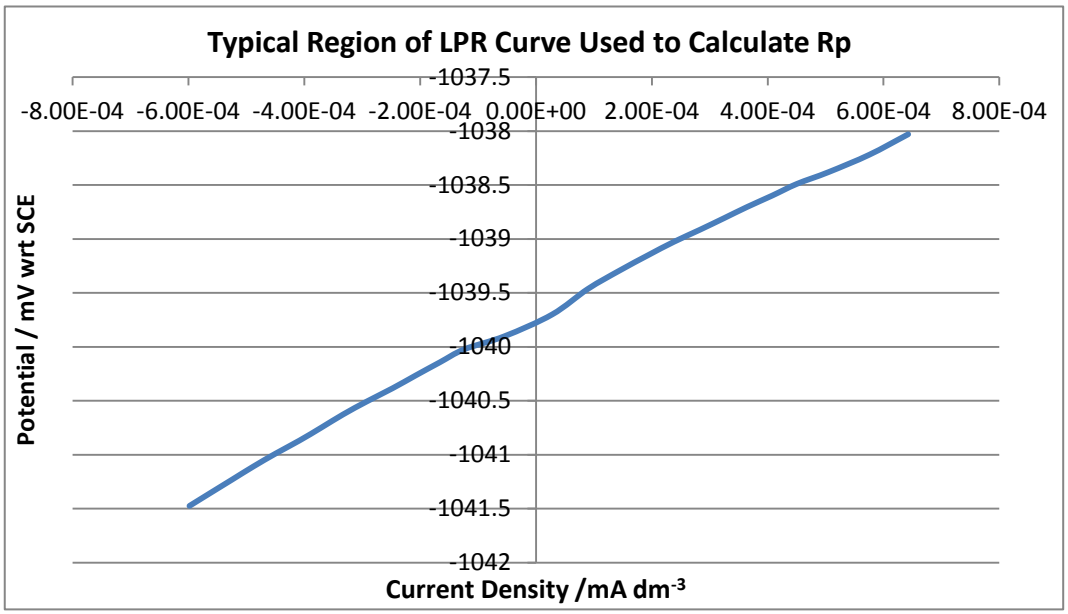

Figure 4-7: *Data showing Typical Region of LPR Curve Used to Calculate Rp*

4.2.2 Neutral Salt Spray Corrosion Testing

Neutral Salt Spray (NSS) corrosion testing is a commonly used corrosion test in the surface finishing industry. It is essentially an accelerated marine environment test, where the samples are subjected to a continuous spray of 5% wt. /vol. NaCl (salt) solution at 35°C at pH 6.5-7.2 according to ASTM B117-07 (2007). This is an extremely corrosive environment and allows the relative corrosion resistance of materials to be compared.

NSS tests are much simpler than actual service conditions and are designed to be a more accelerated and controlled version of service life. Data obtained is limited to being comparable between materials and coatings but not directly relational to actual service conditions. This is because of the controlled and harsh corrosive nature of the NSS test; it can seldom be used to predict actual service life of a material. Corrosive environments encountered in service tend to be more complex in terms of species present and have periodic temperature variations. This makes it unfeasible to recreate these conditions in a 'lab-based' corrosion test; meaning that the NSS test is useful as a 'ranking' test rather than as a direct correlation to actual service conditions.

4.2.2.1 NSS Sample Preparation and Testing

Samples were masked around the edges and rear with chemically inert tape, exposing as large an area as possible without exposing the edges. Testing took place in either an CandW Equipment Ltd. Model SFS450CASS or an Ascott Analytical Ltd. Model S450s neutral salt spray corrosion chamber according to the ASTM B117-07 standard (2007); pH 6.5-7.2, 35 °C, 100 % humidity and a continuous spray of 5 % wt./ vol. NaCl (aq.) at

25-30 ml. min^{-1}. The fallout rate of the chamber was 1-2 ml /hour per 80 cm^2 of horizontal collection area. Values for fallout rate were checked periodically to ensure homogeneity regardless of sample position. Samples were placed on racks at 30 ° to the vertical in random positions throughout the chamber (Figure 4-8). Samples were also tested at least in triplicate to give statistical viability to the results gained.

Figure 4-8: *Digital Image showing a typical sample configuration for an NSS test.*

4.2.2.2 Sample Examination

Examination of sample surfaces took place every hour for the first 8 h and then at 24 h intervals from the original start time, digital images were taken each time the samples were checked. Times to 5% 'white rust' (Figure 4-9a) and 5% 'red rust' (Figure 4-10b) were recorded, when the samples had reached the point at which they showed 5% 'red rust' the test was terminated for that sample. The appearance of 5% of white rust (from Zn corrosion), is of upmost importance in NSS tests, as it indicates a significant failure of the conversion coating. Time to 5% red rust (from Fe corrosion) is of secondary importance, as it indicates failure of the zinc surface. The main significance

of this failure is to monitor any effects that the conversion coating has on the zinc surface's ability to protect the mild steel substrate.

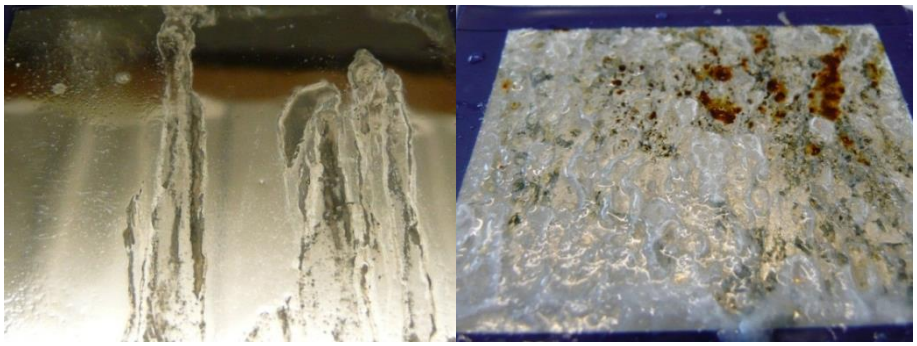

a b

Figure 4-9: *a: Digital image showing the appearance of 5% white rust on an electrodeposited zinc surface. b: Digital image showing the appearance of 5% red rust on an electrodeposited zinc surface.*

4.3 Sample Morphology Characterisation

With corrosion performance being the main determinant of performance, subsequent investigation took place using FEG-SEM to relate surface features to corrosion resistance.

4.3.1 Field Emission Gun Scanning Electron Microscopy (FEG-SEM)

Scanning electron microscopy, (SEM), is widely used to characterise surfaces on a scale that is impossible with optical microscopy. For molybdate coatings, it is especially useful to reveal topographical features such as pores and 'microcracks', on the surface that are not visible to optical microscopes. The Field Emission Gun Scanning Electron Microscope (FEG-SEM) has the advantage over a conventional SEM of providing higher resolution images due to the electron beam being smaller in diameter. This also gives a higher signal to noise ratio and improvements in spatial resolution. With molybdate films studied having thicknesses as low as 60 nm, it was imperative that FEG-SEM was used, particularly for cross-sectional images. The model used for characterisation was a Leo Elektronenmikroskopie GmbH model 1530 VP with an EDAX Pegasus (EBSD/EDXA) unit.

4.3.1.1 FEG-SEM Experimental Technique

Samples were mounted onto conventional aluminium sample holders with a surface of approximately 1 cm in diameter. The chamber was evacuated to ~ 5 x 10^{-1} Pa, for imaging, Secondary Electron (SE) and Inlens detectors were used with accelerating voltages of 5 - 10 keV and a working distance of 5 – 10 mm, depending on type of sample. For general topographic images, SE imaging gave sufficient resolution. For

higher resolution images, the Inlens detector was used. The Inlens detector has the effect of reversing the edge contrast, making edges appear bright instead of dark as shown in Figure 4-10.

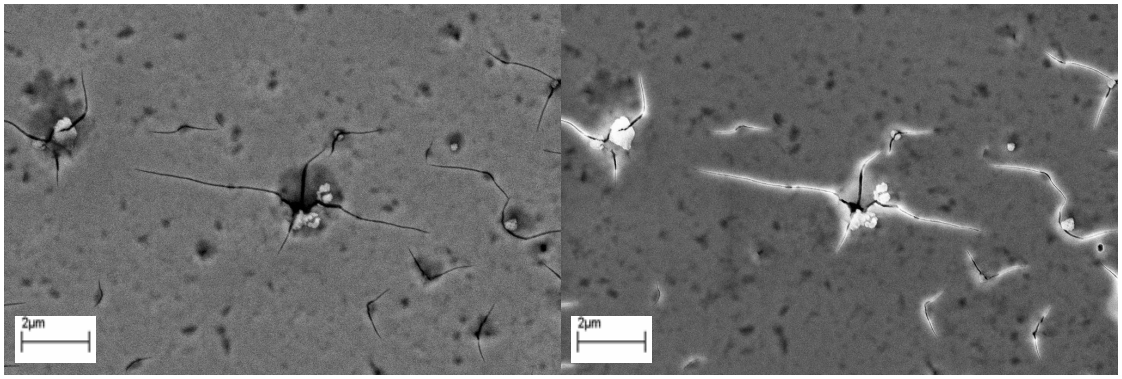

a b

Figure 4-10: *a: FEGSEM Image taken in SE Mode. b: FEGSEM Image taken in Inlens Mode.*

4.3.1.2 FEG-SEM Cryofracture Sectioning Technique

In order to determine coating thickness and reveal information about the coating structure; cryofracture was used. The technique followed was to cut a strip of approximately 10 x 40 mm from the sample, this was then held with appropriate pliers and immersed in liquid nitrogen for ~ 30 s or until the liquid nitrogen had stopped bubbling. When removed, the coating was sufficiently brittle to be fractured by bending the sample through 180 °, the sample was then mounted onto a conventional SEM sample holder (see Figure 4-11).

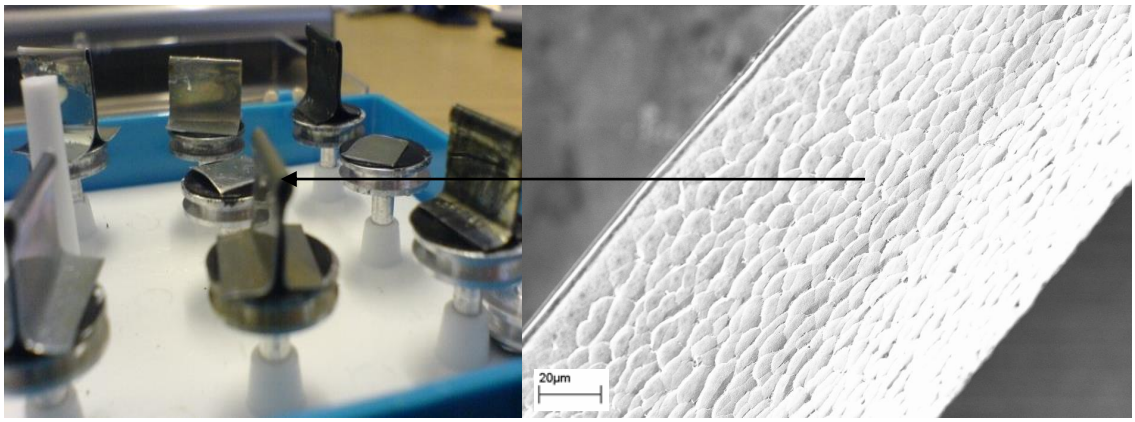

a b

Figure 4-11: *a: Image showing the mounting configuration for cryofractured sample. b: FEG-SEM image showing cryofractured surface in plan view.*

The sample was viewed from directly above the fractured surface (see Figure 4-13), a cross-section was then viewed from around the edge of the curved surface, where the coating and substrate could be viewed (see Figure 4-12a). The beam was then rotated to enable viewing of the coating at an angle parallel to the surface; Figure 4-12b shows an example of a typical cross-section of a conversion coating.

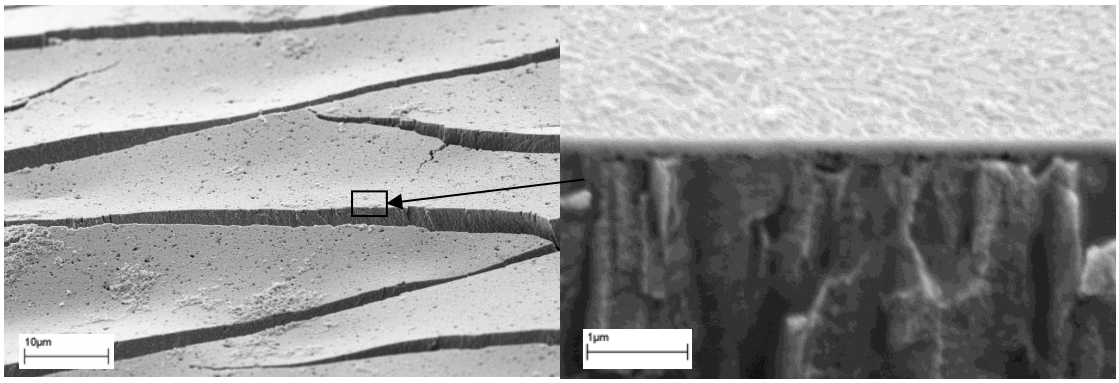

a b

Figure 4-12: *a: FEG-SEM image showing a crofractured surface. b: FEG-SEM image showing a typical cross-section.*

4.3.2 FEG-SEM Examination for Corrosion Nucleation Experiments

Samples were first prepared using the technique described in Section 4.1.4. They were then viewed using FEG-SEM to investigate any appearance of corrosion products, such

as pores, blisters and any de-lamination of the film. An example of a pore can be seen in Figure 4-13. The appearance of any corrosion products allowed for theories on the film breakdown modes to be made. This was also useful in improving the performance of subsequent coatings due to more knowledge about the breakdown characteristics.

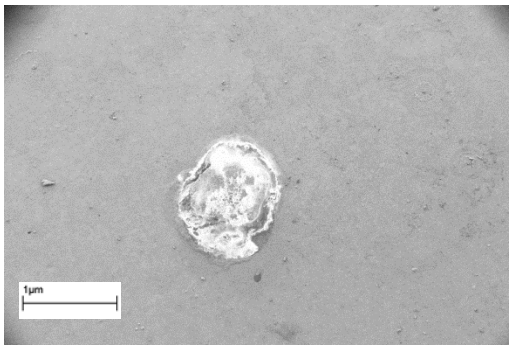

Figure 4-13: *FEG-SEM image showing a pore on a partially corroded sample.*

4.3.3 Focussed Ion Beam Scanning Electron Microscopy (FIBSEM) Technique for Cross-Sectional Investigation

Investigation was carried out using a FEI Nova 600 Nanolab Dualbeam FIB/FEG-SEM focussed ion beam electron microscope. Sample preparation was the same as for general FEG-SEM investigations. Each sample was viewed at a magnification to enable the surface morphology to be examined (typically around 20 000x). To protect the surface and produce a 'clean' edge for ion ablation; a cuboid of 10 x 1 x 0.5 µm of platinum was deposited on the surface by sputter coating (see Figure 4-14a). A rectangular section was then etched by bombardment of Ga^+ ions to a depth that would enable the thickness of the respective coating to be seen, typically from 1-10 µm (see Figure 4-14b). The cross-section was viewed by both electron and Ga^+ ion

imaging techniques in the secondary electron mode, the sample was tilted so that coating thickness could be recorded using the integrated computer software.

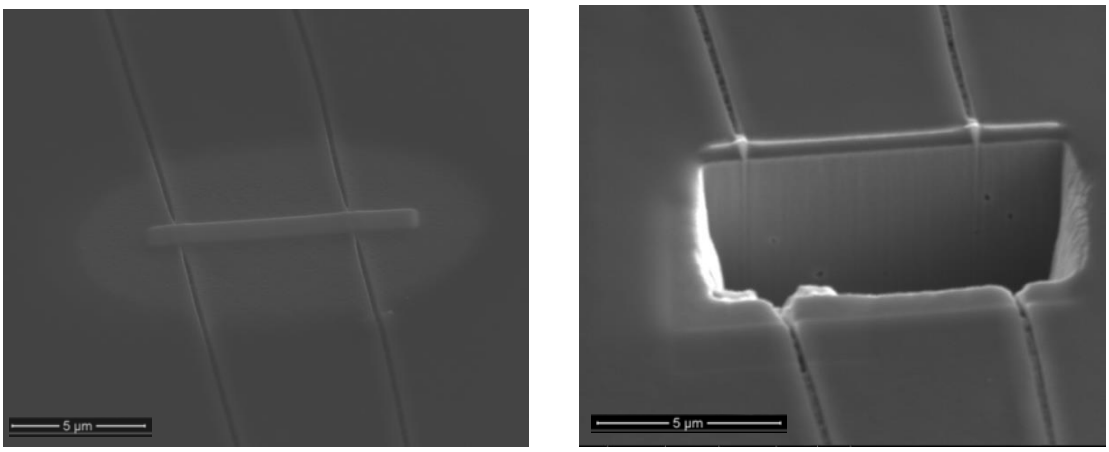

a b

Figure 4-14: *a: SE imaging mode micrograph showing a layer of Pt deposited on the surface of chromate conversion coated zinc surface. b: SE imaging mode micrograph showing the Ga^+ ion beam etched surface of a chromate conversion coated zinc surface for cross-sectional analysis.*

4.4 Sample Compositional Characterisation

4.4.1 Energy Dispersive X-Ray Analysis (EDXA)

The FEG-SEM used was also fitted with an Energy Dispersive X-Ray Analyser (EDXA), this is a useful technique because of its ability to detect the elemental composition of the surface. When the surface is irradiated with electrons, electrons are removed from their respective energy levels. The subsequent movement of an electron from a higher energy level to take the removed electron's place releases a characteristic amount of energy. This energy is emitted in the form of an X-ray and is detected by EDXA; this gives an elemental composition of the surface, with a sampling depth of ~1 µm and a sampling area that can be thought of to be a teardrop shape.

Specific features as well as broad representative areas were tested. An electron beam accelerating voltage of 20 keV was used so that a wide range of elements could be detected. EDXA was a useful and simple technique that could give a representation of the surface. But, because of its relatively high sampling depth and inability to give chemical information such as oxidation state, other techniques, such as AES and XPS were employed.

4.4.2 Auger Electron Spectroscopy (AES)

Auger Electron Spectroscopy (AES) is a surface analytical technique that can be used to determine the composition and chemical species present on a surface. The technique was developed in the 1960s and is named after the French scientist Pierre Auger, who discovered what became known as the Auger effect in the 1920s (Briggs and Sheah 1990).

The Auger effect is illustrated in Figure 4-15, the surface is subjected to a focussed beam of electrons which range in energy from 2 to 50 keV (Briggs and Sheah 1990), if the incident electron has enough energy, it can remove a K-energy level electron from the atom. This removal causes a shift in the electrons in the higher energy levels to fill the vacancy left by the removed electron in the K level. When an electron moves to a lower energy level, energy which is characteristic of the element is emitted, this can either be released as a photon (which is the basis of X-Ray Fluorescence) or it can be transferred to another electron at the same or higher energy level, which is then emitted. This emitted electron is termed the Auger electron and has a characteristic

energy and can be detected and used to give information on the surface composition. A schematic of the Auger electron emission process can be seen in Figure 4-15.

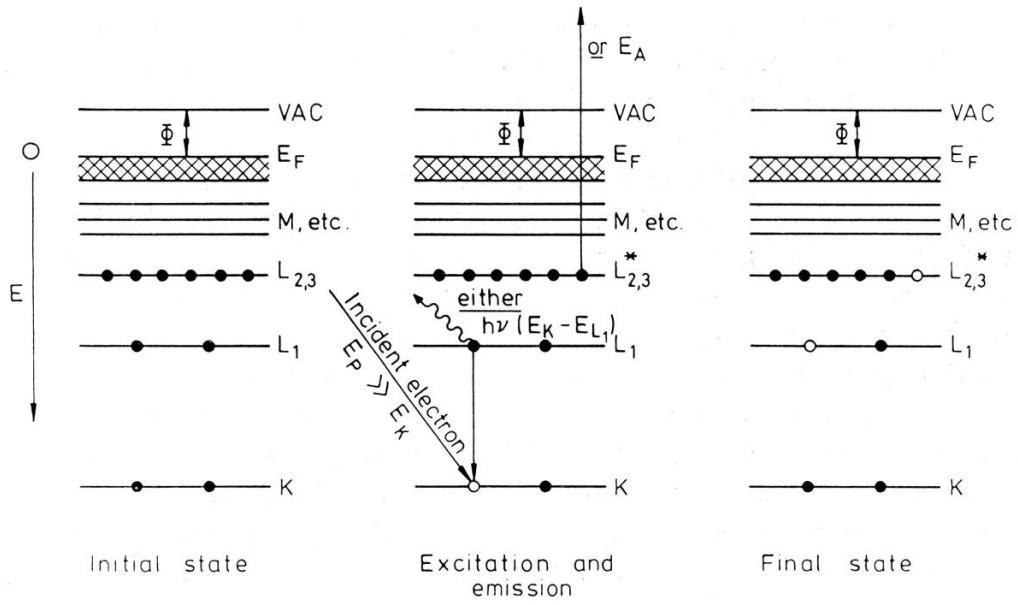

Figure 4-15: *Diagram illustrating the process of Auger electron emission (after Briggs and Sheah 1990).*

This technique can be used to detect elements from lithium (Z=3) to uranium (Z=92) in the periodic table.

4.4.2.1 AES Experimental Technique

Characterisation was carried out using an Auger Electron Spectrometer. Samples were cleaned using acetone and deionised water to remove surface contamination, coupons of 5 x 10 mm were cut from the samples and mounted into the sample holder. The chamber was then evacuated to approximately 1.0 x 10^{-9} torr, and spectra were taken.

4.4.2.2 AES Depth Profiling

The AES equipment used was fitted with an Ar^+ ion beam that was used to ablate the surface to allow depth profiling to be carried out. Spectra were taken at ion etching

times of 0, 20, 60, 120, 300 and 1200 s; this allowed the surface composition to be measured through the coating and coating substrate interface.

5 Results

5.1 DC Linear Polarisation Resistance

Experimental work was focussed on corrosion performance analysis, with the primary indicator being DC LPR. It was discussed in the literature review that the commonly used ASTM B 117 NSS test, was too aggressive an environment to be of use in determining small changes/ improvements in conversion coatings. LPR is a more sensitive technique and allowed small differences in corrosion performance of coatings to be detected.

Additives to the simple molybdate treatment solution were investigated in stages, with the most promising treatment parameters being carried forward to the next stage for further improvement. Additives selected were determined from the literature studied, with the rationale that further investigation of these could produce an enhanced molybdate-based coating system.

5.1.1 Simple Molybdate

Simple molybdate coatings were studied to give a baseline so that any improvements in corrosion resistance with subsequent treatments could be seen. The treatment conditions can be found in Table 5-1.

Table 5-1: Table showing the classification and treatment conditions for the simple molybdate conversion coatings.

Name	Na_2MoO_4 Conc. g. dm^{-3}	pH	Acid	Imm. Time (s)	Temp (°C)
Simple Molybdate	25	5	H_2SO_4	30, 60 and 120	25

Acid zinc samples were passivated with the simple molybdate solutions with immersion times of 30, 90 and 120 s. Immersion times of 30 s gave an iridescent finish. Whilst the finish has full surface coverage, its colouration is uneven. The lustrous finish of the substrate was also evident. During treatment, the coating was seen to change colour a number of times appearing blue/ grey after 10 s, then green, purple, yellow and gold, after 90 s they appeared brown, then lustrous black after 120 s then finally matt black after this time.

90 s immersion times were used to investigate whether a thicker, matt black coating as reported by a number of authors could be formed. The appearance of the samples treated for 90 s was darker than the MoS30 samples, the iridescent finish was maintained. There were also problems with adhesion, where part of the coating became detached during drying.

Immersion times of 120 s gave a dark black/ iridescent green/ purple coating, which still maintained some of the reflective properties of the original electrodeposited acid zinc surface. The coating did however suffer from poor adhesion, with some of the coating flaking off during rinsing and air drying. When subsequent samples were treated, more careful rinsing and drying was employed and this did ensure that the surface remained largely intact.

The Simple Molybdate samples generally showed highly cracked surfaces (see Figure 5-1a-c), with the frequency of these cracks increasing with immersion time. The appearance of pores is evident on the surface of all the simple molybdate treated samples, with longer immersion times leading to more porous surfaces.

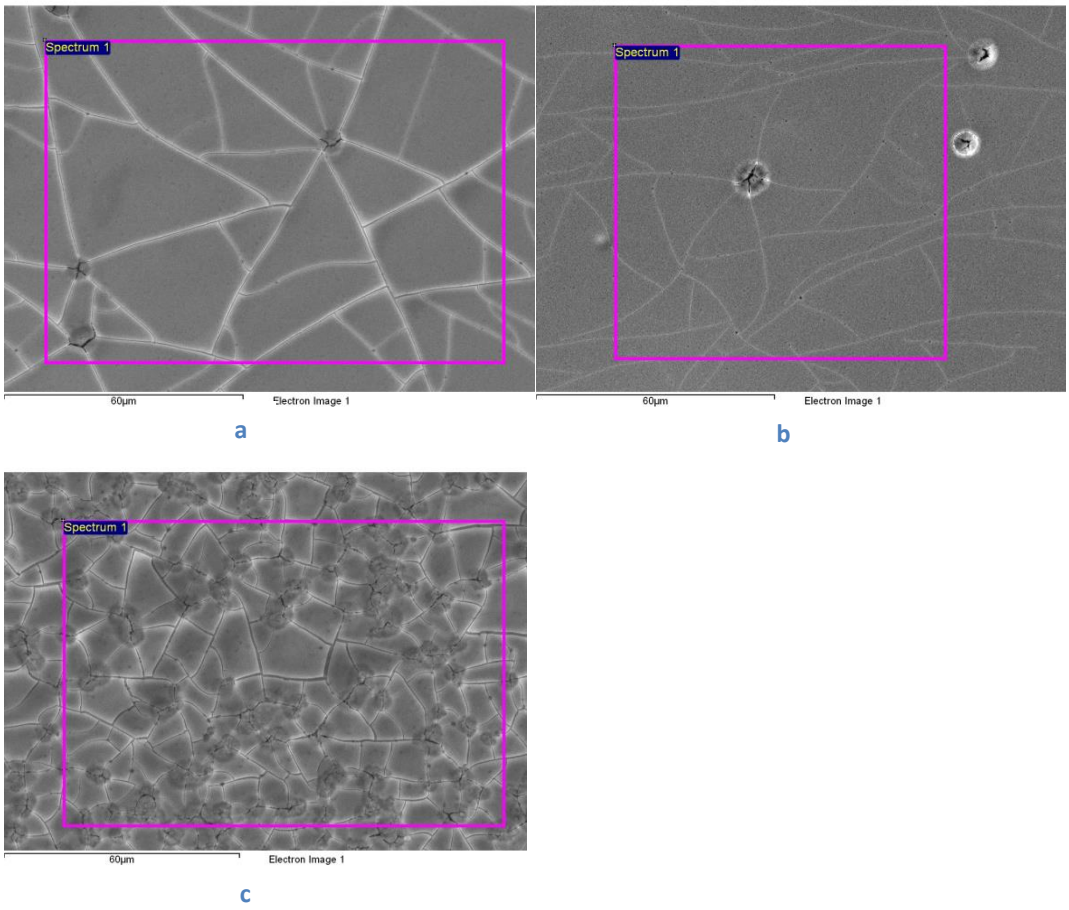

Figure 5-1: *a: Scanning electron micrograph of MoS30. b: Scanning electron micrograph of MoS90. c: Scanning electron micrograph of MoS120.*

5.1.2 Acids Used to Adjust pH

The work carried out by Magalhães *et al.* (2003) highlighted the importance of the acid used to adjust the pH on the characteristics of the coating achieved. Previous researchers have used a number of different acids to adjust the solution pH and these do seem to have had an effect on the nature of the coating attained. Sulphuric acid has been used by many authors from the late 1980s to present, namely, Wilcox *et al.* (1988, 1989), Wharton *et al.* (1996), Almeida *et al.* (1998) and more recently Lewis *et al.* (2006).

Nitric acid has been utilised by Treacy *et al.* (1999) and also as an additive in the 'MPSS' system proposed in 2006 by Song *et al.* Orthophosphoric acid has been used in to acidify molybdate baths for passivating steel surfaces by Kurusawa *et al.* (1989), as well as on zinc surfaces by Tang *et al.* (1994), Magalhães *et al.* (2003) and Rout and Bandyopadhyay (2007). Hydrochloric acid has not been reported to be used by authors in the literature studied, but, as another mineral acid, it was chosen to be investigated.

5.1.2.1 Acid Used to Adjust pH DC Polarisation Results

Immersion time, temperature and molybdate concentration were constant for the following tests, with the isolation of the acid used to adjust pH studied. An industrial chromate system ('CrVI') was also tested, using the same acid zinc samples and the results for LPR also included in Figure 5-2. Table 5-2 shows the treatment conditions for the coatings studied.

Table 5-2: Table showing the classification and treatment conditions for the named samples.

Name	Na_2MoO_4 Conc. g. dm^{-3}	pH	Acid	Imm. Time (s)	Temp (°C)
CrVI	200 ($NaCr_2O_7$)	1.2	HNO_3, 200 ml H_2SO_4	10	25
MoP120	25	5	H_3PO_4	120	25
MoN120	25	5	HNO_3	120	25
MoH120	25	5	HCl	120	25

5.1.2.2 Experimental Observations

It was clear that pH adjusting acid had a great effect on the appearance of the coatings formed. Sulphuric and hydrochloric acids gave black coatings with some iridescence,

adhesion was poor for these coatings, as they flaked off under contact. Nitric acid gave a blue coating with gold edges. Orthophosphoric acid gave coatings that retained the lustrous silver appearance of the substrate, with brown tinges at the edges. The chromate samples were typically iridescent where yellow and green colours could be seen.

5.1.2.3 LPR Results

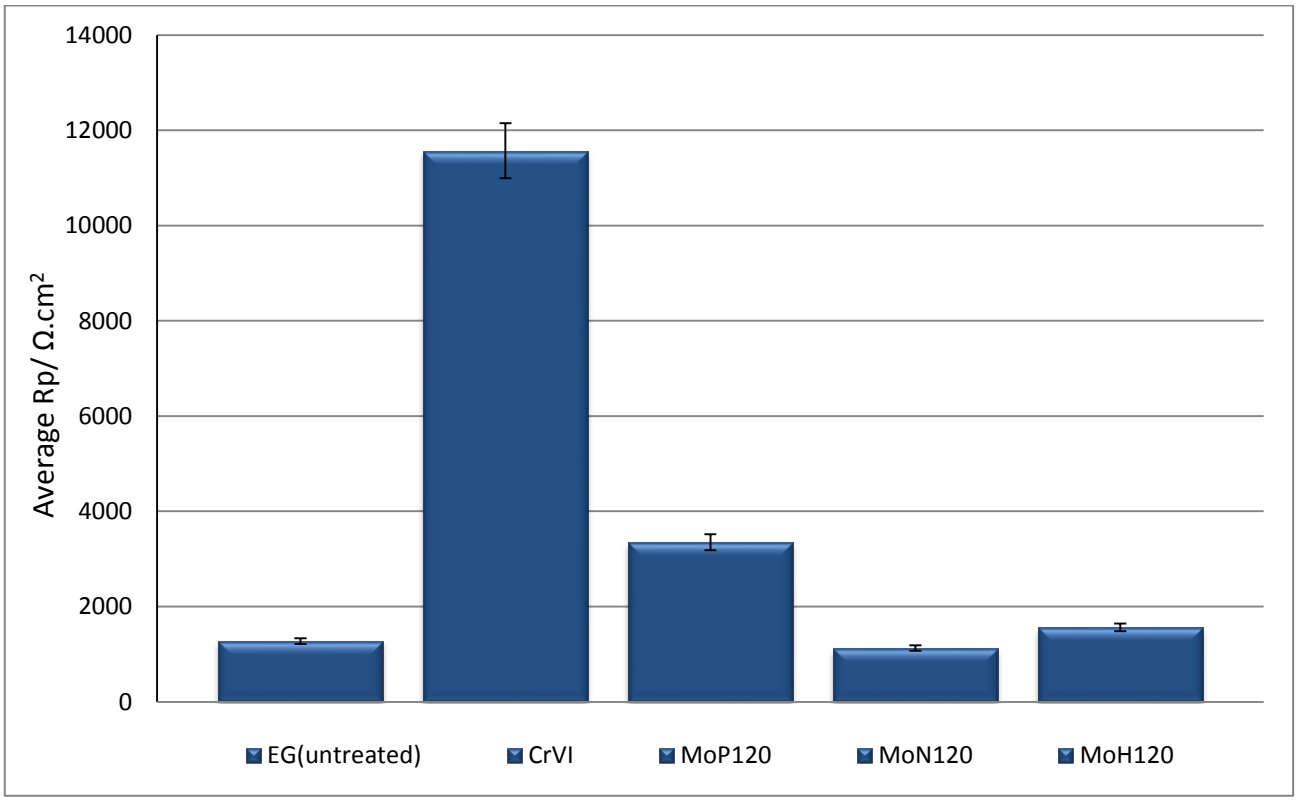

Figure 5-2: *Data showing the average linear polarisation resistance (LPR) of named samples.*

It can be seen from the data shown in Figure 5-2, that the acid used to adjust pH had a marked effect on the polarisation resistance of the coatings tested. Orthophosphoric acid gave coatings with the highest polarisation resistance. It was decided to carry out further investigations using this acid as the agent to reduce the solution pH.

5.1.3 Immersion Time

The rationale for investigating the effect of immersion time was highlighted in Section 2.1.19 in the literature review, where treatment times of 10 to 600 s were investigated by the authors named in Table 2-3. It is thought that coating thickness is broadly proportional to immersion time, up to a point where diminishing gains are seen (Gabe and Gould 1988). It was seen from the selection of acid used that the coating formation rate from the molybdate/ H_3PO_4 treatments was relatively low, so in order to increase thickness, immersion times of up to 600 s were trialled. Table 5-3 shows the treatment conditions of the samples tested.

Table 5-3: Classification and treatment conditions for molybdate/ H_3PO_4 treated samples.

Name	Na_2MoO_4 Conc. g. dm^{-3}	pH	Acid	Imm. Time (s)	Temp (°C)
Mo5P30	25	5	H_3PO_4	30	25
Mo5P60	25	5	H_3PO_4	60	25
Mo5P90	25	5	H_3PO_4	90	25
Mo5P120	25	5	H_3PO_4	120	25
Mo5P180	25	5	H_3PO_4	180	25
Mo5P300	25	5	H_3PO_4	300	25
Mo5P600	25	5	H_3PO_4	600	25

5.1.3.1 Experimental Observations

Coatings generally appeared silver with brown tinges, analogous to similar coatings described previously. Increase in immersion time led to more brown tinges at the edges of the samples and a slightly darker silver overall colouration.

5.1.3.2 LPR Results

The LPR results from this stage are shown in Figure 5-3. It can be see that LPR is increased with immersion time up to 120 s, with a decrease being seen at the longer immersion times.

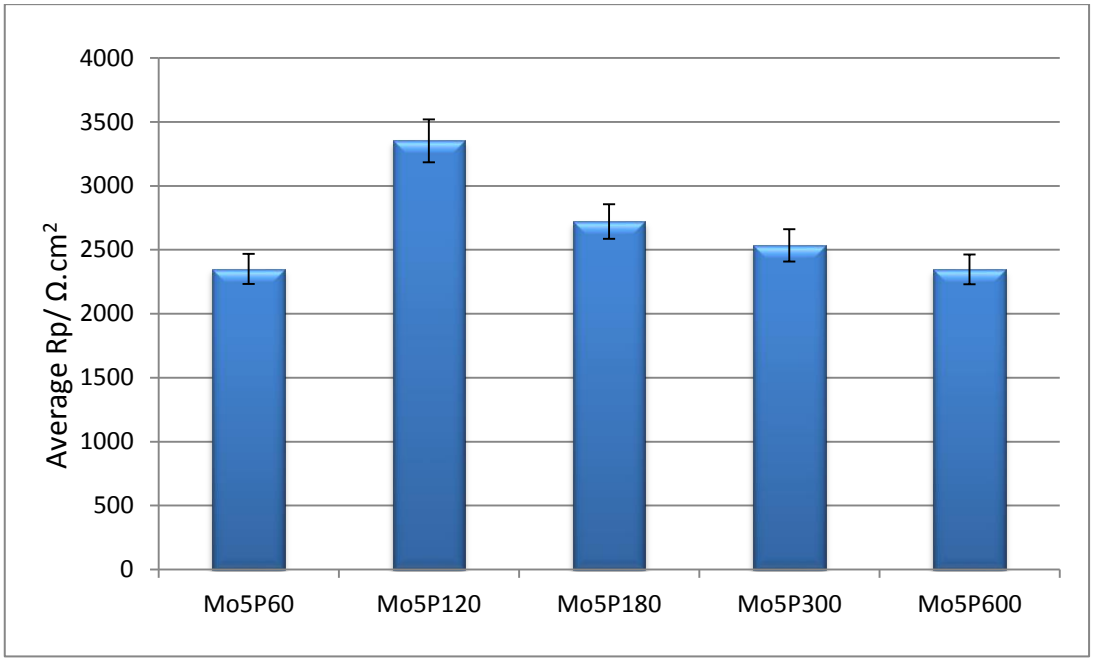

Figure 5-3: *Data showing the average LPR of molybdate/ H_3PO_4 treated samples.*

From these results 120 s was considered the optimum immersion time to be used with subsequent variables in the investigation.

5.1.4 Solution pH

Solution pH has been found to have a great effect on the performance and appearance of molybdate and indeed most, conversion coatings. Detailed information about other authors' observations of the effects of changing solution pH can be found in Section 2.1.23. Lower pHs have been reported to give an increased coating formation rate. In the case of conversion coatings this is not always desirable, because thicker coatings

are not always well adhered and free of porosity. The treatment solution must be acidified to enable the coating process to take place, therefore acidic pHs were used. The lowest pH selected was 2.5, as authors have found that substrate etching occurs below this pH. Many authors have reported either pH 3 or 5 to give the coating with optimum properties. Because of this rationale, pHs of 2.5, 3, 4 and 5 were tested. The treatment conditions can be found in Table 5-4.

Table 5-4: Classification and treatment conditions for molybdate/ H_3PO_4 treated samples.

Name	Na_2MoO_4 Conc. g. dm^{-3}	pH	Acid	Imm. Time (s)	Temp (°C)
Mo2.5P120	25	2.5	H_3PO_4	120	60
Mo3P120	25	3	H_3PO_4	120	60
Mo4P120	25	4	H_3PO_4	120	60
Mo5P120	25	5	H_3PO_4	120	60
Mo6P120	25	6	H_3PO_4	120	60

5.1.4.1 Experimental Observations

Coatings generally appeared lustrous silver with a brown colour being present at the edges. Coatings from the lower pHs (2.5 and 3) appeared duller, with a predominantly grey surface appearance.

5.1.4.2 LPR Results

The values gained for average LPR can be found in Figure 5-6. The results show a trend of increasing LPR with pH to pH 5.0 and then a decrease at pH 6.

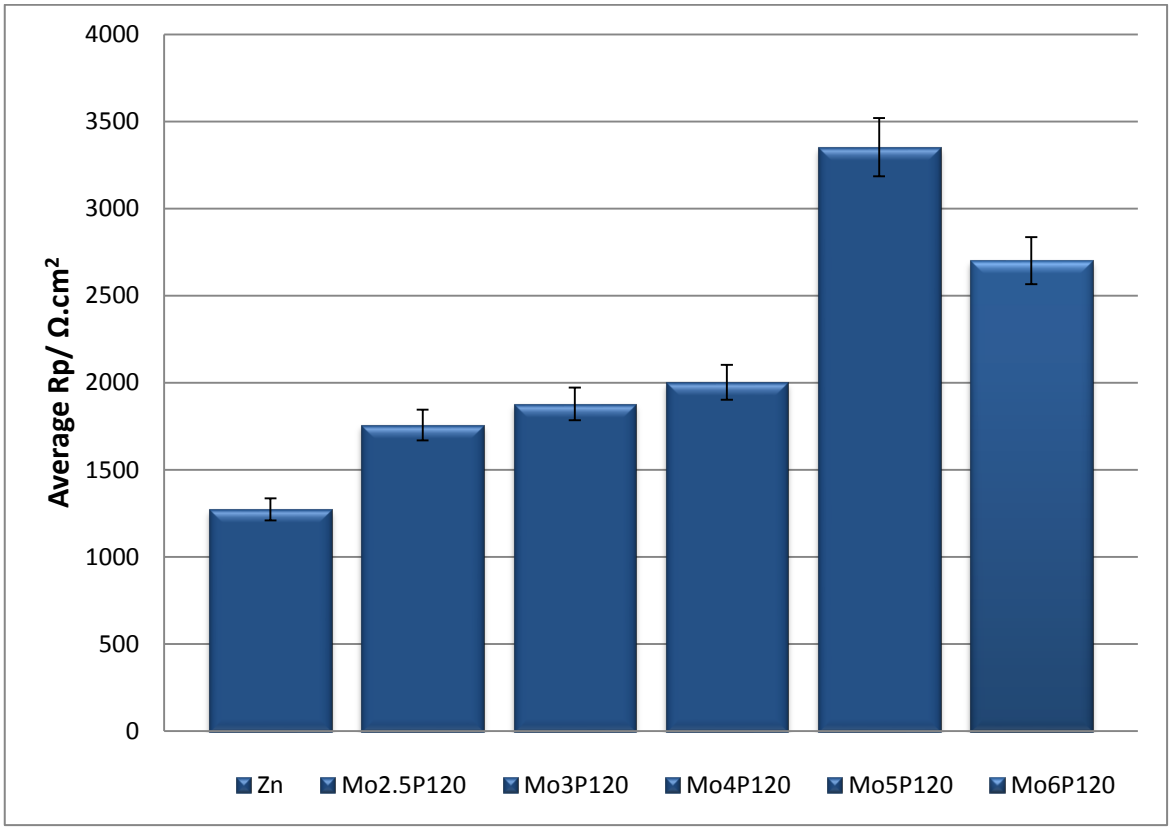

Figure 5-4: *Graph showing the average LPR of named samples.*

From these results it was clear the pH 5 offered the largest enhancements in corrosion resistance, this is in agreement with the majority of authors who used pH as a variable (Treacy *et al.* 1999, Wharton *et al.* 1999, Almeida *et al.* 1998, Rout *et al.* 2007). Subsequent experimental investigations were based on solutions at pH 5.

5.1.5 Additives

Additives investigated were determined from the literature studied in the literature review. Phosphate was added as a heteropolymolybdate former, it was added as sodium orthophosphate, $Na_3PO_4.12H_2O$ at a concentration of 90 g dm^{-3} (Tang *et al.* 1994, Boose *et al.* 2001, Song and Mansfeld 2006). Nitrate was added as an oxidising

agent, in the form of HNO_3, or sodium nitrate, $NaNO_3$ (the solution pH was not effected) (Song and Mansfeld 2006). The rationale for the addition of an oxidising agent was the chromate anion is known to have a strong oxidising potential, whereas the molybdate anion does not, therefore they do not easily form reduction and oxidation products on the surface (hence longer immersion times being commonplace), therefore compounds to increase the oxidising 'power' of the treatment solution were tested.

Sodium gluconate, $NaC_6H_{11}O_7$, was added as a complexant, because it was found by Boose and co-workers that it was successful at increasing the corrosion resistance of a similar coating system (2001). Also investigated was an increase in molybdate concentration from 25 to 60 g cm^{-3}, because of positive results seen in work carried out by Song and Mansfeld (2006). Treatment conditions and sample names can be seen in Table 5-5

Table 5-5: Sample classification and treatment conditions for named additives used in DC LPR trials.

Name	Na_2MoO_4 Conc. g. dm^{-3}	pH	Acid	Additive 1 (g . dm^{-3})	Imm. Time (s)	Temp (°C)
40Guc	25	5	H_3PO_4	40 Sodium gluconate	120	60
10HNO3	25	5	H_3PO_4	10 HNO_3	120	60
10NaNO3	25	5	H_3PO_4	10 $NaNO_3$	120	60
90PO4	25	5	H_3PO_4	90 Na_3PO_4	120	60
60Mo	60	5	H_3PO_4	N/A	120	60

5.1.5.1 *Experimental Observations*

The increase in molybdate concentration had the effect of making the coatings appear dark blue/ brown. Iridescence was seen on the surfaces of gluconate, phosphate and nitric acid additive treatments, with 40Gluc and 90PO4 appearing gold and purple. Samples 10HNO3 and 10NaNO3 appeared green and purple with dark brown edges.

5.1.5.2 *LPR Results*

The Figure, 5-5 shows the results gained from the polarisation resistance tests.

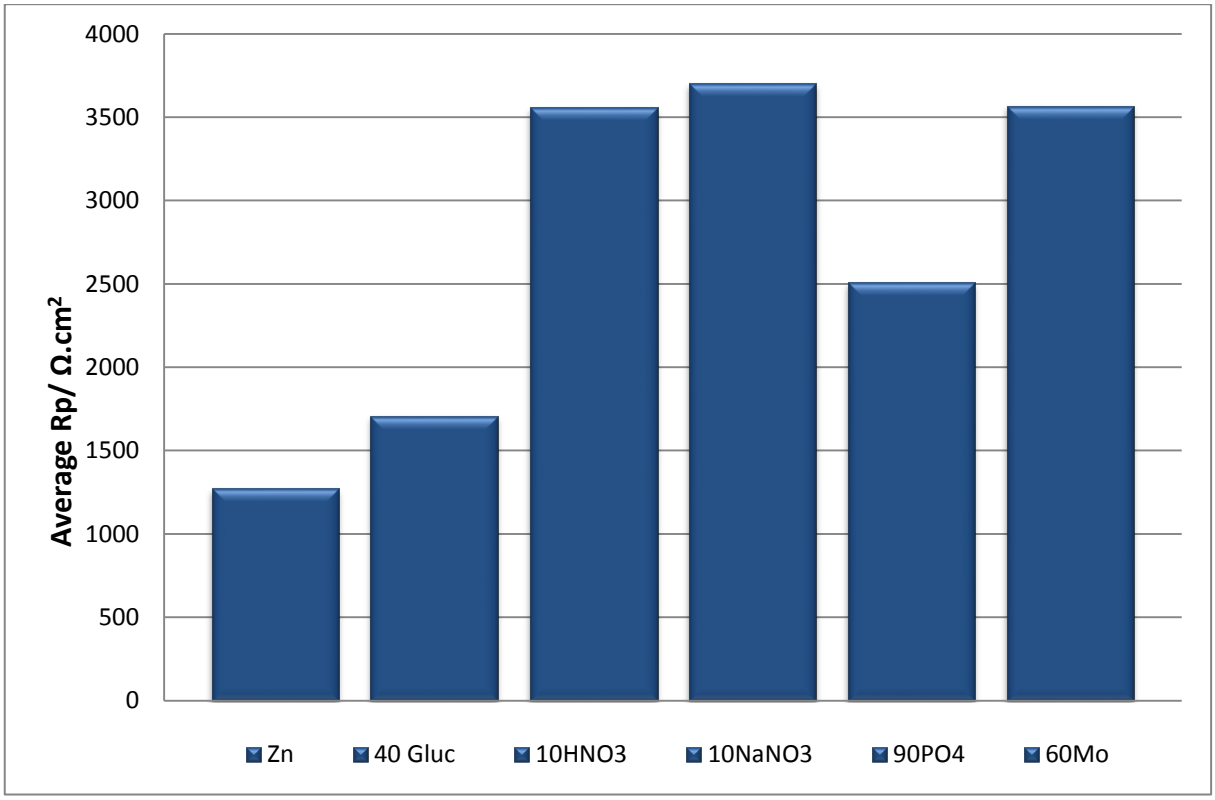

Figure 5-5 : *Data showing the average LPR of samples with the named additives.*

All treatment solutions offered increased protection over the Zn substrate. Significant increases in polarisation resistance over Mo5P120 system (3 350 $\Omega.Cm^2$) were seen with the addition of 10 g dm^{-3} $NaNO_3$ and increasing the sodium molybdate

concentration to 60 g dm^{-3}. Additions of sodium gluconate and Na_3PO_4, showed decreased polarisation resistance over the Mo5P120 system.

Because of the increase in corrosion resistance seen with increasing the molybdate concentration to 60 g dm^{-3}, this was used for subsequent experiments. The next stage of investigation was to determine whether these additives could confer higher corrosion resistance when used synergistically. They were therefore tested in combinations and the effects of this measured. The treatment conditions and sample naming can be found in Table 5-6.

Table 5-6: Data showing sample classification and treatment conditions for named additives

Name	Na_2MoO_4 Conc. g. dm^{-3}	pH	Acid	Additive 1 (g . dm^{-3})	Additive 2 (g . dm^{-3})	Additive 3 (g . dm^{-3})	Imm. Time (s)	Temp (°C)
60MoNo3	60	5	H_3PO_4	10 $NaNO_3$	N/A	N/A	120	60
60MoNO3PO4	60	5	H_3PO_4	10 $NaNO_3$	90 Na_3PO_4	N/A	120	60
60MoNO3Gluc	60	5	H_3PO_4	10 $NaNO_3$	40 Sodium gluconate	N/A	120	60
60MoNO3PO4 Gluc	60	5	H_3PO_4	10 $NaNO_3$	90 Na_3PO_4	40 Sodium gluconate	120	60

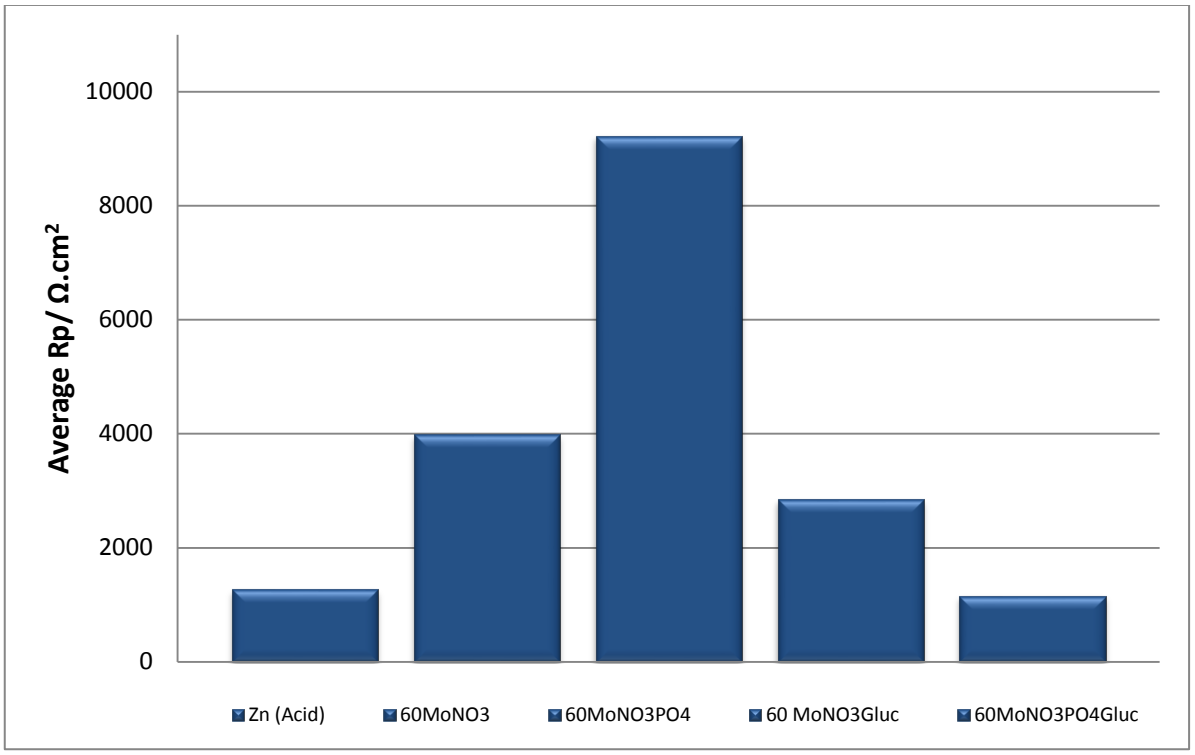

Figure 5-6: *Data showing the average LPR of named samples.*

The data shown in Figure 5-6 shows that with nitrate and phosphate additions, the average LPR values were much higher than those previously found. This was a very encouraging result, being significantly higher than comparable molybdate systems studied. The addition of gluconate species decreased the corrosion resistance to a level similar to the substrate alone.

For further analysis, the 60MoNO3PO4 system was termed 'MoP', for ease of determination of subsequent improvements as an improved molybdate-phosphate system.

5.1.6 Investigation of Enhanced Coatings without the Addition of Molybdate

It became apparent from the results obtained from AES, determining the atomic composition of the MoP type coating, that there was a fairly small amount of molybdenum (4 at. %) present in the coating. To determine whether the Mo present in the coating lead to an increase in corrosion resistance, a coating system was made, without the addition of molybdate. Table 5-7 shows the composition of this treatment solution.

Table 5-7: Data showing the treatment conditions for the named coating.

Name	Na_2MoO_4 Conc. g. dm^{-3}	pH	Acid	Additive 1 (g . dm^{-3})	Additive 2 (g . dm^{-3})	Imm. Time (s)	Temp (°C)
NP	N/A	5	H_3PO_4	10 $NaNO_3$	90 Na_3PO_4	120	60

The coating was similar in appearance to the MoP treated sample, appearing grey and homogeneous. FEG-SEM investigation showed the coating to be porous and have a crystalline structure. LPR testing was carried out on the coatings, these showed only a slight improvement over the untreated electrodeposited Zn surface and offered much lower corrosion resistance than the MoP samples (see Figure 5-9).

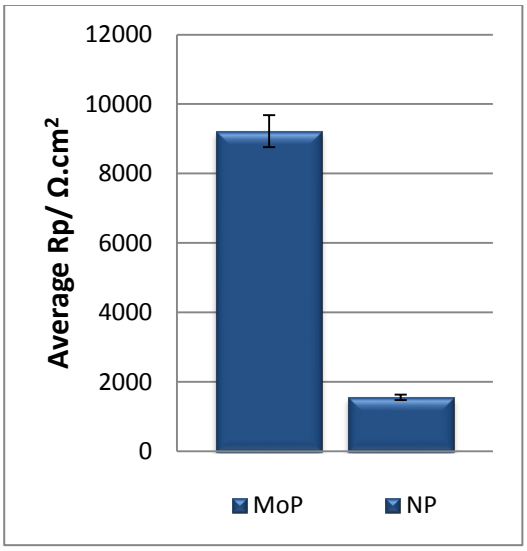

Figure 5-7: *Data showing the values for LPR for the named coatings.*

5.1.7 Silica and Silicate Additives

Silica and silicate were studied as additives to the improved 'MoP' system. Silica was colloidal and 5 nm in diameter. Sodium metasilicate was used at a concentration of 50 $g.dm^{-3}$ to mirror the work carried out by Song and Mansfeld in 2006. Nano-sized colloidal silica was used due to its efficacy in work carried out by Thiery and Pommier (2004) when used as a sealant for conversion coatings. Hara *et al.* (2003), used colloidal silica to produce a thick (> 5 µm), corrosion resistant conversion coating.

One and two stage processes were used, which would produce a silica rich coating or topcoat. It was also found that when sodium silicate was added to the acidified solution it would gelatinise, therefore it was used as a second solution to add a topcoat. The formulations listed in Table 5-8 were used.

Table 5-8: Table showing the treatment conditions and classification for silica and silicate coated samples.

Name	Na_2MoO_4 Conc. g dm^{-3}	pH	Acid	Additive 1 (g dm^{-3})	Additive 2 (g dm^{-3})	Additive 3 (g dm^{-3})	2nd Stage Treatment	Imm. Time (s)	Temp (°C)
MoP50Si	60	5	H_3PO_4	10 $NaNO_3$	90 Na_3PO_4	50 5 nm SiO_2	N/A	120	60
MoP50Silicate	60	5	H_3PO_4	10 $NaNO_3$	90 Na_3PO_4	50 Na_2SiO_3	N/A	120	60
MoP+MoP50Silicate	60	5	H_3PO_4	10 $NaNO_3$	90 Na_3PO_4	N/A	120 s MoP50Silicate	240	60
MoP20Si	60	5	H_3PO_4	10 $NaNO_3$	90 Na_3PO_4	20 5 nm SiO_2	N/A	120	60

5.1.7.1 Experimental Observations

Acidification increased the viscosity of the silicate containing solution to the point where it was gelatinised after a short period of time. Coatings from nano-colloidal silica treatments appeared dark grey, whereas silicate additions led to more of a blue iridescence. A white sediment was formed overnight when nano colloidal silica was used at 50 g dm^{-3}, because of this it was decided to decrease the silica concentration to 20 g dm^{-3}. White sediment did not form at this lower concentration.

A two stage process 'MoP+50silicate', was investigated, with the view to adding an outer layer of a silicate rich molybdate film to an inner MoP (molybdate-phosphate) conversion coating. This was not successful because the LPR was actually decreased over the MoP coating alone. All of the coatings gave an increase over the Zn substrate, the LPR results can be found in Figure 5-8.

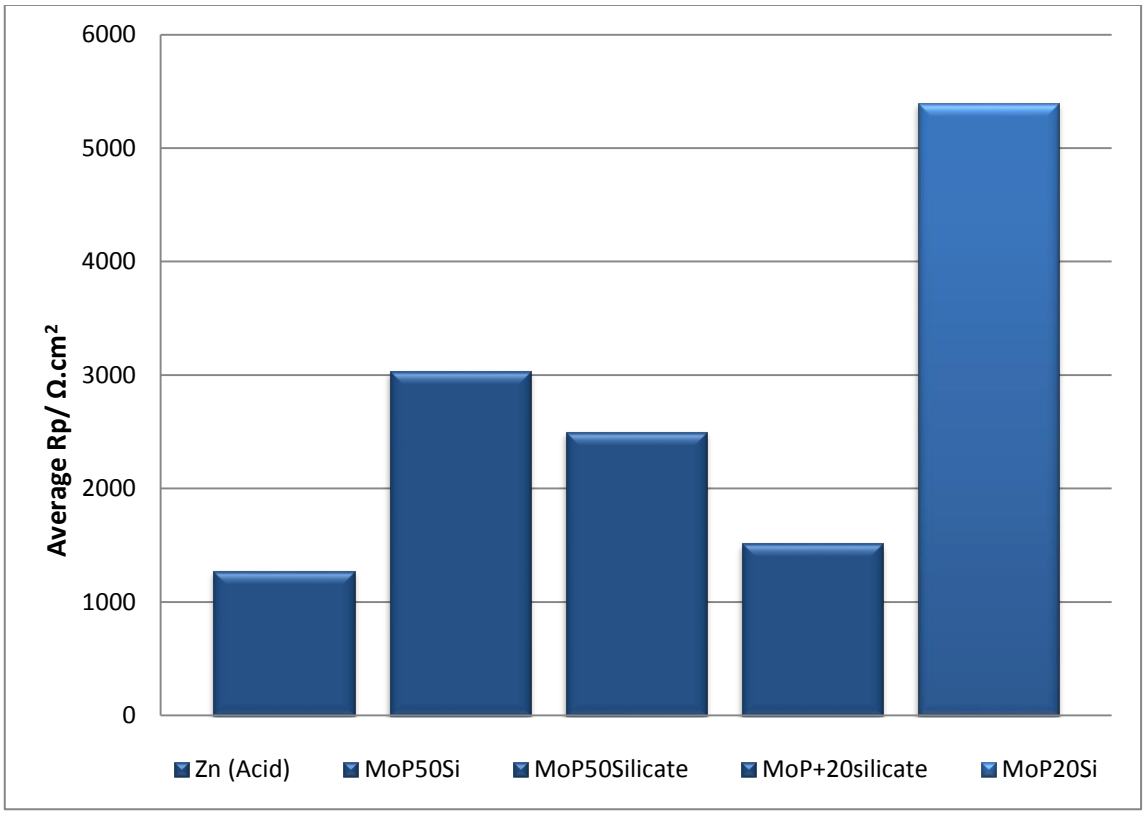

Figure 5-8: *Data showing the LPR values for the named treatments with silica and silicate additives.*

The highest performing silca or silicate coating was MoP20Si, this coating was investigated further, this is described in the relevant sections; being referred to as 'MoPSi'.

5.1.8 Cobalt Additives

Investigation was carried out into cobalt additives, primarily because of work carried out by Meyers *et al.* (1994), where a cobalt and molybdenum based conversion coating's efficacy as a chromate replacement was described. Cobalt has also been used as an additive for Cr(III) based systems, where it is thought to be a catalyst to the surface reactions producing thicker trivalent chromium coatings (Crotty 1981). Co(II) is also capable of forming heteropolymolybdates in solution (Stiefel 2001).

Cobalt nitrate was selected as this is analogous with an industrially used Cr(III) system this was added to the highest performing MoP system and investigated at immersion times of 30, 60 and 120 s at 60 °C. The naming convention for the samples can be seen in Table 5-9.

Table 5-9: Table showing sample classification for cobalt nitrate additions.

Name	Na2MoO4 Conc. g. dm-3	pH	Acid	Additive (g . dm-3)	Imm. Time (s)	Temp (°C)
MoPCo30	25	3	H_3PO_4	7.5 $Co(NO_3)_2$	30	60
MoPCo60	25	3	H_3PO_4	7.5 $Co(NO_3)_2$	60	60
MoPCo120	25	3	H_3PO_4	7.5 $Co(NO_3)_2$	120	60

5.1.8.1 Experimental Observations

The addition of cobalt nitrate gave the solution a purple colour with a blue precipitate at pH 7.0, as the pH was reduced to pH 5.0, the precipitate started to dissolve, this did not fully dissolve with heating, therefore the pH was reduced until the precipitate dissolved, this occurred at pH 3.0, where the solution was a clear pink colour. Therefore treatment was carried out at this pH. Three treatment times were used, mainly because of the reported catalysing effect of cobalt possibly leading to a higher coating rate.

Coatings appeared light brown with a 30 s treatment time with more of a prominence of dark brown to black at the longer immersion times.

The coatings were subjected to LPR tests, the results of these tests can be seen in Figure 5-9.

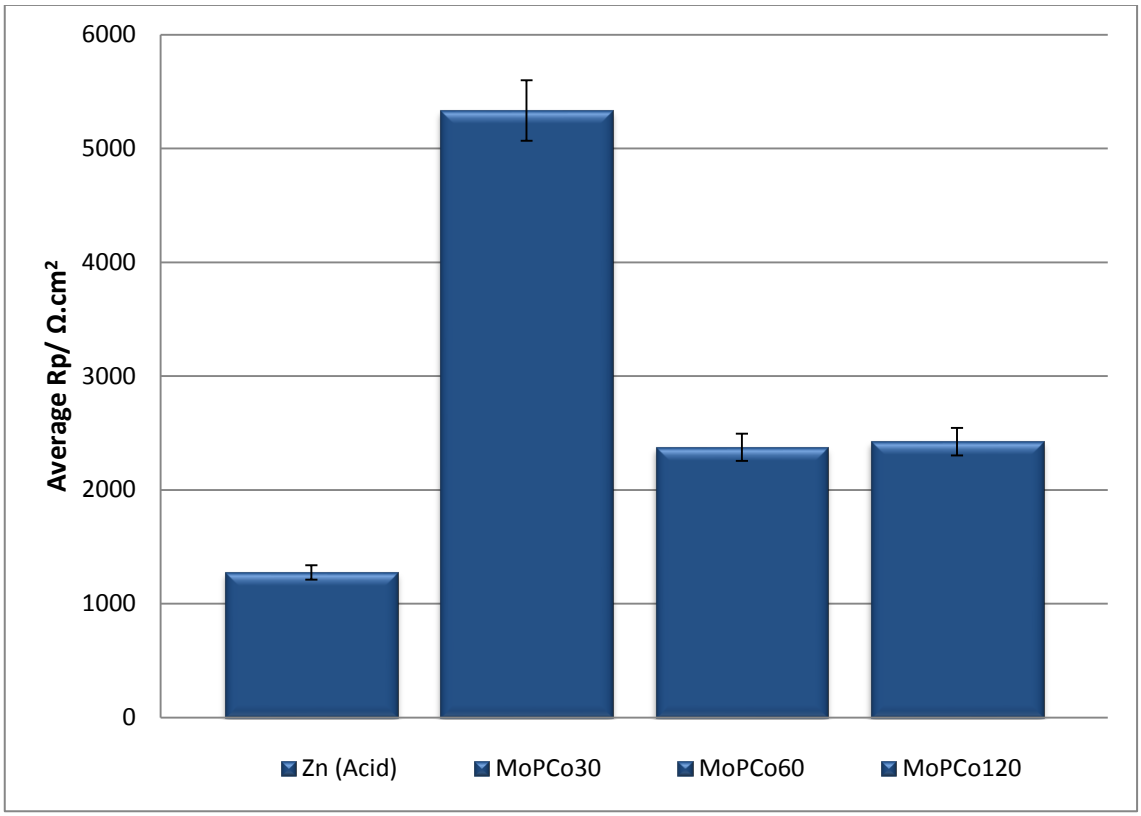

Figure 5-9: *Graph showing LPR results for named coatings with cobalt nitrate additions.*

The results show the LPR values at 30 s immersion to be significantly higher than the longer immersion times. Further research into Co additives was curtailed due to Co(II) species being classified as a class 2 R49 carcinogen, known to cause cancer by inhalation and are listed in annex I of directive 67/548/EEC (1967).

5.1.9 Silicate Sealants

Two silicate sealant systems were investigated, each to impart a layer of silicate onto the molybdate coating to enhance corrosion resistance analogous to early Cr(III) systems (Bibber 2008). Two systems were studied, the first, adapted from a patent for sealing a Cr(VI) conversion coating system, filed by Maiquez in 1993, US Patent number 5178690, termed 'silicate-1'. The second being adapted from work on sealing

a zinc phosphate conversion coating published by Lin and co-workers (2008), this is termed 'silicate-2'. Table 5-10, shows the treatment formulations for the named coating systems.

Table 5-10: Table showing sample classification and treatment conditions for silicate sealed, molybdate coatings.

Name	Na_2MoO_4 Conc. g. dm^{-3}	pH	Acid	Additive 1 (g . dm^{-3})	Additive 2 (g . dm^{-3})	Additive 3 (g . dm^{-3})	2nd Stage Treatment	Imm. Time (s)	Temp (°C)
MoP-S1	60	5	H_3PO_4	10 $NaNO_3$	90 Na_3PO_4	N/A	Silicate-1	120+60	60
MoP-S2	60	5	H_3PO_4	10 $NaNO_3$	90 Na_3PO_4	N/A	Silicate-2	120+600	60
MoPSi-S1	60	5	H_3PO_4	10 $NaNO_3$	90 Na_3PO_4	20 SiO_2 (nano)	Silicate-1	120+60	60
MoPSi-S2	60	5	H_3PO_4	10 $NaNO_3$	90 Na_3PO_4	20 SiO_2 (nano)	Silicate-2	120+600	60
S1	N/A	N/A	N/A	Silicate 1	N/A	N/A	N/A	120	25
S2	N/A	N/A	N/A	Silicate 2	N/A	N/A	N/A	120	25

Silicate 1:

- 200 g dm^{-3} sodium silicate
- 0.3 g dm^{-3} sodium carbonate
- 3 g dm^{-3} sodium fluoride
- 60 s immersion

Silicate 2:

- 5 g dm^{-3} sodium silicate
- 85 °C
- 600 s immersion

LPR Results can be seen in Figure 5-10.

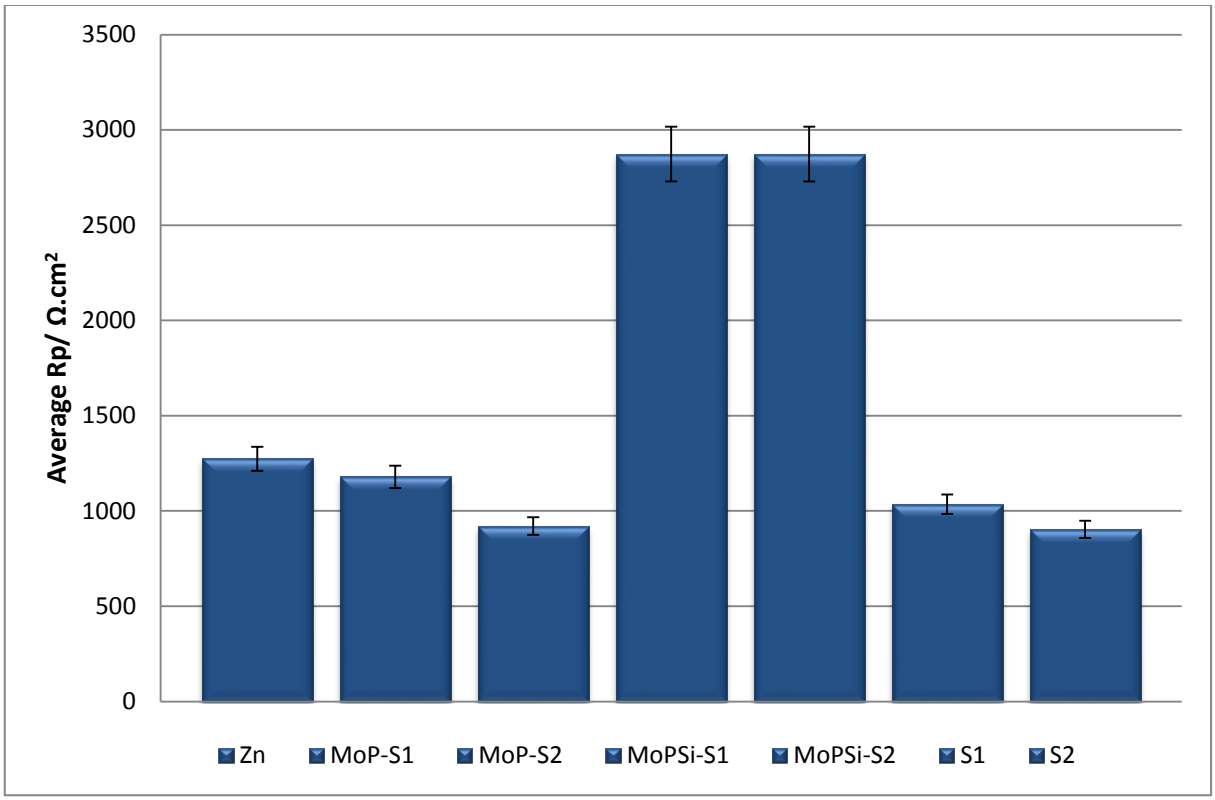

Figure 5-10: *Data showing the LPR for the named coatings on Zn surfaces.*

The data shown in Figure 5-12 shows that the MoP system had LPR levels decreased to below the substrate alone, whilst the MoPSi system did not show as much of a decrease, the values are still significantly lower than those of the MoPSi system alone.

Silicate sealants were investigated on the untreated Zn substrate as a control. These coatings were termed S1 and S2, relating to their respective silicate sealant systems used. Their visual appearance and corrosion resistances were similar to the coatings formed over conversion coatings.

5.1.10 Rare Earth Metal Systems

Rare earth metal (REM) coatings were investigated with a view to evaluating whether they could be incorporated into a composite molybdate/ REM system. REM coatings

were investigated primarily to give a baseline to compare any composite coatings to in the future.

There has been increased interest in REM nitrate and chloride compounds for producing conversion coatings on Zn, Mg and Al surfaces (See Section 1.5.1). REM coatings with no other additives based on those proposed by Rudd *et al.* (2000) and Hosseini *et al.* (2007), (based on cerium and lanthanum nitrates ($Ce(NO_3)_3$ and $La(NO_3)_3$) at a concentration of 50 $x10^{-3}$ M) were investigated. Treatment times studied by authors generally ranged from 10 s to 1 day (see Table 1-4). Promising results were found using simple immersion for only 7 minutes at room temperature (Hosseini *et al.* 2007), so this treatment condition was investigated.

Details of sample naming and treatment conditions can be found in Table 5-11.

Table 5-11: Data showing the treatment conditions for the named samples.

Name	Na_2MoO_4 Conc. g. dm^{-3}	pH	Acid	Additive (g . dm^{-3})	Imm. Time (s)	Temp (°C)
CeNO3 RTP	N/A	7	N/A	21.7 $Ce(NO_3)_3$	420	25
CeNO3 50C	N/A	7	N/A	21.7 $Ce(NO_3)_3$	420	50
LaNO3 RTP	N/A	7	N/A	21.6 $La(NO_3)_3$	420	25
LaNO3 50C	N/A	7	N/A	21.6 $La(NO_3)_3$	420	50

5.1.10.1 Experimental Observations

Room temperature cerium nitrate coatings appeared silver with brown staining, lanthanum nitrate coatings had much more of brown coverage and even colouration. At 50 °C, cerium nitrate coatings had an even coverage of a blue/ light brown colour, lanthanum nitrate coatings appeared around 50 % silver and 50 % dark brown.

5.1.10.2 LPR Results

The LPR results can be found in Figure 5-11.

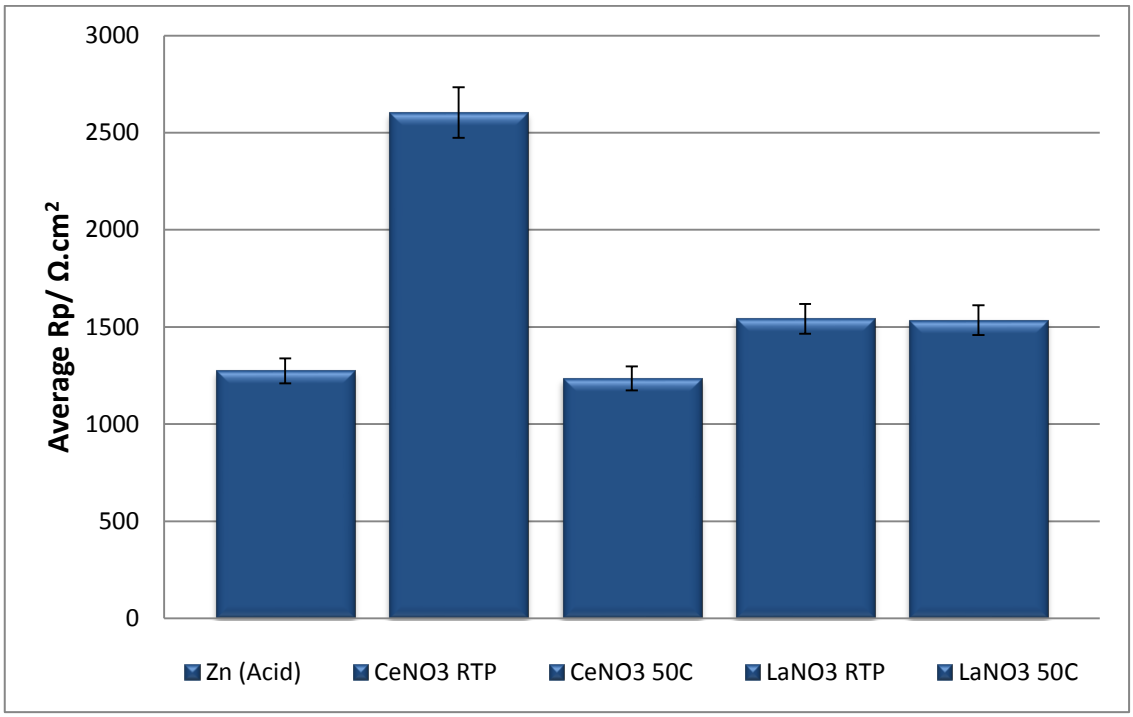

Figure 5-11: *Data showing the LPR values for the named coatings.*

Data in Figure 5-11 shows that the cerium nitrate coating at room temperature produced the only significant increase in LPR over an uncoated electrodeposited zinc coatings. Other coatings offered only small enhancements in corrosion resistance.

5.1.11 Rare Earth Metal and Molybdate Dual Layer Systems

Dual layer coatings were investigated consisting of a two stage process of REM/ molybdate. Two stage processes were necessitated because of the very poor solubility of REM nitrate in the molybdate treatment solution. Molybdate treatments were based on the improved 'MoP' system. The treatment conditions can be found in Table 5-12.

Table 5-12: Data showing the treatment conditions for the named molybdate/ REM coatings.

Name	Na_2MoO_4 Conc. g. dm^{-3}	pH	Acid	Additive (g . dm^{-3})	2nd Stage Treatment	Imm. Time (s)	Temp (°C)
CeNO3 RTPMo	N/A	7	N/A	2.17 $Ce(NO_3)_3$	MoP	420	25/ 60
CeNO3 50CMo	N/A	7	N/A	2.17 $Ce(NO_3)_3$	N/A	420	50/ 60
LaNO3 RTPMo	N/A	7	N/A	2.16 $La(NO_3)_3$	MoP	420	25/ 60
LaNO3 50CMo	N/A	7	N/A	2.16 $La(NO_3)_3$	MoP	420	50/ 60

5.1.11.1 Experimental Observations

Coatings were generally similar in appearance, with the prominence of iridescence similar to the 'MoP' type coatings although a little lighter.

5.1.11.2 LPR Results

The results from LPR testing can be found in Figure 5-12.

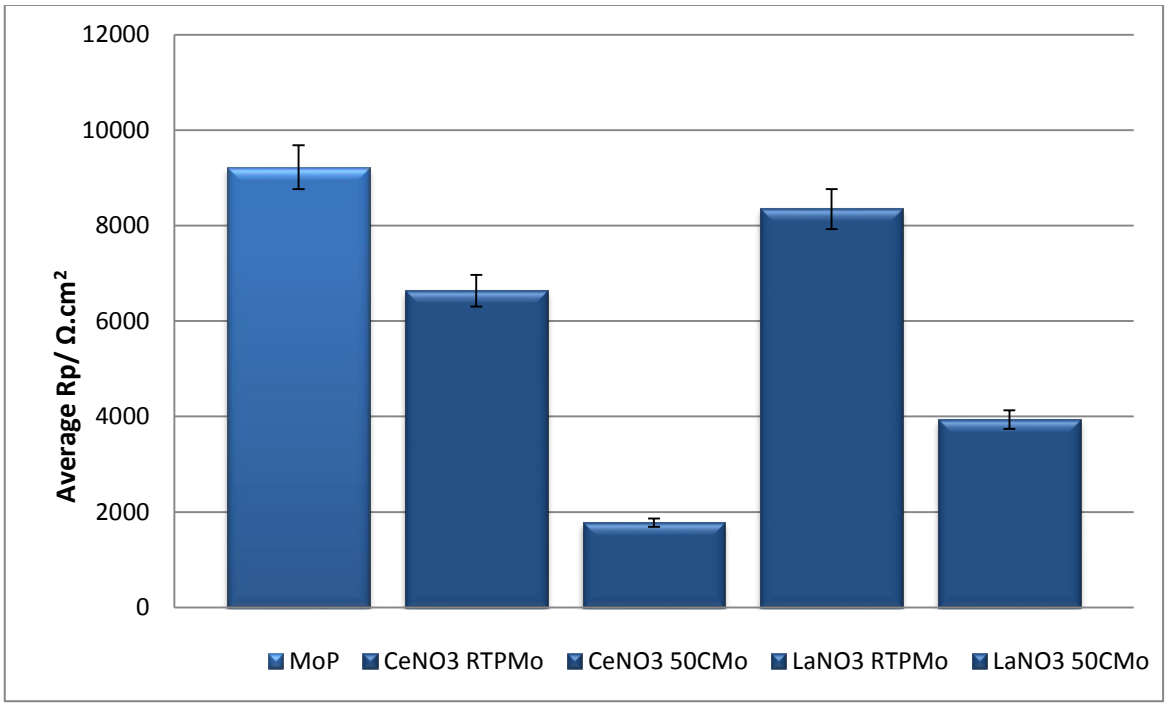

Figure 5-12: *Data showing the values for LPR for the named coatings.*

All coatings gave enhancements over the unpassivated zinc electrodeposited substrate, although none of the composite coatings gave any enhancement over the MoP single stage treatment. Lanthanum nitrate / MoP was the highest performing coating of those tested.

5.1.12 Summary of LPR Testing

LPR investigations allowed for a wide variety of conversion coating variables to be tested and any effects that they had on the protective properties to be seen. Samples that performed well, this being defined as > 5000 Ω cm^2 a 5 x improvement over the un-passivated electrodeposited surface were investigated further using neutral salt spray corrosion testing. The coatings that met these criteria were, MoP, MoPSi, CeNO3 RTPMo and LaNO3 RTPMo.

5.2 Neutral Salt Spray Corrosion Testing

5.2.1 Introduction

Neutral salt spray corrosion tests were carried out to the ASTM B117 (2007). Examination of sample surfaces took place every hour for the first 8 h and then at 24 h intervals from the original start time, digital images were taken each time the samples were checked. Times to 5% 'white rust' and 5% 'red rust' were recorded, when the samples had reached the point at which they showed 5% 'red rust' the test was terminated for that sample. The appearance of 5% of white rust (from Zn corrosion), was of upmost importance in NSS tests, as it indicated a significant failure of the conversion coating. Time to 5% red rust (from Fe corrosion) was of secondary importance, as it indicated the failure of the zinc surface. The main significance of this failure was to monitor any effects that the conversion coating has on the zinc surface's ability to protect the mild steel substrate.

5.2.2 Results

The best performing coatings determined from LPR testing were selected to be tested using the industry standard ASTM B 117 neutral salt spray test. The untreated zinc electrodeposited substrate as well as the chromate reference surfaces were also tested as a control. Also included was a 'simple' molybdate coating, similar to one studied by many authors in the mid to late 1990s, the 'MoS120' coating was used for this. This was important so that any improvements and changes could be seen relative to this coating. The NSS corrosion data for these coatings and their respective average LPR values are shown in Table 5-13.

Table 5-13: Data showing the corrosion data for the named conversion coatings on Zn surfaces.

Name	Average LPR (Ω. cm^2)	Average Time to 5% White Rust (hrs)	Average Time to 5% Red Rust (hrs)
Zn (acid)	1273	1	48
CrVI	11571	120	248
MoS120	2223	6	120
MoP	9222	24	144
MoPSi	5333	20	144
CeNO3 RTPMo	6637	6	96
LaNO3 RTPMo	8345	10	96
MoP-S1	1178	6	96
MoP-S2	921	6	96
MoPSi-S1	2873	10	144
MoPSi-S2	2873	10	120

LPR results are stated so that a comparison can be made between the NSS and LPR techniques. It can be seen that NSS results broadly follow the ranking trend shown by LPR testing, with a few exceptions, namely the rare earth metal – molybdate composite coatings, which performed relatively poorly. Average times to 5% white rust of 20 and 24 h for the MoPSi and MoP coatings are amongst the highest studied for any molybdate based coatings reported in the literature (see Section 2.1.24).

5.2.2.1 Experimental Observations

5.2.2.1.1 Zn

The untreated Zn showed 5% of WR after 1 h of exposure. Corrosion occurred initially as a prominence of a powdery dark grey product. This increased in volume until the end of the test when 5 % red rust could be seen.

5.2.2.1.2 CrVI

The chromate treated surface resisted the formation of white rust until an average of 120 h NSS exposure. Surface appearance did not remain constant throughout the whole test, as when examined, the surface lost some of its iridescence after 24 h and lost most of its pigment after 48 h, appearing silver. Small patches of white rust were seen after 120 h.

5.2.2.1.3 MoP

The MoP treated surfaces resisted the formation of white rust for an average of 24 h NSS exposure. Corrosion occurred quite locally, with the majority of the surface remaining intact. The white rust became voluminous after 96 h of exposure, leading to substrate corrosion and the appearance of red rust after 144 h.

5.2.2.1.4 MoPSi

The MoPSi treated surfaces resisted the formation of white rust for an average of 20 h, making it inferior in terms of corrosion resistance to the MoP treatment that it is based upon. Corrosion occurred locally, in a similar way to the MoP treated surface. After 96 h, the white rust started to become locally voluminous, eventually leading to failure by red rust after 144 h.

5.2.2.1.5 Rare Earth Metal Molybdate Composite Coatings

In general, the REM/ molybdate coatings performed poorly offering 8 and 10 h until 5 % white rust for CeNO3-MoP and LaNO3-MoP respectively. Although the initial onset of corrosion was relatively quick, the REM-molybdate samples did not show the

voluminous white rust zinc corrosion product until after 48 h exposure, failing to red rust shortly after.

5.2.3 Summary of NSS Corrosion Testing

NSS corrosion testing for the single stage molybdate treatments was quite successful, with good correlation shown with the ranking from the LPR testing and times to 5 % white rust from NSS testing. The breakdown mechanisms for the MoP and MoPSi coatings appeared to be quite similar, with localised film weaknesses leading to the onset of corrosion. The REM/ molybdate coatings behaved in this way too, although they showed the initial corrosion much sooner. The chromate coatings changed their appearance initially, losing their iridescence, but remained quite similar in appearance for a long period of time until they eventually showed 5 % white rust corrosion.

It was decided, due to the poor corrosion resistance that the REM-MoP coatings had shown, to not involve them in the characterisation stages, instead focussing on the MoP and MoPSi coatings.

5.3 Sample Morphology Characterisation

5.3.1 Field Emission Gun Scanning Electron Microscopy (FEG-SEM)

5.3.1.1 Acid Zinc Surface

The electrodeposited acid Zn substrate is shown in Figure 5-13. At lower magnification, the surface appears relatively smooth. However, viewing at higher magnification reveals a micro-roughness on the surface.

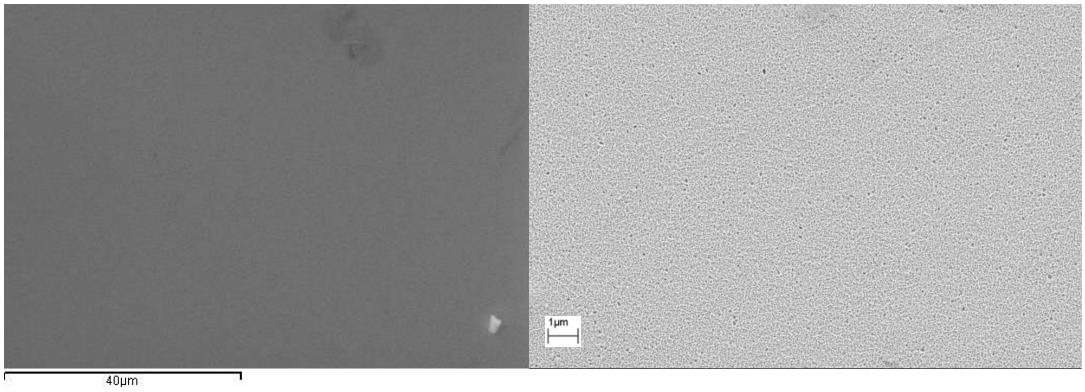

Figure 5-13: *a: SEM image showing an electroplated Zn surface at low magnification. b: FEG-SEM Image at high magnification showing the surface of a Zn electrodeposited surface, after pre-treatment.*

The electroplated coating had a nominal thickness of 8 µm, the cryofracture method was unsuccessful in allowing this to be viewed in cross-section as the technique employed was only effective for viewing sections of up to ~ 5 µm. This necessitated the use of the FIB-SEM ion beam cross-sectioning method. Figure 5-14 shows the thickness, with the approximate thickness being 8 µm.

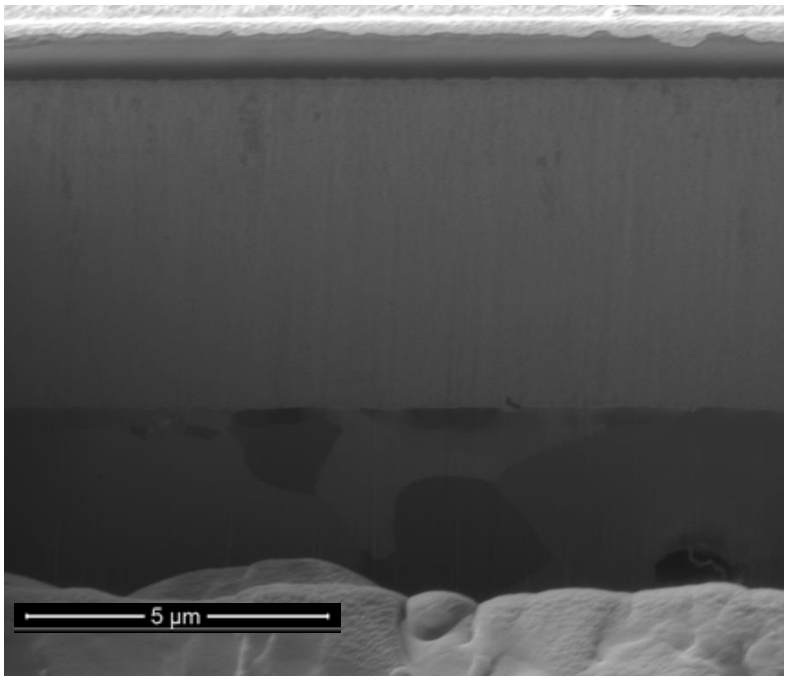

Figure 5-14: *Ga^+ ion image showing the cross-section of an electrodeposited Zn surface.*

The EDXA data shown in Table 5-14 shows that the electrodeposited Zn coating was 99 % pure Zn, with a small amount of chloride present.

Table 5-14: Data showing the composition measured by EDXA of an electrodeposited Zn surface.

Element	Weight %	Atomic. %
Zn	99	99
Cl	1	1

5.3.2 CrVI Treated Surface

The Cr(VI) treated surface exhibited a typical crack structure in common with coatings of this type reported by other authors (Biestek and Weber 1976, Lewis *et al.* 2006). The cracks themselves appeared in an aligned manner (see Figure 5-15), which is not analogous to other chromate coatings reported.

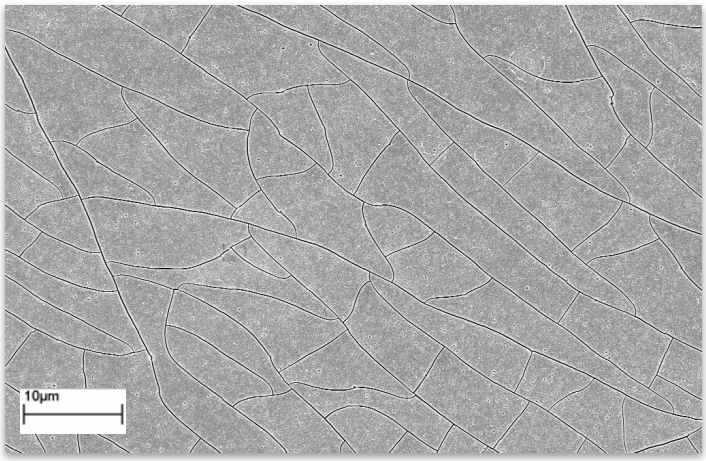

Figure 5-15: *FEG-SEM image showing a Cr(VI) coated electrodeposited Zn surface.*

FIB-SEM was used to determine the coating thickness, as conversion coating adhesion was lost when using the cryofracture technique. Figure 5-16 shows the coating thickness to be around 350 nm.

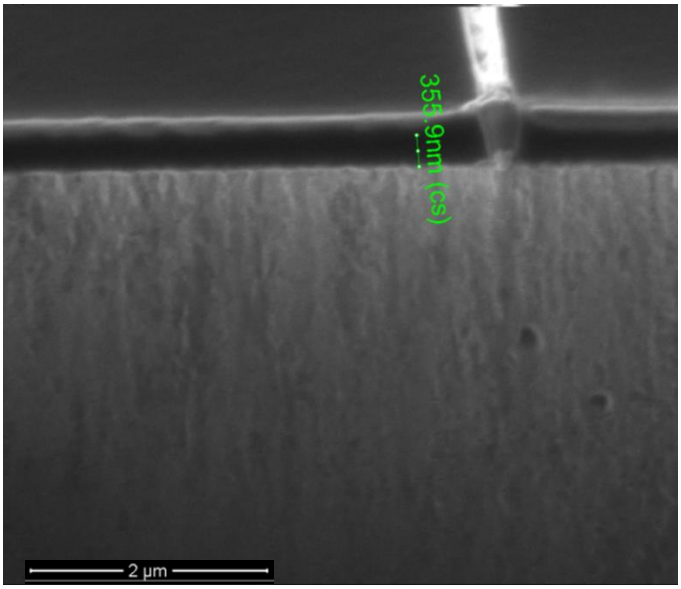

Figure 5-16: *FIBSEM Ga^+ ion image showing the coating thickness of a Cr(VI) treated electrodeposited Zn surface.*

5.3.2.1 'Simple' Molybdate Treated Surface

SEM investigation of the simple molybdate surface showed the prevalence of a network of cracks (see Figure 5-17a). It was also apparent that, at the junctions of some cracks there was the formation of dimple like structures measuring around 7 µm in diameter (see Figure 5-17c). These were unique to this treatment condition, and were not found when investigating the substrate.

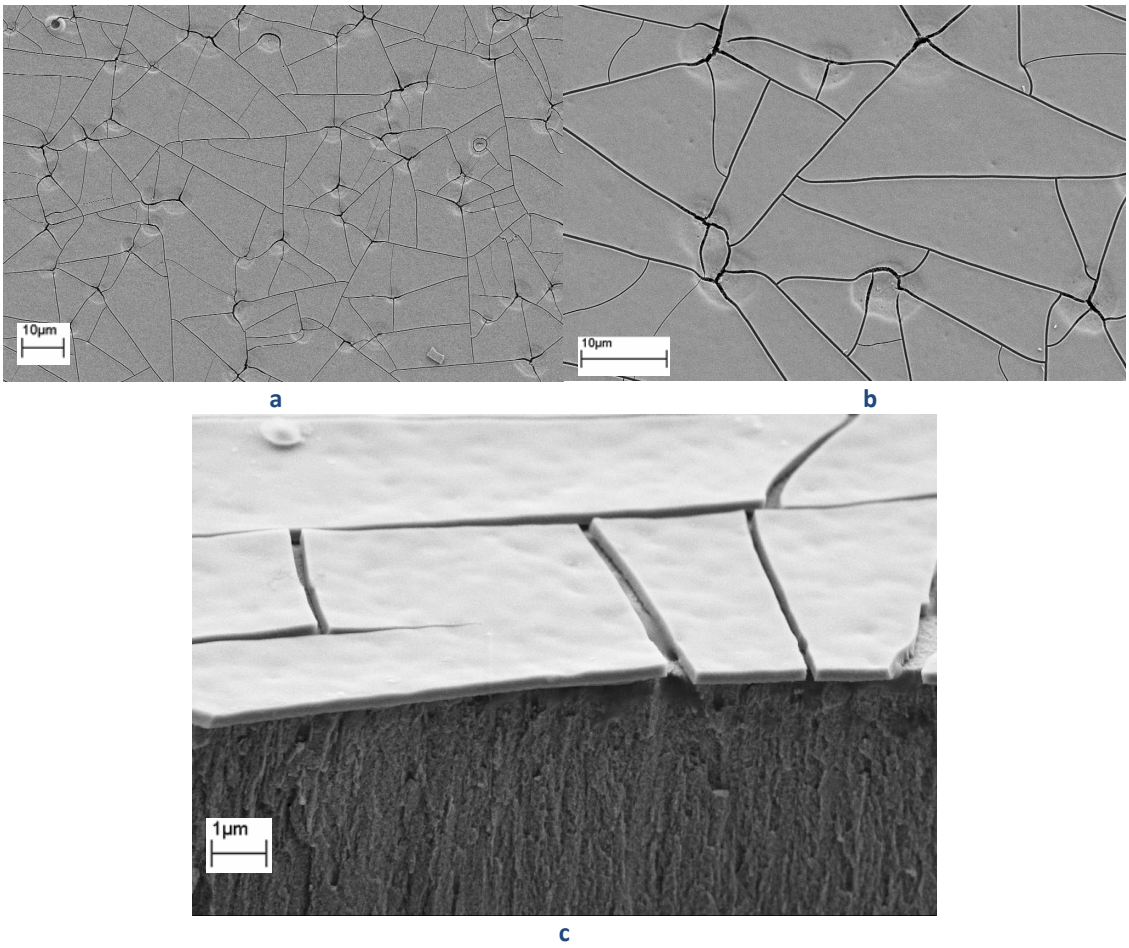

Figure 5-17: *a: FEG-SEM image showing the cracked structure of a simple molybdate treated electrodeposited Zn surface. b: FEG-SEM image showing the cracked structure of a simple molybdate treated electrodeposited Zn surface. c: FEG-SEM Cryofracture image of a simple molybdate treated electrodeposited Zn surface.*

The cryofracture technique showed the coating to be approximately 300 nm thick. A platelet type structure could be seen where the cracks on the surface appeared to expose the substrate. It was also apparent that coating adhesion was quite poor as voids could be seen at the substrate coating interface.

EDXA analysis showed the surface composition to be quite high in Mo with a large amount of Zn (from the substrate) present as well as a large amount of O (see Table 5-15).

Table 5-15: Data showing the composition measured by EDXA of simple molybdate treated electrodeposited surface.

Element	Weight %	Atomic. %
O	16	47
Mo	26	13
Zn	57	40

5.3.2.2 MoP Treated Surface

When viewed at high magnification, the MoP surface appeared to have a large amount of porosity, which can be seen in Figure 5-18. The coating structure was in contrast to many other molybdate-based coatings, studied previously, both by the author and other authors, which were generally smoother and cracked (Gabe and Gould 1988, Wilcox and Gabe 1988, Wharton *et al.* 1996, Jahan *et al.* 1997, Almeida *et al.* 1998, Wharton *et al.* 1999, Lu *et al.* 2001, Magalhães *et al.* 2003, Wilcox 2003, Lewis *et al.* 2006).

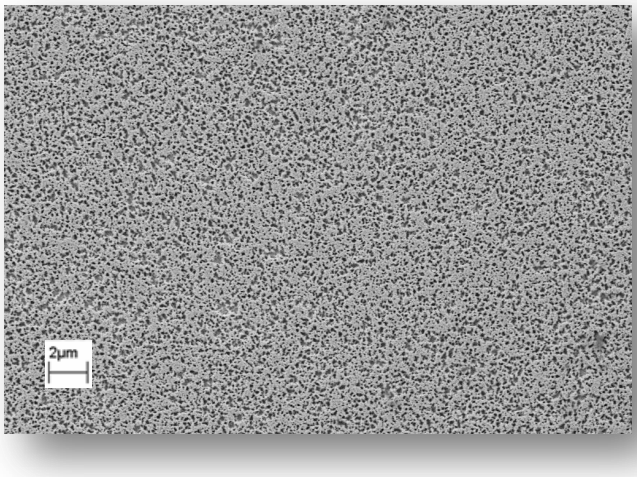

Figure 5-18: *FEG-SEM image showing the porous structure of an MoP treated electrodeposited Zn surface.*

Cryofracture was used to determine coating thickness and view the coating structure (see Figure 5-19). The coating was found to be approximately 300 nm thick and appeared to have a columnar structure. The pores appeared to penetrate to the substrate, although this investigation was inconclusive, as it may be that there is a thin coating present at the bottom of the pores.

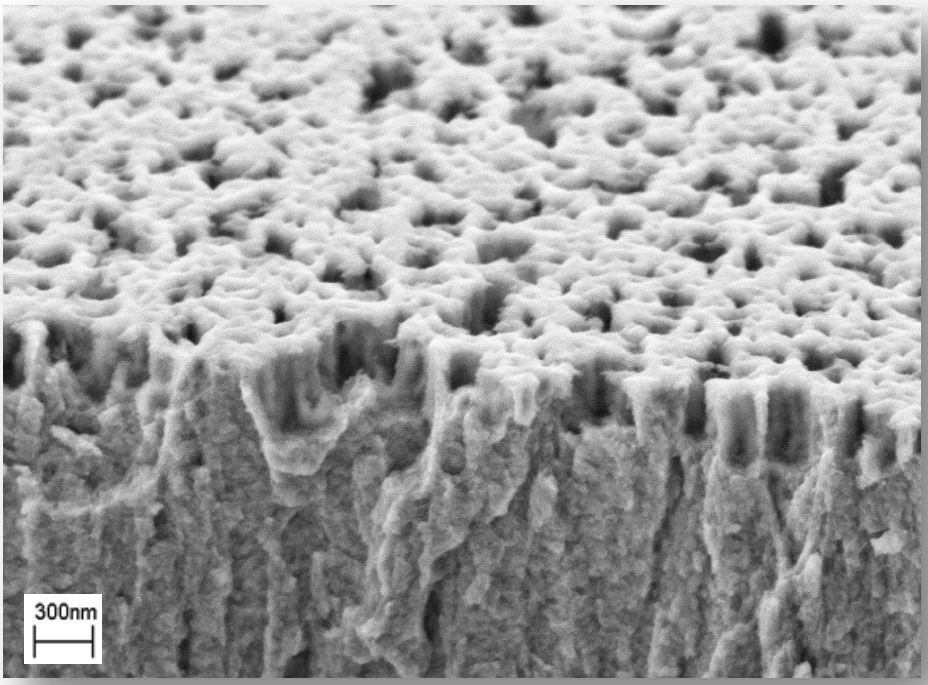

Figure 5-19: *FEG-SEM Cryofracture image showing the thickness and structure of an MoP treated electrodeposited Zn surface.*

EDXA showed that the surface was made up almost exclusively of Zn with only small amounts of Mo and O present (see Table 5-16). Also present was a small amount of Fe, it is possible that this could have been detected due to the mild steel substrate, as the treatment solution did not have any Fe content.

Table 5-16: Data showing the composition measured by EDXA of an MoP treated electrodeposited surface.

Element	Weight %	Atomic. %
O	2	8
Mo	1	1
Zn	92	86
Fe	5	5

5.3.2.3 MoPSi Treated Surface

The addition of nano sized silica led to a more conventional type molybdate conversion coating, with a cracked surface. However, the cracks were quite different to those seen on a simple molybdate, appearing less angular and discontinuous, with smaller distance between platelets of coating. The porosity was lost and a random crack structure was prominent (see Figure 5-20).

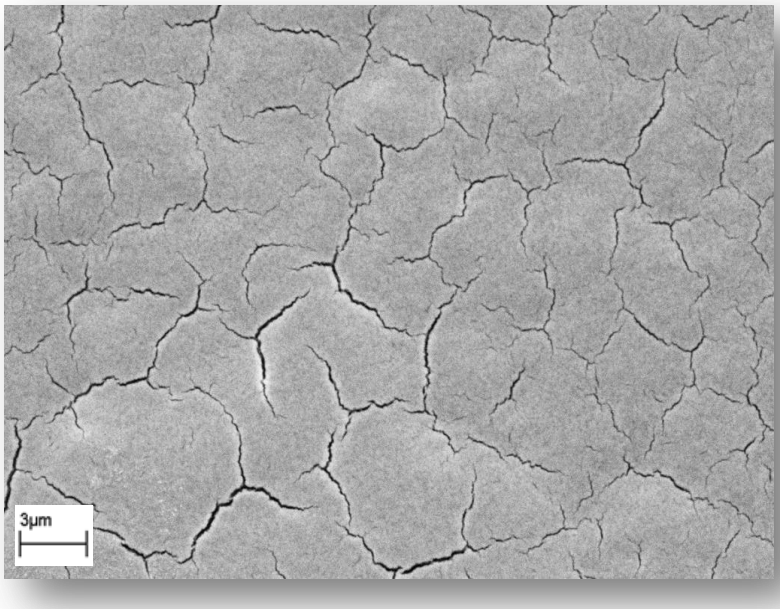

Figure 5-20: *FEG-SEM image showing the crack structure of a MoPSi treated electrodeposited Zn surface.*

Cryofracture was again used to view the coating cross-section; the coating was relatively thick, at approximately 1 µm, see Figure 5-21. There appears to be slight a loss of adhesion or porosity at the coating/ substrate interface, this can be seen in the dark areas at beneath the coating in Figure 5-21. The coating appeared homogeneous and dense, with a particulate structure.

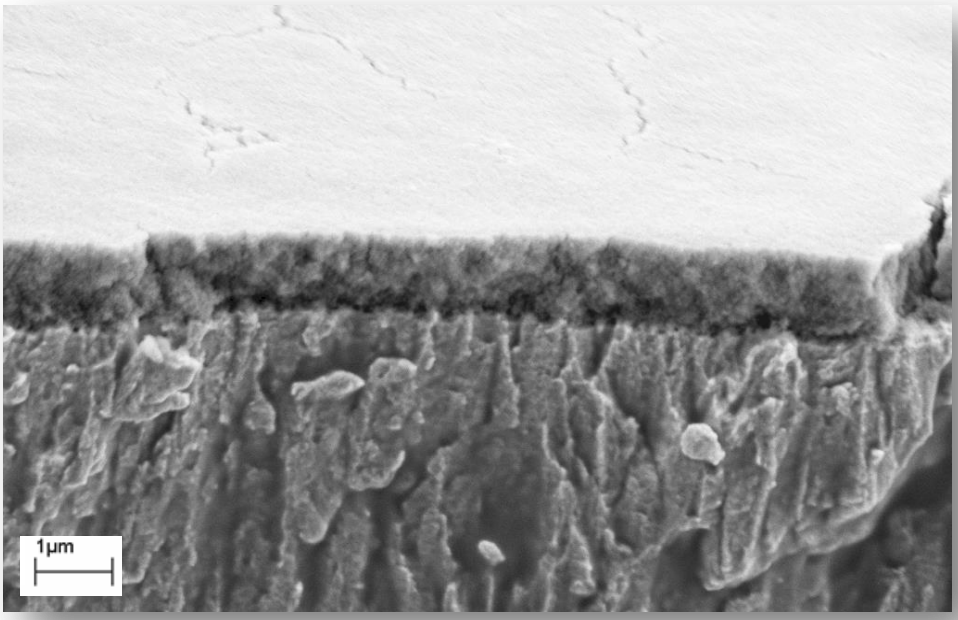

Figure 5-21: *FEG-SEM Cryofracture image showing the approximate thickness and structure of a MoPSi treated electrodeposited Zn surface.*

EDXA experiments (Table 5-17) showed a large amount of Zn with a significant amount of O present. Mo, Si and P were prominent albeit in amounts of less than 5 wt. %. Analogous to the MoP coating studied previously, there was an appearance of a small amount of Fe.

Table 5-17: Data showing the composition measured by EDXA of an MoPSi treated electrodeposited surface.

Element	Weight %	Atomic. %
O	14	39
Mo	4	2
Zn	74	49
Si	1	1
P	5	7
Fe	3	2

5.3.2.4 Silicate Sealants

The morphology of the silicate sealed samples was investigated, to provide further insight into their poor corrosion resistance. It can be seen in Figure 5-22, that the coatings had large pores, both on the surface and at the substrate coating interface. The cross-section also appeared to show that the conversion coating that was present before silicate immersion had been removed, leaving the electrodeposited Zn surface exposed through the pores.

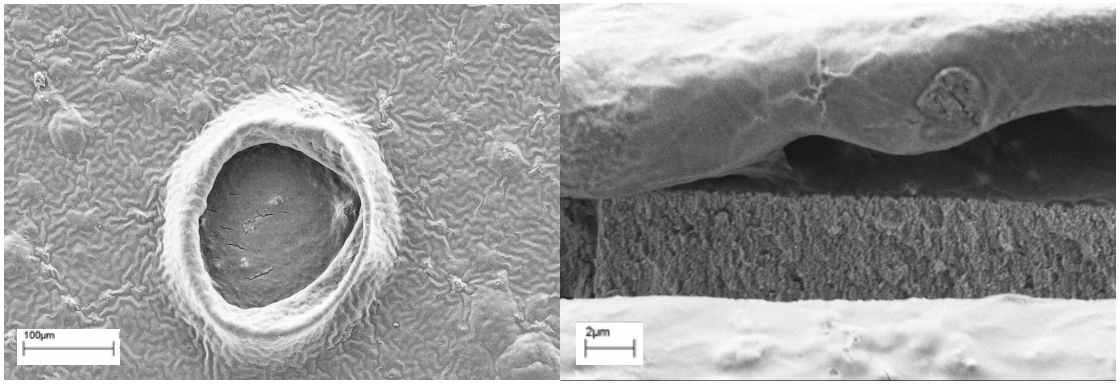

Figure 5-22: *a: FEG-SEM image showing the appearance of a pore in the silicate sealant layer on a molybdate coated, electrodeposited zinc surface. b: FEG-SEM image showing the cross-section of a silicate sealant layer on a molybdate coated, electrodeposited zinc surface.*

5.3.2.5 REM-Molybdate Composite Surfaces

REM-molybdate composite surfaces appeared to have a microrough, non-porous surface throughout (see Figure 5-23). Cryofracture revealed a thickness of about 200 nm and what appeared to be porous areas due to lack of adhesion at the substrate coating interface.

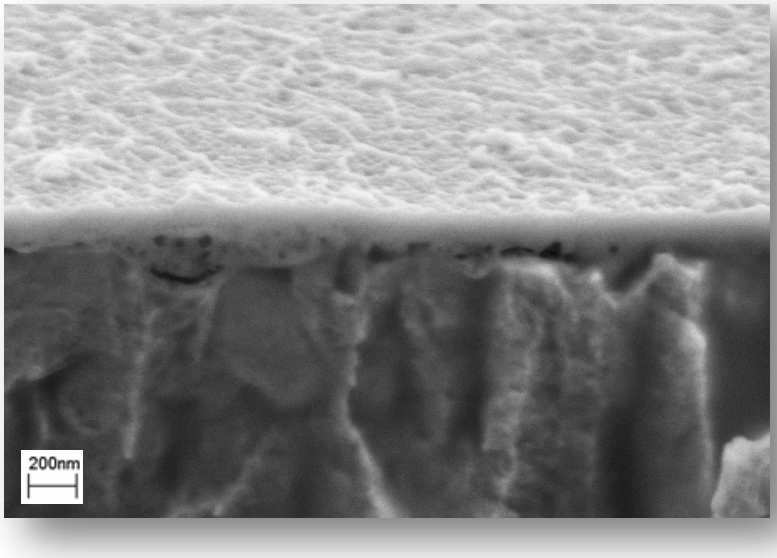

Figure 5-23: *FEG-SEM image showing the cross-section of a LaMoP coated, electrodeposited zinc surface.*

5.3.2.6 Cobalt Nitrate Additions

Surfaces formed from treatment solutions with cobalt nitrate additions appeared similar to the MoP type surfaces, in that they were porous and well adhered to the substrate. They appeared much rougher than the MoP coatings, with a crystal like growth on the coating surface (Figure 5-24).

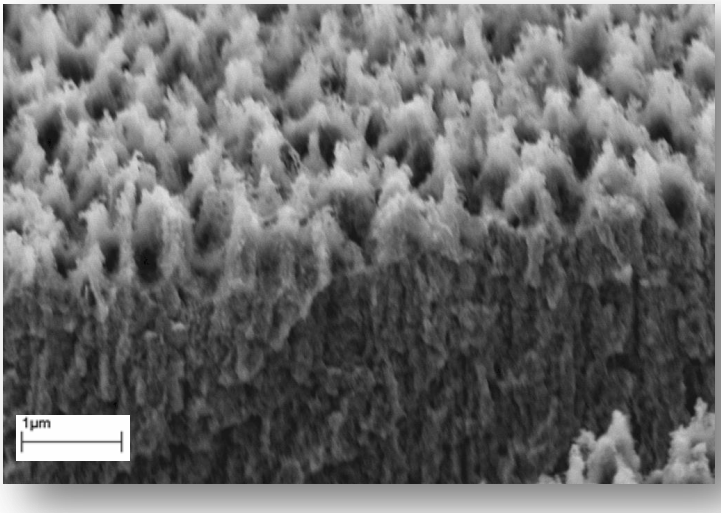

Figure 5-24: *FEG-SEM image showing the cross-section of a molybdate cobalt nitrate added coated electrodeposited zinc surface.*

5.3.3 Summary of FEG-SEM

Molybdate coatings were formed on Zn surfaces. The simple molybdate coating had a smooth, cracked surface. 'Improved' coating appearance was influenced by the additives used. The MoP type coating produced a porous coating, which was relatively thin. Silica produced a dense, pore-free coating, with the appearance of micro-cracks. Chromate coatings appeared cracked and had poor substrate adhesion.

5.4 Auger Electron Spectroscopy Surface Composition Measurements

Auger electron spectroscopy was used to investigate the surface composition of the coatings investigated in the previous section. AES is a more appropriate technique to measure the composition of the types of coatings studied here because of the limitations of EDXA sampling depth. Data shown in Figures 5-25 to 5-28 shows the average compositions of the surfaces measured using AES.

5.4.1.1 CrVI Treated Surface

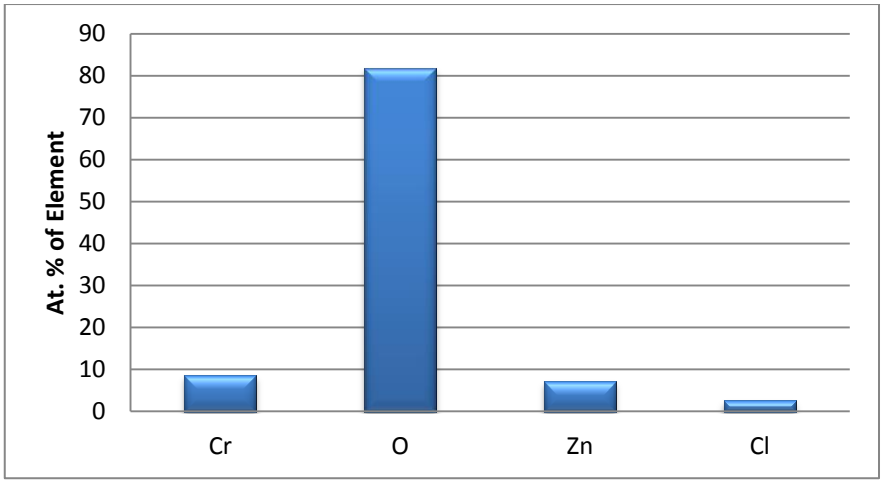

Figure 5-25: *Data showing the average composition measured using Auger Electron Spectroscopy of a CrVI treated electroplated Zn surface.*

5.4.1.2 Simple Molybdate Treated Surface

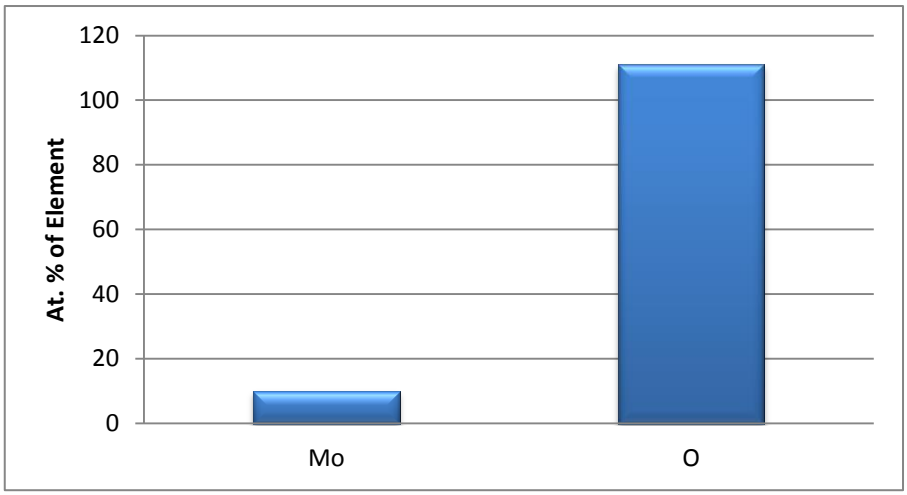

Figure 5-26: Data showing the average composition measured using Auger Electron Spectroscopy a Simple Molybdate treated electrodeposited Zn surface.

5.4.1.3 MoP Treated Surface

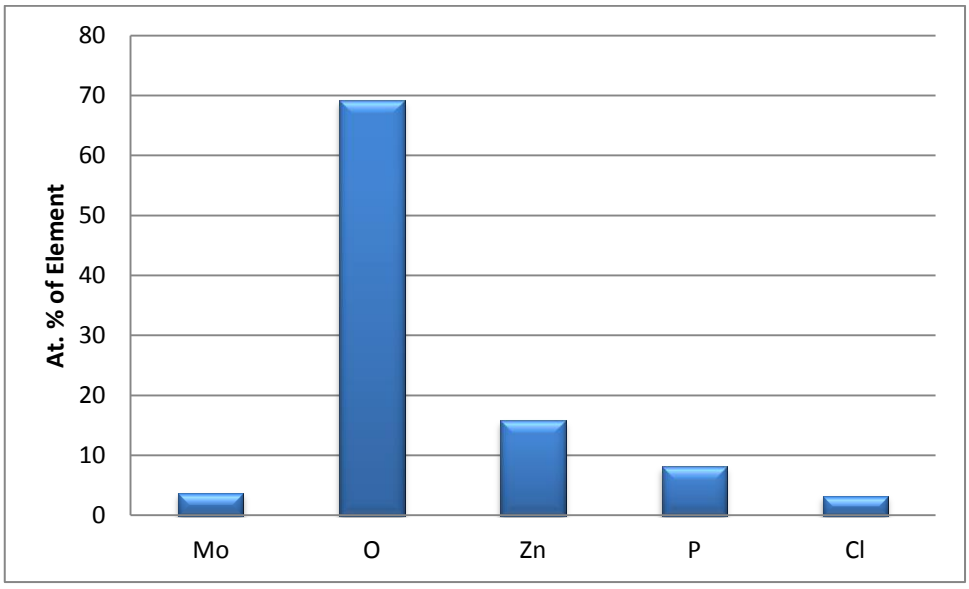

Figure 5-27: *Data showing the average composition measured using Auger Electron Spectroscopy a MoP treated electrodeposited Zn surface.*

5.4.1.4 MoPSi Treated Surface

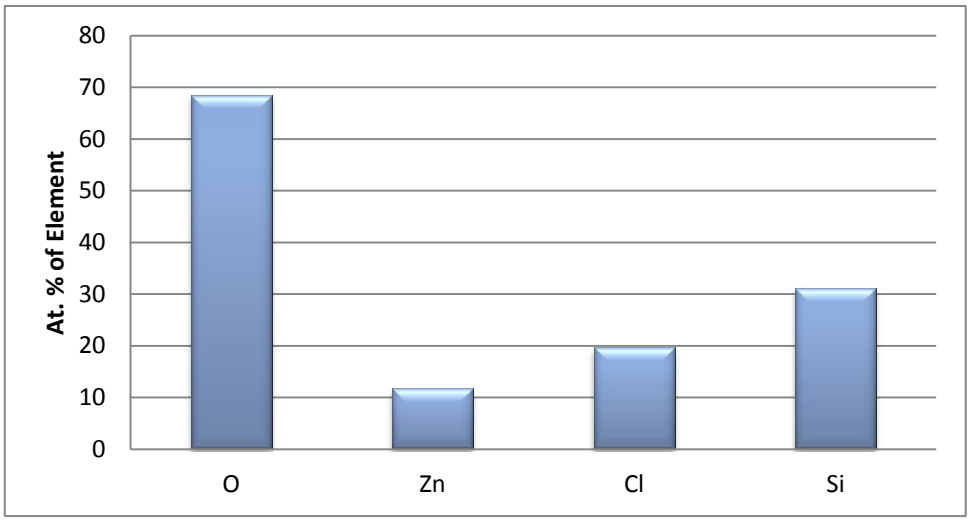

Figure 5-28: *Data showing the average composition measured using Auger Electron Spectroscopy a MoPSi treated electrodeposited Zn surface.*

The data shown in Figures 5-25 to 5-28 shows all of the coating surfaces to be rich in oxygen. The metal constituent atom is present at a much smaller percentage and not present at all on the surface of the MoPSi surface Figure 5-28. Phosphorus makes up over 8 at.% of the MoP coating (Figure 5-27) which is in contrast to the bulk composition found using EDXA, which did not find any. The hexavalent chromium and MoP treated samples had 2.5 and 3.2 at% of Cl respectively.

5.5 Corrosion Initiation Experiments

5.5.1 Introduction

In order to give more information regarding how the coatings perform, it was decided to investigate the *initiation* of corrosion. This can be thought of as an investigation to determine the point(s) of weakness or the mechanism that causes coating failure. The experimental technique is described in detail in Section 4.1.4.

The samples selected for investigation were the Zn, chromate and 'simple' molybdate reference coatings, as well as the improved MoP and MoPSi coatings. Coatings were immersed in 5 % wt/ vol $NaCl_{(aq)}$ until they showed any surface change. Initial signs of corrosion were deemed to be any appearance of pitting or discolouration of the film, not a voluminous corrosion product.

Compositional data was found using EDXA and AES where possible, to give an indication of the composition of the corrosion products.

5.5.2 Electrodeposited Zn

After a short period of exposure, 20 min, in 5 % NaCl (aq), there was already evidence of corrosion on the Zn surface. These initial signs of corrosion took the form of crystalline structures of around 5 µm across (see Figure 5-29a). The visual appearance after 2 h was a slight surface dulling and a light matt effect. After 4 h, these features were much more prominent and covered much more of the surface (see Figure 5-29b). The visual appearance after 4 h was of a definite white rust corrosion product which was prominent.

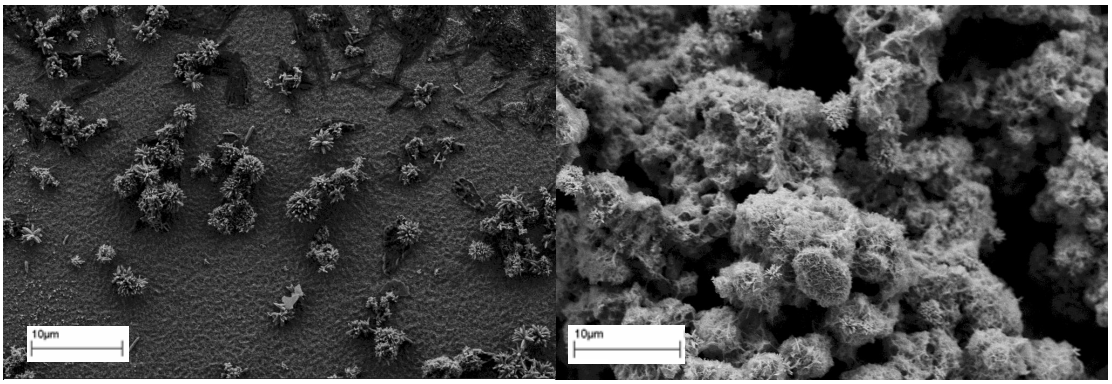

a b

Figure 5-29: *a: FEG-SEM image showing the appearance of crystalline corrosion product on a partially corroded electrodeposited Zn surface. After 20 minute,s 5 % NaCl (aq) exposure. b: FEG-SEM image showing the appearance of voluminous crystalline corrosion product on a partially corroded Zn surface. After 4 h, 5 % NaCl (aq) exposure.*

It was decided to study the composition of the samples corroded for 2h, as these had areas of the corrosion initiation, as well as areas that were more intact. Scanning Auger Microscopy (SAM) made it possible to determine the two distinct areas and gain spectra from these. The image shown in Figure 5-30a represents the areas that this data was taken from.

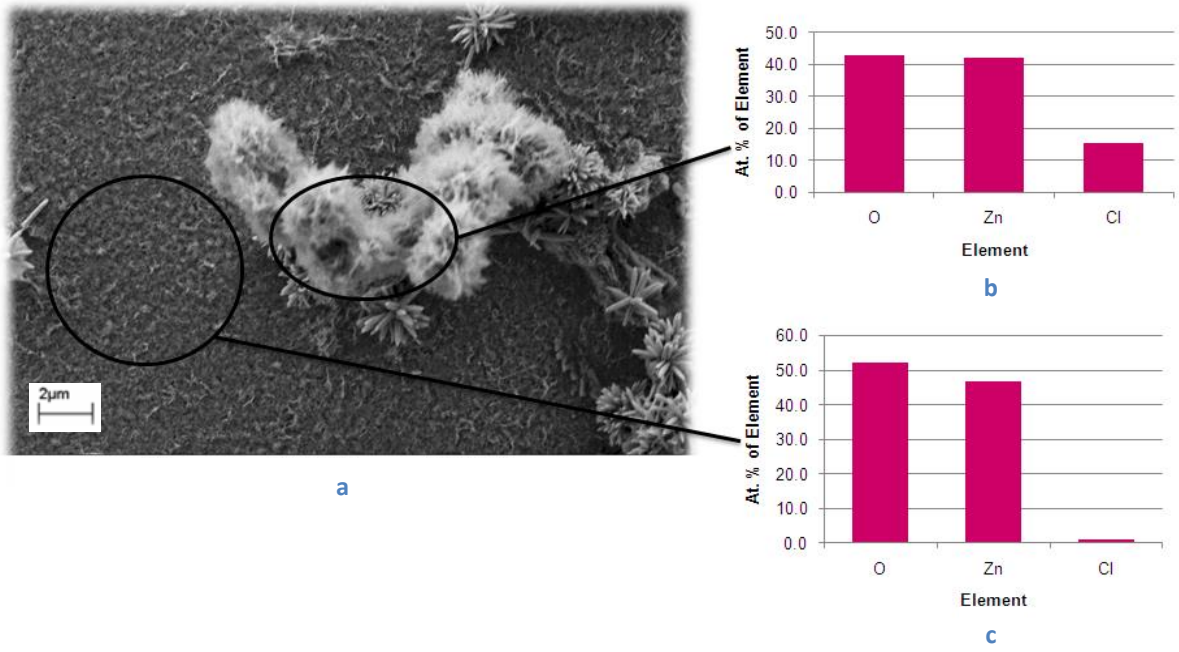

Figure 5-30: *a: FEG-SEM image of an electrodeposited Zn surface after 2 h 5 % NaCl (aq) exposure. The areas circled represent where the AES spectra were taken from. b: AES data representing the corroded area of an electrodeposited Zn surface after 2 h, 5 % NaCl (aq) exposure. c: AES Data representing the intact area of electrodeposited Zn surface after 2 h 5 % NaCl (aq) exposure.*

The data shown in Figures 5-30b and c show that there were significant amount of zinc and oxygen present at both sites, with the 'corroded' area having much more chlorine present.

5.5.3 Chromate Treated Surface

The chromate treated surface did not show any visible corrosion after 4 h of NaCl exposure, the only surface change was a slight loss of surface colour, which went from iridescent to clear. When viewed using FEG-SEM however, it could be seen that the film started to delaminate (see Figure 5-31a), exposing what appeared to be the substrate below (lighter areas in the image). However, AES showed the exposed areas to maintain a concentration of Cr (see Figure 5-31c,). The intact coating area (Figure 5-31b) was made up primarily O (> 80 %) with lesser amounts of Cr and Zn (< 10 % each)

and a small amount of Cl. Where the coating had peeled away, there was a smaller amount of Cr (< 5 %), much more Zn (~ 24 %) and Cl (~ 15 %).

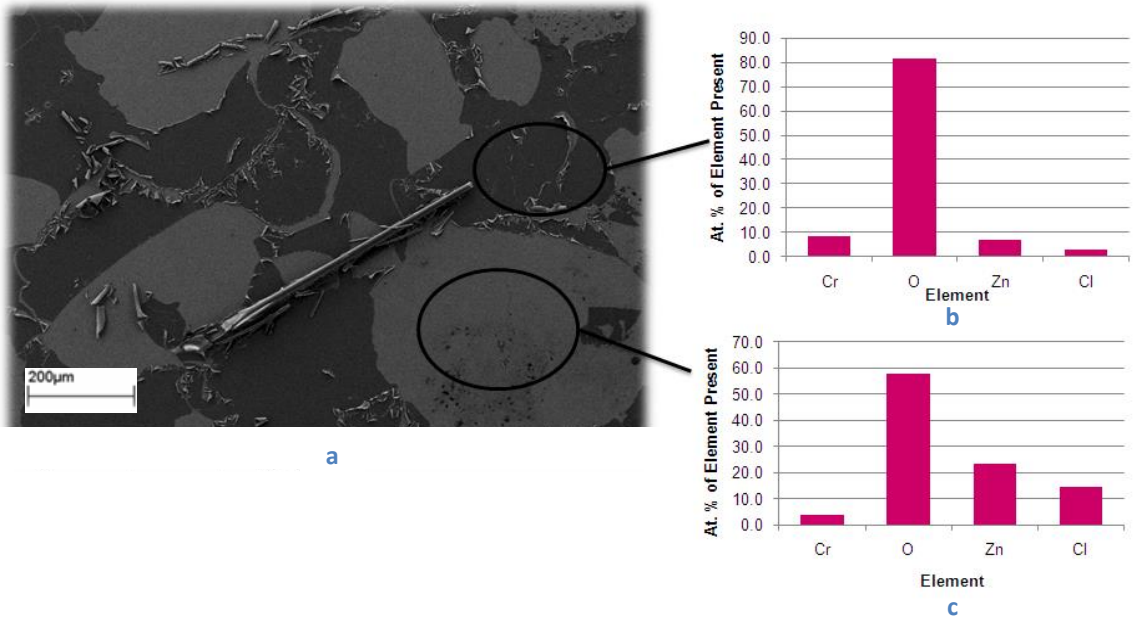

Figure 5-31: *a: FEG-SEM image of a chromate treated, electrodeposited Zn surface after 4 h, 5 % NaCl (aq) exposure. The areas circled represent where the AES spectra were taken from. b: AES data representing the intact area of a chromate treated, electrodeposited Zn surface after 4 h, 5 % NaCl (aq) exposure. c: AES Data representing the corroded area of a chromate treated, electrodeposited Zn surface after 4 h, 5 % NaCl (aq) exposure.*

5.5.4 Simple Molybdate Treated Surface

The 'simple' molybdate treated surface began to show the visual signs of corrosion after 4 h of 5% NaCl exposure, this manifested itself as barely visible areas of powder on the surface.

When viewed using FEG-SEM, corrosion appeared to start at the crack junctions, which can be seen as the dark areas in Figure 5-32. AES data (Figure 5-33) showed that the surface maintained a concentration of Mo, showing that the corrosion was fairly isolated to the crack junctions and the majority of the coating remained intact.

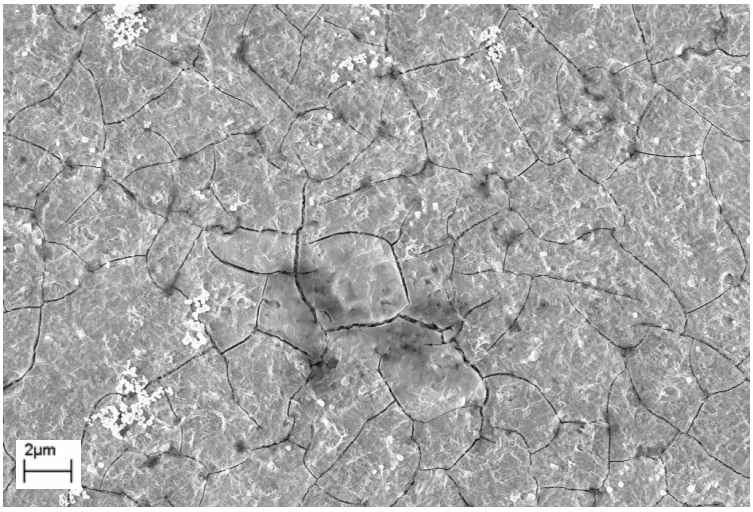

Figure 5-32: *FEG-SEM image showing the surface appearance of a partially corroded 'simple' molybdate treated sample after 4 h, 5% NaCl (aq) exposure.*

Using AES, it was possible to obtain spectra from the partially corroded and the largely intact areas of the coating, see data in Figure 5-33. Both areas were oxygen rich; however, the corroded areas had a much lower concentration of Mo as well as higher Zn and Cl concentrations.

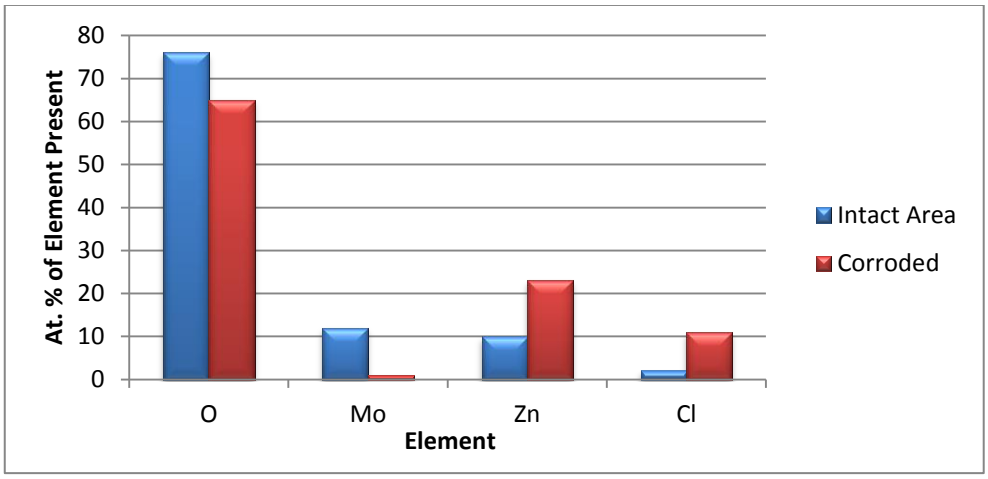

Figure 5-33: *AES data showing the composition of a partially corroded 'simple' molybdate treated sample after 4 h, 5% NaCl (aq) exposure.*

5.5.5 MoP Treated Surface

After 4 h of 5 % NaCl exposure there was an appearance of small white spots that were only just visible to the naked eye. These were less frequent and smaller than those seen on the 'simple' molybdate samples. FEG-SEM investigations revealed these to be blisters in the coating surface of about 70 µm in diameter (see Figures 5-34a and b).

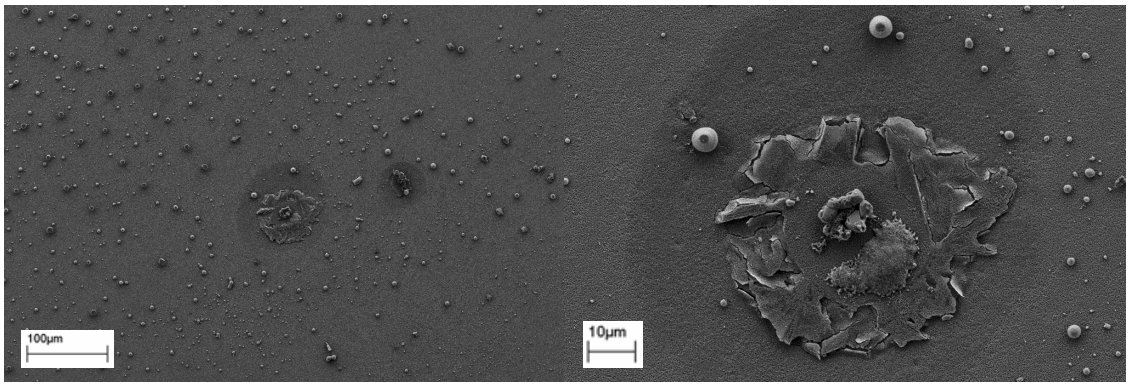

a b

Figure 5-34: *a: FEG-SEM image showing the surface appearance of a partially corroded MoP treated surface after 4 h, 5% NaCl (aq) exposure). b: FEG-SEM image showing the appearance of a blister on a partially corroded MoP treated surface after 4 h, 5% NaCl (aq) exposure.*

The ability to gain site-specific information using AES allowed for compositional analysis to be performed on both the background and blistered areas. The average composition of these areas can be found in Figures 5-35a and b respectively. Both areas were oxide rich, with a high amount of Zn on the surface. A small amount of Mo was present on the background area surface; and not present in the blistered area. A significant amount of P was present in both areas. The blistered area was slightly more Cl rich.

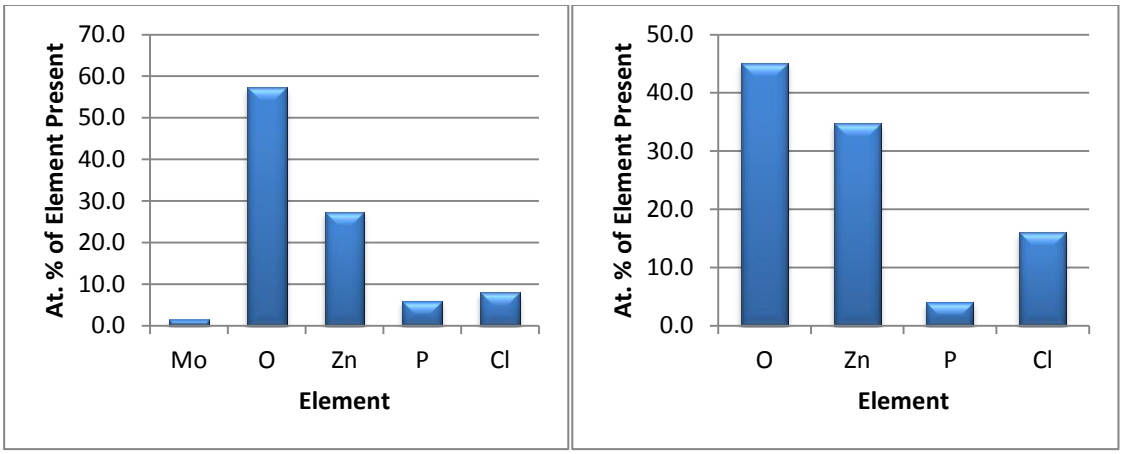

Figure 5-35: *a: AES data from background area on a partially corroded MoP treated surface after 4 h 5% NaCl (aq) exposure. b: AES data from blistered area on a partially corroded MoP treated surface after 4 h 5% NaCl (aq) exposure.*

5.5.6 MoPSi Treated Surface

After 4 h of 5% NaCl exposure, the MoPSi coating appeared un-corroded; the main visual difference was that the surface appeared slightly duller in colouration. FEG-SEM analysis showed the surface to have a structure similar to an un-corroded surface of this type, with only the prominence of pores of around 5 – 10 µm in diameter showing any difference to the un-corroded surface (Figure 5-36).

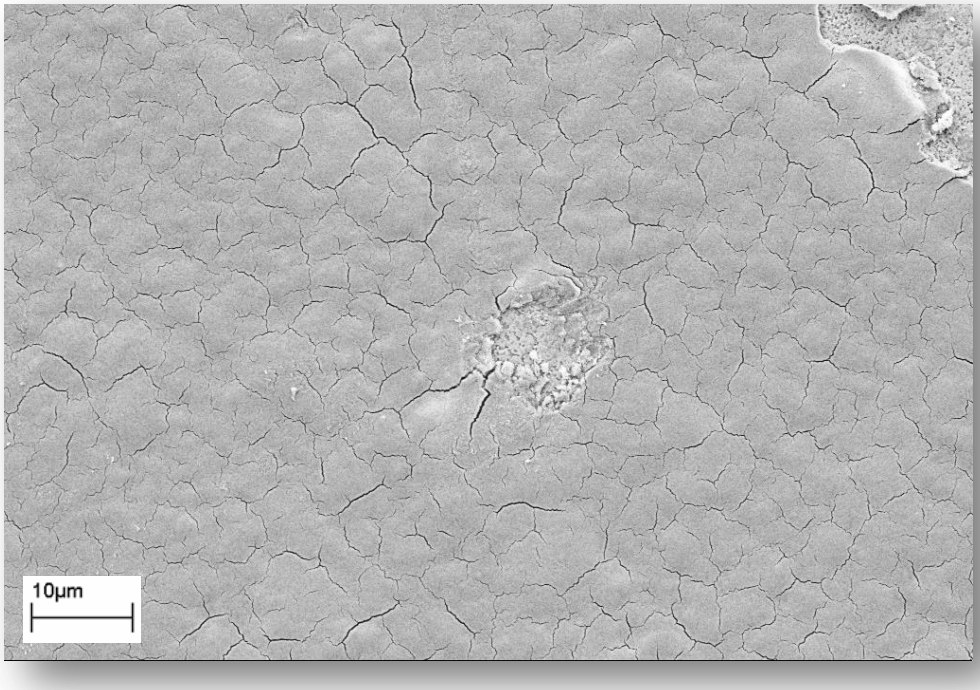

Figure 5-36: *FEG-SEM micrograph showing the surface appearance of a partially corroded MoPSi treated surface after 4 h, 5% NaCl (aq) exposure, a 'pore' can be seen towards the centre of the image.*

Using Scanning Auger Microscopy to locate the porous areas, it was possible to perform AES compositional analysis in both the 'porous' and 'background' areas of the coating. The data shown in Figure 5-37, shows the surface composition of these areas as well as an un-corroded coating of the same type.

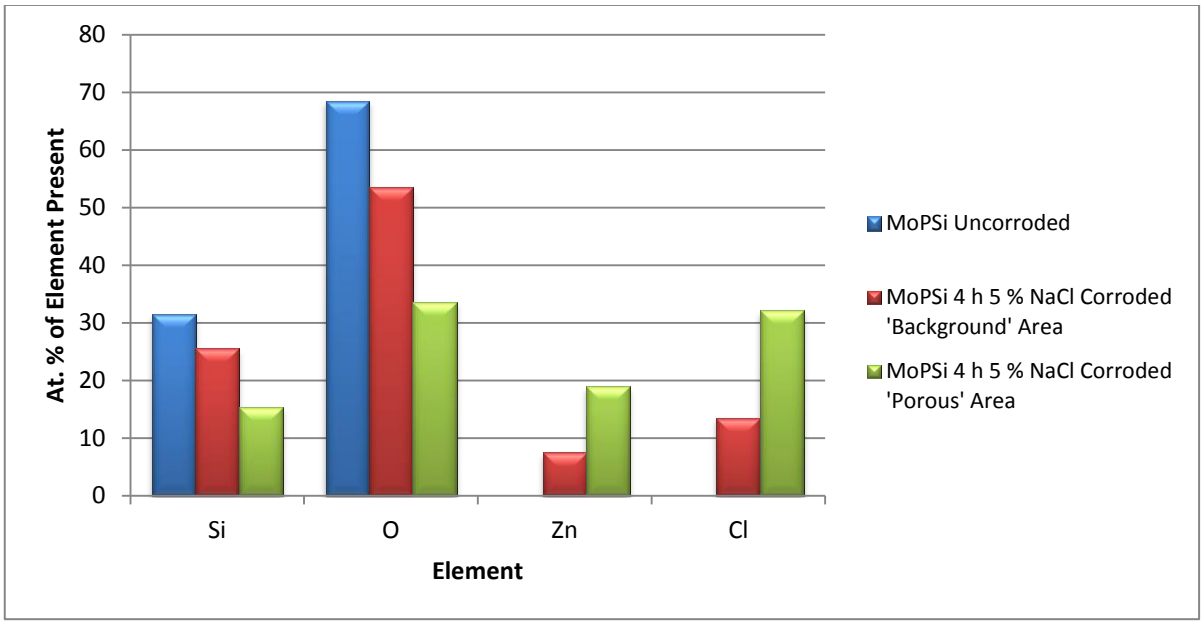

Figure 5-37: *Data obtained from AES measurements of the MoPSi coating in un-corroded and slightly corroded states.*

It can clearly be seen that there was an increase in the prominence of Zn and Cl species as the coating corroded, similar to the MoP type coatings. The ratio of approximately 1:2 Si:O was maintained throughout as well as the same ratio of Zn:Cl as the coating breaks down.

5.5.7 Summary of Initiation of Corrosion Experiments

Corrosion nucleation was a successful technique in evaluating the corrosion protection capabilities of the coatings studied. There were key differences seen with the coatings and these were apparent in both the structure and composition of the coatings.

6 Discussion

This section aims to discuss the development of an enhanced molybdate conversion coating system for electrodeposited zinc surfaces. The section starts with simple molybdate coatings then discusses ways in which improvements to these coating systems were developed. Throughout, there are theories about how the morphology and chemical composition may have affected the corrosion resistance and coating characteristics.

After analysing the development of an enhanced molybdate conversion coating system a determination of the reasons behind this enhancement in corrosion resistance is made. A study into the initiation of corrosion was carried out with the highest performing molybdate based coatings, an untreated zinc substrate and a Cr(VI) coating. A number of techniques were used to investigate how the coatings corrode including FEG-SEM, EDXA and AES.

Results gained from LPR testing can be thought of as representative of the values for the coating, it was important to perform at least 6 repeat experiments and in most cases 12; because the differences in values for some of the simple coatings were quite small. The same can be said with NSS tests, where the average values from two batches of three samples from the same treatment conditions were taken. When values for coating thickness have been quoted, however, these are more indicative of trends as they were averaged from three values from the same coating. Values for EDXA and AES were as

representative as possible and effort was made to perform spectra on areas of the coatings that were representative of the whole coating.

6.1.1 Simple Molybdate Coatings on Zinc Surfaces

Simple molybdate coatings were studied to give a baseline so that any improvements in corrosion resistance with subsequent treatments could be seen. The simple solution consisted of treatment conditions found to be most common in the literature survey by authors that chose to study simple molybdate coatings. Molybdate concentration of 25 g dm^{-3} was utilised, and sulphuric acid was used to acidify the aqueous treatment solution to pH 5.0 at room temperature.

Immersion times of 30 and 90 s produced iridescent coatings. Coatings of this type are well documented by previous authors who have studied molybdates on zinc surfaces (Wilcox and Gabe 1988, Wilcox 1989, Han and Fang 1996, Almeida *et al.* 1998, Konno *et al.* 2001, Lee *et al.* 2002, Magalhães *et al.* 2003, Wilcox 2003). 120 s immersions produced a darker, iridescent gloss black finish, this colouration agrees with that found by many authors using similar treatment solutions (Gabe and Gould 1988, Wilcox and Gabe 1988, Almeida *et al.* 1998, Magalhães *et al.* 2003, Lewis *et al.* 2006).

Simple molybdate coatings offered a 75 % improvement in LPR resistance over the untreated electrodeposited Zn surface, indicating that the coatings did provide a relatively small amount of corrosion protection (Figure 5-2). After LPR testing was carried out, the samples had small amounts of visible pitting on the surface. This could

be due a localised lack of coating adhesion, where the porous areas of the coating acted as initiation points for corrosion.

When viewed using FEGSEM (Figure 5-1) the simple molybdate samples showed the characteristic 'dried riverbed' microstructure of platelets and cracks, which is well documented by authors who have studied similar coatings (Wilcox and Gabe 1988, Wilcox 1989, Wharton *et al.* 1996, Almeida *et al.* 1998, Magalhães *et al.* 2003, Lewis *et al.* 2006). The frequency of these cracks increased with immersion time, suggesting that the cracks are indeed formed from a relief of internal stresses as the coating increases in thickness (Heavens 1970, Wilcox and Gabe 1988, Gabe and Gould 1988).

The cracks between the platelets were quite large, up to and around 150 – 200 nm, there would be a good chance that these would allow the ingress of corrosive species thus leading to the relatively poor corrosion resistance seen.

At around 25 % of the 'crack junctions' there was a prominence of 'pin-holes', around 5 µm in diameter with some coatings formed on top. The presence of these 'pin-holes' could lead to the poor corrosion resistance that these samples exhibited in LPR testing. They could allow the substrate to be corroded by the ingress of aggressive chloride ions and lead to a much faster onset of substrate corrosion, in a similar way to how cracks in the coating are thought to (Treacy *et al.* 1999). Further to this, it was observed that during neutral salt spray corrosion testing, corrosion seemed to occur at a few small points in the coating, whilst most of the coating tended to stay intact for a long period of time. Therefore, it may be at the cracks and pores that corrosion starts and leads to the poor corrosion resistance seen.

'Pin-holes' were not apparent on the untreated substrate, even though it would appear that they were present before the coating was formed. This suggests that they were formed as a product of localised substrate dissolution that occurred in the treatment solution before, and as part of, the coating process. This phenomenon may be due to the acid attacking the surface prior to coating formation.

Studying simple molybdate coatings allowed a performance 'benchmark' so that improvements could be seen that were independent of any slight variations in substrate morphology and composition.

6.2 Enhancing Simple Molybdate Conversion Coatings for Zinc Surfaces

6.2.1 The Effect of Acids Used to Adjust pH

The effect of acid used to adjust the pH of the simple molybdate system created a marked difference in LPR resistance of the coatings (Figure 5-2). Acidification with nitric acid led to a coating that offered reduced performance to the untreated electrodeposited substrate alone. This could be due to the coatings appearing continuous by eye, but being porous when viewed using FEG-SEM. The appearance of pores would inevitably compromise corrosion resistance because they would probably give rise to pitting corrosion.

Pitting corrosion is a localised form of corrosion that creates pores, or pits, in a metal surface. These pits are caused by localised areas of metal dissolution due to the corrosive media. The base of the pits become anodic because of the lack of oxygen

present and the surrounding substrate areas become cathodic, supplying electrons to drive substrate dissolution.

This may occur because nitric acid is a strongly oxidising acid and may have attacked some areas preferentially, causing localised zinc dissolution and leading to the onset of these pores. Coatings of this type have not been widely reported in the literature studied, the only similarities are with coatings investigated by Treacy and Co-workers in 1999, within their investigation they noted that the coating of a similar type was porous and this lead to appreciably rapid corrosion of the substrate (Treacy *et al.* 1999).

Molybdate samples formed from baths acidified with hydrochloric acid ('MoH120') performed around 20 % better than the untreated, electrodeposited Zn substrate in LPR tests (Figure 5-2). The coating had a black and brown finish with iridescence, in common with coatings studied by earlier authors (Gabe and Gould 1988, Wilcox and Gabe 1988, Wilcox 1989, Wilcox 2003, Magalhães *et al.* 2003, Lewis *et al.* 2006). Coating adhesion was observed to be relatively poor with areas of the coating flaking off upon contact. This also agrees with findings from the aforementioned earlier authors, who also noted the lack of adhesion of the darker molybdate coatings. After LPR testing was completed, there were areas visible to the naked eye where the coating had pitted. The combination of the poor coating adhesion and appearance of this surface pitting could be attributable for the relatively poor protective capabilities of these coatings.

It has been theorised that colour is a good indicator of coating thickness (Wilcox and Gabe 1988, Wilcox 1989). Iridescence is an effect that occurs when there is a thin film above a reflective surface. If the film has a thickness in the order of magnitude of the

wavelength of the incoming light, then, as the incident light passes through the film and reflects off the lower surface, some wavelengths are attenuated and some amplified, depending on the film thickness, as the light passes back through the film. Iridescent colour is therefore a good indicator of film thickness.

It may be that the MoH120 coating was formed at too high a rate, possibly because the acid led to rapid deposition of the molybdate coating so that the substrate oxide formed a very small part of it. This would suggest that the coating was more a 'deposit' than a well adherent 'conversion coating', where the substrate oxide forms a significant part of the final coating. By definition a conversion coating is a mixture of substrate and treatment metal oxides and hydroxides (Biestek and Weber 1976). In contrast, a deposit is made up of a substance with little interaction chemically between the substrate and coating. The lack of adherence could be attributable to this coating being made up mainly of a deposited structure. Poorly adhered coatings will, by definition, expose the substrate, leading to localised corrosion in these areas, Figure 5-36 is an example of this phenomenon. SEM investigation of the interface region, using the cryofracture technique would have given more conclusive results of this hypothesis; it was, however not used for the relatively poorly performing samples of this type.

Coatings formed from solutions acidified with orthophosphoric acid (MoP120) retained the lustrous silver finish of the electrodeposited Zn surface, with light brown tinges towards the edges. Magalhães *et al.* (2003) used a similar treatment solution to the one studied here and found that the coatings obtained had a slight brown colouration. This suggests that the coatings were very thin, too thin to interfere with the incident visible

light and hence they did not have the iridescent appearance on the typical thicker conversion coatings. Thin hexavalent and trivalent chromium conversion coatings have been reported with a similar appearance, with thicknesses thought to range from ~ 60 nm for Cr(III) coatings and ~ 80 nm for Cr(VI) coatings (Hulser 1999, Bibber 2008), so it can be deduced that the MoP120 type coating may have had a thickness in this region.

LPR testing showed the MoP120 coatings to increase the protective capability of the untreated electrodeposited Zn surface by over 150 %, as measured in Figure 5-2, a promising result for a simple molybdate treatment. The enhancements in the protective capabilities of the coatings can be thought to be due to the coating being homogeneous and non-porous, in contrast to the cracked simple molybdate coatings discussed previously in this section.

The chromate coated samples had a relatively high protective capability, which was around ten times higher than the electrodeposited Zn substrate and four times higher than the highest performing molybdate coating, MoP120, this was demonstrated using LPR testing, the results of which can be found in Figure 5-2. After testing, the coatings appeared intact and did not show the pitting exhibited by the MoN120, MoH120 and MoS120 molybdate coatings.

When examined using FEG-SEM chromate coatings appeared cracked and fairly poorly adhered to the substrate (Figure 5-15). The cracks were aligned, in contrast to the platelet type structure seen on the surface of the MoS120 (‘simple molybdate’) samples. This is not typical of hexavalent chromium treated surfaces, as discussed in Section 1.4.5.7, usually a more random crack structure analogous to the cracked molybdate

coatings discussed previously is apparent (Biestek and Weber 1976, Gabe 1978). FIB-SEM was used (Figure 5-16) to determine coating thickness and this was found to be around 350 nm, which is in agreement with the iridescent appearance reported by Hulser 1999 (200-300 nm) and Winn and Dalton in 2008 (200 nm).

6.2.2 The Effect of Immersion Time

The rationale for investigation of increasing immersion time was to evaluate whether the MoP120 type coatings could be thickened, thus providing enhanced corrosion resistance. This was because of the increased barrier protection that having a greater coating thickness could afford. Increasing immersion time gave increases in LPR resistance until treatment times of 120 s, then reductions in LPR resistance were seen (see Figure 5-3). It was clear that 120 s was the optimum immersion time. After 120 s treatment time, the coating could have lost adhesion or exposed the substrate, causing poorer corrosion resistance, in common with the thicker molybdate coatings studied previously and by other authors (Wilcox and Gabe 1988, Wilcox 1989, Wharton *et al.* 1996, Almeida *et al.* 1998, Magalhães *et al.* 2003, Lewis *et al.* 2006). It is possible that there was a trade off with the barrier to corrosion provided by thin, non-porous coatings and the increased amount of coating present to be oxidised by the corrosive species in the testing media. As a thicker coating would be able to provide higher corrosion resistance, as thicker types of chromate coatings are known to (Biestek and Weber 1976, Hulser 1999).

6.2.3 The Effect of Solution pH Modification

Investigation of modification of treatment solution pH showed that pH 5.0 was the highest performing in terms of coatings with the highest corrosion resistance (Figure 5-4). This may be due to the theory, discussed in the previous section, that there is an optimum coating thickness for corrosion resistance. Solution pH is known to have an effect on coating formation rate, with lower pHs increasing substrate dissolution. Increased coating dissolution leads to a localised reduction in pH at the substrate to coating interface, leading to increased coating formation rate. This is occurs until the solution pH is too low, less than about pH 2.0. At this low pH dissolution is too high for a coating to be formed as substrate etching occurs where the substrate surface is dissolved before it can react with the molybdate anion and produce a conversion coating (Wilcox and Gabe 1988). Many authors have suggested pH 5.0 as being the optimum pH for molybdate treatments, this is because of the lower dissolution of the substrate surface, which allows the molybdate anions to react with the surface and form a conversion coating. Tang *et al.* (1994) stated that, for their 'molyphos' system, solution pH was not critical but adjustments in immersion times needed to be considered for variances in pH because of the differences in coating formation rate. For subsequent experiments in the present investigations, pH 5.0 was selected as the optimum pH.

6.2.4 The Effect of Oxidising Agent Additions

The rationale for the addition of an oxidising agent was that the chromate anion is known to have a strong oxidising potential, whereas the molybdate anion does not

(Cotton *et al.* 1999), therefore it does not easily form reduction and oxidation products on the substrate surface, hence longer immersion times being commonplace. Therefore compounds to increase the oxidising 'power' of the treatment solution were investigated.

Improvements in LPR resistance were seen with both nitric acid and sodium nitrate additions, with sodium nitrate leading to slightly higher LPR resistances (Figure 5-5). The coatings appeared slightly iridescent, suggesting that they were thicker than the colourless coatings formed without these additions. This suggests that the coating rate was increased by the increase in zinc dissolution that the addition of an oxidising agent would have led to. Coatings with nitrate additives had the highest LPR resistance of any coatings discussed so far, showing an increase of 250 ΩCm^2 over the Mo5P120 coating. This was encouraging and led to nitrate being used in subsequent investigations with a view to producing an enhanced molybdate based conversion coating.

6.2.5 The Effect of Sodium Gluconate Additions

Sodium gluconate was added as a complexant, with the rationale that that it may be able to stabilise the molybdate anions in solution in a state that could produce an effective coating in a similar way to coatings studied by Han *et al.* (1996). LPR values were actually decreased with the addition of sodium gluconate; suggesting that any chemical change that occurred in the treatment solution due to this additive was detrimental to corrosion resistance possibly changing the coating composition or morphology (see Figure 5-5). Coatings appeared iridescent blue, suggesting that they were thicker than the Mo5P120 coatings and that the addition of sodium gluconate had

increased coating formation rate, this may have led to porosity. When studied using FEG-SEM, they appeared cracked and porous. In common with coatings discussed previously, the cracked surface may have led to the acceleration of corrosion and significant decrease of protective capabilities demonstrated by the poor results for LPR resistance seen.

6.2.6 The Effect of Increased Molybdate Concentration

Molybdate concentration was increased to 60 g cm^{-3} to mirror the coating system proposed by Song and Mansfield in 2006 and to evaluate whether a more effective coating could be produced. Coatings appeared very similar to the Mo5P120 coatings, showing only a light brown staining on the edges. The increase in LPR resistance was small, at ~150 ΩCm^2, but was consistent nonetheless (see Figure 5-5). Subsequent coatings were investigated using this increase in molybdate concentration.

FEG-SEM investigations revealed a microstructure that was very similar to the Mo5P120 type coatings, with a porous structure mirroring the untreated, electrodeposited Zn surface. Coating thickness was around 60 nm, a slight increase over the Mo5P120 surface.

6.2.7 The Effect of Sodium Orthophosphate Additions

Phosphate was added in the form of sodium orthophosphate, with a view to forming a phosphate containing heteropolymolybdate solution in the form of $PMo_{12}O_{40}^{3-}$ (Steifel 2001). It was theorised that this ion would react with the Zn substrate, forming a well adhered, unreactive coating.

Coatings appeared iridescent gold with purple edges, suggesting that a thicker coating was formed. LPR resistance was actually decreased to ~2 000 ΩCm^2 (Figure 5-5). This was a significant decrease and this may be as a result of too high a concentration of phosphate present, leading to a mainly phosphate coating instead of a molybdate phosphate formulation. It may have also been that the coating deposited onto the surface instead of forming a true conversion coating, leading to poor coating adhesion. It was important to continue to investigate the addition of further phosphate species, as this had been found to be effective, by Tang *et al.* (1994) and Song and Mansfeld (2006), in producing an effective molybdate conversion coating system.

6.2.8 Synergistic Effects of Additives

The rationale for investigating the synergistic effects of additives was to enhance the coating system further, using combinations of additives that have been identified to work synergistically with molybdate in the literature survey (Wilcox *et al.* 1986, Kurosawa *et al.* 1989, Tang *et al.* 1994, Han *et al.* 1996, Boose *et al.* 2001, Magalhães *et al.* 2003, Song *et al.* 2006). Increased molybdate concentration and sodium nitrate additions were investigated first. An increase in LPR resistance to ~ 4 000 Ω cm^2 was seen, significantly higher than the values obtained from these additions alone (Figure 5-6). The theory of the action of sodium nitrate in producing an enhanced coating has been discussed previously in Section 6.1.6 and the results remained encouraging with the addition to a higher concentration of molybdate to the treatment solution.

The addition of sodium gluconate to all of the treatment solutions decreased the LPR resistance to as low as ~ 1 100 Ω cm^2 (less than the untreated substrate alone) (Figure 5-

6). It was concluded that sodium gluconate was detrimental in creating a protective coating, in contrast to the positive findings of Boose and co-workers (2001) who stated the addition of sodium gluconate improved the corrosion resistance of a similar coating system, albeit on more corrosion resistant zinc-iron alloy surfaces. Gluconate is a complexant and although the authors did not state their reasons for its addition, it was thought that it was able to change the chemical state of the molybdate in solution, creating more favourable conditions for an effective coating to be formed. The poor corrosion resistance of coatings obtained from treatment solutions with sodium gluconate additives has been discussed previously in Section 6.2.5.

6.2.8.1 MoP Type Coating Characteristics

The effect of the combination of increased molybdate concentration, sodium nitrate and sodium orthophosphate additions produced a molybdate coating, termed '60MoNO3PO4'. This coating, named 'MoP' for subsequent discussion had an LPR resistance of > 9 200 Ω cm^2. There has been little reporting of LPR for molybdate based coatings on Zn surfaces, however, in the context of this study this value was very encouraging as it was ~75 % as high as a chromate sample (Figures 5-2 and 5-6).

The MoP coating appeared grey and continuous, suggesting that it was thicker than the clear/ stained coatings and possibly thinner than the iridescent type coatings. FEG-SEM investigation showed coatings of this type to have a rough, porous, columnar microstructure, which the cryofracture technique revealed to be around 300 nm thick (see Figure 5-19). Coating adhesion was much better than the cracked coatings studied previously. Pores were around 100 nm in diameter, high magnification at the base of

the pores showed that there was a coating present; but it was very thin, at around 30-50 nm (similar to the simple MoP treated samples).

AES (Figure 5-27) showed the coating surface composition to be mainly made up of O, with approximately 16 % Zn, 8 % P and 4 % Mo, with an amount of chloride present that can be thought of as an impurity due to atmospheric exposure. This suggests that the coating was made up of a mixture of Zn, P and Mo oxides in an approximate ratio of 4:2:1 respectively. This suggests that it was a true conversion coating, where the coating is made up of a mixture of substrate and coating metal oxides. This would inevitably lead to the improved adhesion, supported by the fact that the coatings did not detach when the cryofracture technique was used to view them in cross-section.

6.2.8.2 MoP Coating Formation Theory

Using the data gained from AES surface composition measurements as well as documented data from similar coatings studied in the literature survey, it was possible to theorise about the coating stoichiometry and formation.

The presence of nitrate in the acidic media would have increased the substrate surface dissolution. The presence of molybdate and phosphate would have formed a heteropolymolybdate compound similar to $PMo_{12}O_{40}^{3-}$ which formed a compact coating containing Mo and P in a dense oxide layer. The Zn dissolved by the acid on the surface was incorporated back into the coating, either as a Zn oxide, hydroxide or zinc phosphomolybdate. Due to the conditions and species in the treatment bath, above 25°C in acidic media, it can be assumed that a heteropolymolybdate species, incorporating phosphorous was formed (see Equation 25) (Stiefel 2001).

$$PO_4^{3-} + 12MoO_4^{2-} + 16H^+ \rightarrow [H^+\ 25°C] \rightarrow PMo_{12}O_{40}^{3-} + 8H_2O$$ .....*Equation 25*

On the substrate surface there would have been dissolution and simultaneous hydrogen evolution (Equation 20).

Equations 33 and 34 show a possible coating formation route from a heteropolymolybdate, phosphomolybdate species to a zinc phosphomolybdate species that may have formed the coating.

The formation of zinc phosphomolybdate:

$$PMo_{12}O_{40}^{3-} + 24Zn^{2+} + 11PO_4^{3-} + 176H^+ + 164e^- \rightarrow 12Zn_2PMoO_7 + 88H_2O$$ .....*Equation 26*

The zinc phosphomolybdate compound could also have been formed from the simple molybdate and phosphate species present in the treatment solution (Equation 27):

$$MoO_4^{2-} + PO_4^{3-} + 2Zn^{2+} + 2H^+ + 2e^- \rightarrow Zn_2PMoO_7 + H_2O$$ .....*Equation 27*

The composition of zinc phosphomolybdate (2:1:1, Zn:P:Mo) is fairly close to the ratios of atoms found using AES (4:2:1), but there is still an amount of Zn and P that have not been accounted for. It may be the case that the coating also has a significant amount of zinc phosphate analogous to a phosphate conversion coating. The formation of this is shown in Equation 28 (Wiederholt 1965):

$$Zn^{2+} + PO_4^{3-} + H^+ \rightarrow ZnHPO_4$$ .....*Equation 28*

The formation of zinc phosphate as a constituent of the conversion coating would agree with the observations that the surface is micro-porous when viewed using FEG-SEM, as

phosphate coatings are known to be porous and crystalline when formed on zinc surfaces (Wiederholt 1965). Phosphate coatings are also known to have fairly poor corrosion resistance as a standalone treatment and need subsequent finishes, such as oils and lacquers to be applied to them to enhance their corrosion resistance to an acceptable level (Biestek and Weber 1976).

6.2.8.3 Investigation of Enhanced Coatings without the Addition of Molybdate

To evaluate whether the MoP types coatings' good performance in corrosion tests was due to the molybdenum being present, samples were treated in the same conditions, without the addition of molybdate to the treatment solution. The results from LPR testing of this coating showed little improvement over the untreated Zn (Figure 5-7). Visually, the surface appeared similar to the surface of the MoP sample, with a grey colour. These results suggest that although it was not a major constituent of the MoP coating, the presence of Mo lead to the significant enhancement of corrosion resistance seen.

6.2.9 Dual Layer Coatings

It was clear that attempts to thicken the coating by modification of pH and immersion time created coatings that had poorer corrosion resistance than the clear and grey MoP type coatings. Therefore, to further improve the LPR and corrosion resistance of the coatings different techniques for thickening the coating were employed. These were, the use of silica and silicates as well as dual layer systems using rare-earth metal containing solutions.

6.2.9.1 Silica Additions

Nano-sized colloidal silica was added to the molybdate solution with a view to creating a thick and dense, corrosion resistant coating. Coatings formed from solutions containing colloidal silica appeared dark grey, with the higher (50 g dm^{-3}) silica concentration having a matt finish and the lower (20 g dm^{-3}) concentration appearing glossy. Both coatings had a lower LPR value than the MoP system at ~ 3 000 ΩCm^2 and ~ 5 400 ΩCm^2 for the high and low silica concentrations respectively (Figure 5-8). The high concentration silica added sample appeared darker, suggesting that it was thicker and FEG-SEM investigations confirmed this. They also showed that this coating had a crack structure similar to the simple molybdate coating, with crack widths of up to 5 µm. The substrate exposure that these cracks caused would have inevitably led to the lower corrosion resistance seen with these samples.

The result for the low concentration solution was encouraging however, and because it produced a thicker coating than the MoP solution it was investigated further with an investigation to assess if it performed better in NSS tests.

Low concentration nano-silica containing coatings, termed 'MoPSi', were NSS tested. They resisted the formation of 5 % white rust for an average of 20 h. This was a very promising result and among the highest of any molybdate based conversion coatings reported on electrodeposited acid zinc surfaces. The dense, silica rich outer layer improved the corrosion resistance of the coating as has also been reported to by other authors (Jesionowski *et al.* 2001, Hara *et al.* 2003 , Palanivel *et al.* 2003, Dalbin *et al.* 2005, Liu *et al.* 2006). However, the NSS resistance was lower than expected, despite

the fact that the coating was thicker and denser than the MoP coating (Table 5-13). This suggested that there was another mechanism leading to the poorer corrosion resistance other than the density of the coating, such as porosity or coating adhesion. These factors were investigated for partially corroded coatings in Section 5.5.6, discussion for this can be found in Section 6.3.4.

FEG-SEM investigation of the 'MoPSi' coatings revealed a cracked microstructure similar to 'simple' acid molybdate and chromate coatings studied (see Figure 5-20). The cracks were different because their widths were much reduced and they were discontinuous. These coatings were also free of the pores and 'pinhole' phenomena that were thought to have led to corrosion on some of the other types of simple acid molybdate coatings.

AES depth profiling (Figure 5-28) showed the surface coatings to be made up of a dense layer of Si and O in the ratio of 1:2, suggesting that it was made up of SiO_2. Ion ablation was used to determine the composition through the depth of the coating, 1200 s of ablation was required to produce a signal from zinc, suggesting that the coating was relatively dense and thick. There was not any molybdenum detected in the coating using this method, but it may have been that the silica coating formed as a deposit over a thin zinc molybdate conversion coating because EDXA data showed that Mo was present. Table 5-17 shows the EDXA data and there is a difference between the composition of the coatings examined with the two techniques, this is to be expected, because as explained in Section 4. Experimental Techniques, AES is considered a surface sensitive technique, whereas EDXA, with a sampling depth of ~ 1 µm, a bulk technique. The EDXA data clearly showed the Mo and P to be present in the bulk of the coating,

suggesting that a conversion coating was formed and the colloidal silica was present throughout the coating.

The use of nano-sized silica as an additive to increase the coating thickness was successful in creating an improved coating system.

6.2.10 Silicate Sealants

Silicate sealants were investigated to impart a layer of silicate onto the coating surface, thus sealing the coating. It was hoped that this would provide an un-reactive barrier to corrosion. LPR results were much poorer than the MoP base system, but it was hoped that the vast increases in coating thickness would lead to improvements in NSS resistance. FEG-SEM investigations revealed that the silicate sealed coatings were in excess of 9 µm thick (Figure 5-22a) and had large pores that were in excess of 100 µm in diameter (Figure 5-22b). These would inevitably lead to pitting corrosion in local areas, giving the relatively poor corrosion resistance indicated by the LPR values. The coatings also had poor adhesion, which was evidenced by the voids seen between the coating and substrate in the micrograph of the cross-section.

To investigate whether the porosity was a product of the silicate layer thickness, and whether the appearance of pores could be decreased by producing thinner coatings, silicate coatings were formed with immersion times of 10, 20 and 30 seconds. These coatings gave lower corrosion resistance than the 120 s treated sample and FEG-SEM investigation showed that they remained porous, so they were not investigated further.

As a control, silicate sealants were investigated without the molybdate coated layer. They were LPR tested and the average values were only slightly less than the coatings with the MoP initial treatment (Figure 5-10). This suggests that the conversion coating was at least partially dissolved by the alkaline silicate treatment solution and was only able to provide a minimal level of protection to the surface. The LPR results as well as the findings from the FEG-SEM analysis were not encouraging. However, because of the coating thickness and findings from the authors investigating coatings of this type previously, it was decided to NSS test these coatings.

In NSS tests the highest performing coatings were MoPSi-S1 and MoPSi-S2, which showed 5 % WR after 10 hrs (Table 5-13). This was a poor result, but was somewhat expected due to the poor results seen with LPR corrosion testing. Initiation of corrosion was localised, with some areas showing WR corrosion after < 8 h, whilst other areas remained uncorroded for much longer, more than 24 h. This suggests that the pores in the coating lead to the onset of pitting corrosion and the areas of continuous coating offered much more corrosion protection to the surface.

The addition of sodium metasilicate to the MoP molybdate treatment solution led to the silicate gelatinising, coatings were still able to be formed, however, the increase in solution viscosity made agitation difficult. LPR results were poor, at around 2 500 Ωcm^2, therefore investigation of coatings of this type was discontinued (Figure 5-10).

In conclusion, silicate sealants were not effective in producing a more corrosion resistant molybdate-based conversion coating. This was probably due to their poor adhesion and high porosity. Attempts to reduce these factors were also unsuccessful

and the resultant coatings performed much poorer than the highest performing enhanced molybdate based coatings studied so far.

6.2.11 Rare Earth Metal Conversion Coatings

Rare earth metal (REM) coatings were investigated with a view to evaluating whether they could be incorporated into a composite molybdate/ REM system. REM coatings were investigated primarily to give a baseline to compare any multi-layer coatings to. REM nitrates are good semiconductors and are relatively un-reactive, therefore it was hoped that they could provide an effective protective surface. They have also been hypothesised to be capable of 'self-repair' in a similar way to chromate coatings, making them an ideal candidate to be investigated as a replacement for the aforementioned coatings (Trabelsi *et al.* 2005).

Lanthanum and cerium nitrates were investigated as these were thought to be capable of forming coatings on Zn surfaces (Mansfeld *et al.* 1992). The majority of research, however has focussed on their use on Al surfaces (Rudd *et al.* 2000, Aramaki 2005, Conde *et al.* 2008) with little documented evidence of their performance on Zn surfaces.

Cerium nitrate coatings formed at room temperature gave the highest LPR resistance of ~ 2 600 Ωcm^2 (Figure 5-11). Interestingly, they were similar in appearance and LPR resistance to the 'simple' molybdate-orthophosphoric acid treated samples studied previously, suggesting that there could be similarities with the coating structure and thickness. Other REM treatments did not convey a similar level of protection to the

substrate, imparting only slight improvements over the untreated electrodeposited acid Zn substrate.

The coatings formed at 50 °C were interesting because they produced a more iridescent coating, suggesting that they were thicker. Even though they were poorer in LPR tests, they were investigated further with their incorporation into dual layer systems. This was because none of the coatings performed particularly well in LPR tests so it was decided to investigate all of the coatings further to evaluate any benefits they may have had when used in a composite coating.

6.2.12 Rare Earth Metal and Molybdate Dual Layer Systems

Investigations to incorporate the REM nitrates into a molybdate solution proved unsuccessful because of the poor solubility of the REM nitrates. Solubility was investigated at a variety of temperatures, times and concentrations, with no significant improvements seen. Instead, dual layer coatings were investigated, with first an immersion in an REM solution, then an immersion in the MoP solution.

REM-MoP coatings appeared similar to the MoP type coatings, with a grey finish and some iridescence. LPR resistance was inferior to the MoP type coating, with the lanthanum nitrate-MoP coating at room temperature being the highest performing treatment of this type with a LPR value of ~ 8 300 Ω cm^2 (MoP 9 300 Ω cm^2) (Figure 5-11).

Because REM-Molybdate coatings did have some of the highest recorded LPR values for molybdate coatings, they were corrosion tested using NSS testing.

NSS testing indicated that the coatings of this type showed 5 % white rust corrosion after 8-10 h, this was a fairly poor result. In this case, the enhanced LPR data did not correlate with the NSS results (Table 5-13).

The coatings were examined using FEG-SEM to view the coating structure in cross-section using the cryofracture technique. The coatings appeared approximately 200 nm thick, with a non-porous outer layer (see Figure 5-23). There were voids at the substrate-coating interface that may have caused poor NSS performance due to loss of adhesion and allowing the ingress of corrosive species.

6.2.13 Cobalt Nitrate Additions

Investigation was carried out into cobalt additives, primarily because of a report carried out by Meyers *et al.* (1994), that mentioned the effectiveness of a cobalt and molybdenum based conversion coating as a chromate replacement, the authors did not give specific details about the coating composition. Cobalt has also been used as an additive for Cr(III) based systems, where it is thought to be a catalyst to the surface reactions. Co(II) is also capable of forming heteropolymolybdate compounds in solution in a similar way that phosphates are (Stiefel 2001).

Cobalt nitrate was used as an oxidising agent and there was already a nitrate oxidising agent present in the treatment solution, therefore would serve to increase the oxidation rate of the surface slightly, without having a significant influence on the other species present in the treatment solution.

Solubility was not complete at pH 5.0, trials with heating and pH modification showed full solubility at pH 3.0. Coating formation rate appeared to be quite high, with the appearance of black coatings after 120 s immersion. It has been suggested that the Co (II) ions act as a catalyst for surface reactions to create the conversion coating. This theory was certainly plausible in this case, as black conversion coatings are generally thicker than clear and grey ones. It can be deduced that although the addition of cobalt nitrate did produce some coatings that appeared promising, in that they were thick and homogeneous. Their candidacy for being incorporated into a possible chromate replacement system is limited, because of the issues with cobalt being identified as a carcinogen and the possibility of restriction of use in the future by the EU (2009).

FEG-SEM investigations showed the surface to be rough and crystalline, with a thickness of around 750 nm (Figure 5-24). Like the MoP type coating, this coating appeared porous, but investigation showed pores did not expose the substrate (Figure 5-24). The coating composition was determined by AES, and there was a significant amount of Co present, suggesting that not only was the Zn surface catalysed by the Co but also it formed part of the coating. The dark iridescence can be thought of to be due to the surface roughness as well as the interference effect of the coating thickness.

6.3 Corrosion Initiation Analysis

Partially corroding coatings to investigate the onset of coating failure using 5 % NaCl immersion and FEGSEM was a successful technique that had not been widely reported in the literature studied. Its usefulness was such that the ability to investigate failure modes of coatings could be seen and conclusions made about the weaknesses of the

coatings that led to their failure. Theories for the failure modes for the samples studied can be found in the relevant sections below.

6.3.1 Initiation of Corrosion of Electrodeposited Zinc Coatings

After a short period of exposure, 20 min, in 5 % NaCl (aq), there was already evidence of corrosion on the Zn surface. These initial signs of corrosion took the form of crystalline structures of around 5 µm across (see Figure 5-30a). The visual appearance after 2 h was a slight surface dulling and a light matt effect. As mentioned in the results section, the samples corroded to 2 h were selected for further analysis. There were two distinct areas that were apparent, the more intact 'background' and 'corroded' areas. 'Corroded' areas were areas where crystalline corrosion product was present. AES was used to measure the composition of these areas; Figures 5-30b and c show the results of these measurements.

The AES data, shown in Figures 5-30b and c, show the surface composition in the two areas of the 2 h corroded substrate. The 'intact background' area can be thought of to be made up of zinc oxide (ZnO) some zinc hydroxide ($Zn(OH)_2$) as a layer on the surface along with a small amount of zinc chloride ($ZnCl_2$) (Slunder *et al.* 1971). The crystalline corrosion product, where the 'corroded' spectra has been taken from can be thought to be made up of a mixture of corrosion products mentioned earlier, but with a much greater prominence of chloride corrosion product.

6.3.2 Initiation of Corrosion of Chromate Coatings

The primary initial failure mode for coatings of this type was coating delamination. The coating lost adhesion by a mechanism where it appeared high internal stresses rolled the coating up. This could have been caused due to localised corrosion occurring in the cracks of the outer layer of the coating causing local high stress which produced a localised loss of adhesion. Despite the delamination, areas that appeared to have the coating removed still had a significant amount of Cr present. This suggests that there was a well adhered 'under-layer' of coating below the highly stressed layer, leading to substrate protection despite the removal of a large amount of the coating. It is not clear whether this layer was formed before the coating delamination; or whether it was evidence of re-passivation through a 'self-repair' process that coatings of this type have been documented to be capable of. Leachable Cr(VI) species are said to re-passivate the damaged areas of the coating with the subsequent formation of Cr(III) oxides (Biestek and Weber 1976). The data shown in Figure 5-31a and b show the approximate composition of the two areas of the chromate coatings.

The intact coating was probably made up of a mixture of chromium oxides and hydroxides, along with some zinc oxide and hydroxide (Cr_2O_3, $Cr(OH)_3$, ZnO, $Zn(OH)_2$). Some chloride corrosion product was also probably present, most likely as $ZnCl_2$ as zinc corrodes preferentially to chromium. The 'corroded' area of the coating can be thought of to be made up of a mixture of the products mentioned above, but with a higher ratio of zinc and chloride corrosion product.

6.3.3 Initiation of Corrosion of Simple Molybdate Coatings

Simple molybdate coatings appeared to fail due to localised corrosion at the crack junctions that were present due to it being a highly cracked surface (Figure 5-32). This lends credence to the theory that the substrate is exposed at the crack junctions, similar to the coatings studied by Treacy and co-workers (1999). This theory is supported by the localised depletion of Mo at the corroded areas, which were crack junctions (Figure 5-33). This corrosion would have inevitably led to the appearance of 5 % white rust from the Zn substrate in NSS tests with less than 6 hours of exposure which was apparent in NSS testing.

In contrast, the protective capabilities to 5 % red rust were relatively good, suggesting that the coating was able to provide a level of protection to the substrate after white rust was apparent. This either suggests that the coating failed fairly exclusively at the crack junctions or that there was a large amount of the coating that was insoluble and provided protection long after the appearance of 5 % white rust (Table 5-13).

The corrosion behaviour was certainly contrary to the Cr(VI) coatings, that had film delamination and appeared to expose more of the substrate than these coatings did. The fact that the Cr(VI) coatings were not corroded and these coatings were, does suggest that molybdate coatings were not capable of ‘self-repair’. This agrees with the assertion that molybdate is a weaker oxidising agent than chromate, discussed in the literature survey.

The site specific AES data (Figure 5-33) showed that the intact areas of the coating also have a much higher Mo concentration than the corroded areas; there are two reasons that may have led to this. The first reason could be that the corrosion occurred in areas with low Mo concentration initially which would be cracks or pores in the un-corroded coatings. The second possible reason could be that the corroded areas were depleted of Mo, because of the formation of soluble Mo chlorides, which could have been removed from the surface during rinsing, after the immersion. It is likely that a combination of these two mechanisms occurred, with corrosion initiating at the areas where less coating was present and forming local soluble Mo(IV) and Mo(III) chloride compounds as reported by Treacy and co-workers (1999).

6.3.4 Initiation of Corrosion of MoP Coatings

After 4 h of 5 % NaCl exposure there was an appearance of small white spots that were only just visible to the naked eye. These were less frequent and smaller than those seen on the 'simple' molybdate samples. FEG-SEM investigations revealed these to be blisters in the coating surface of about 70 µm in diameter (see Figure 5-34b). The appearance of pores would inevitably lead to localised coating weakness and eventually failure through pitting corrosion. The pores were fairly infrequent, in agreement with the observations from the NSS testing; that corrosion occurred in local areas, with the majority of the coating remaining intact long after 5 % white rust was seen.

Site specific AES was carried out on the 'background' areas, which appeared un-corroded and the 'blistered' areas described above. The data in Figure 6-1 shows the atomic composition of these areas as well as an un-corroded coating of the same type.

This was used to make conclusions about the coating breakdown mechanisms; these can be found in the relevant sections below.

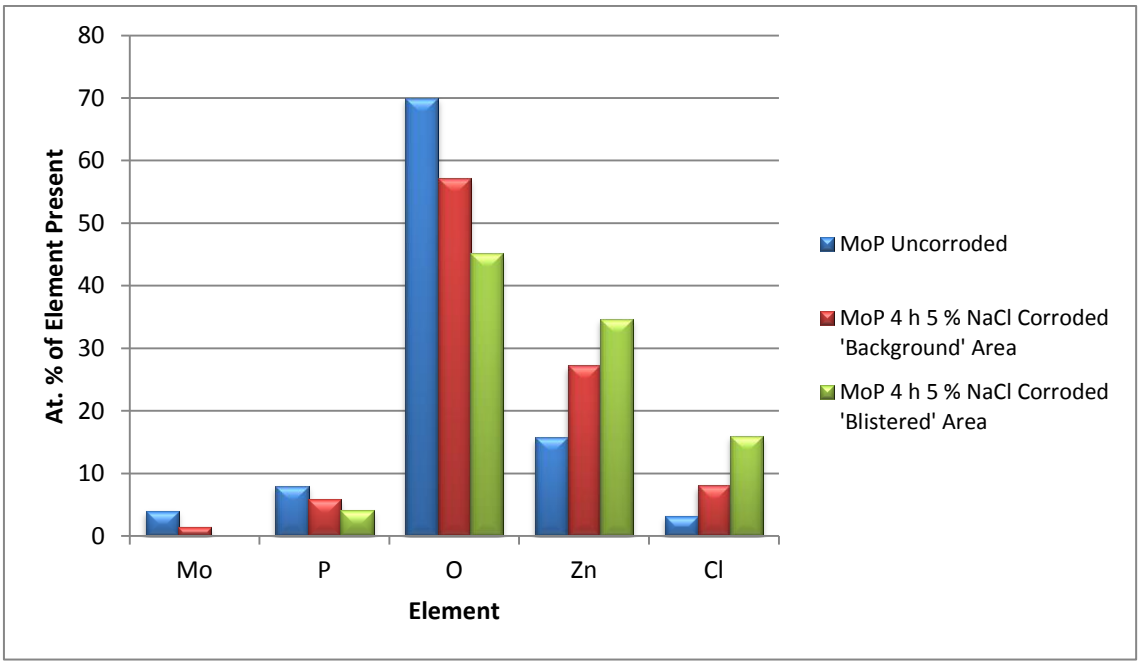

Figure 6-1: *Data obtained from AES measurements of the MoP coatings in un-corroded and slightly corroded states.*

6.3.4.1 Background Area

The background area of the coating can be thought of as made up of zinc phosphomolybdate compounds similar to the un-corroded coating discussed in Section 6.1.10.1. It is likely that there was some chloride corrosion product present in the form of Zn or Mo chlorides. Even in the apparently un-corroded background area, there was an increase in Zn concentration, coupled with a decrease in Mo and P concentrations (see Figure 6-1); which would have led to the onset of Zn corrosion. So it can be deduced that when the coating was exposed to chloride media; some of the coating was removed and substrate corrosion ensued. Because of the good corrosion resistance that these coatings exhibited, the 'background' area after 4 h, 5 % NaCl immersion was

probably quasi-stable. These areas of the coating resisted voluminous white rust formation for much longer than the latter, appearing unchanged even after 5 % red rust was seen in the blistered areas and the test was terminated (after 144 h).

6.3.4.2 Blistered Area

Coating breakdown appeared to initiate at the blistered areas of the coating. Blisters were not present before any exposure to chloride media; therefore they can be thought of to be the precursor to coating failure (Figure 6-1). After 4 h exposure to 5 % NaCl, some of the blisters were just apparent to the naked eye as very small white spots. Site-specific AES scans showed these features had a lack of Mo species present, which suggests the latter were removed by corrosive dissolution in the chloride media. The blistered areas also had a much larger amount of chloride present; this can also be thought of to be due to localised corrosion in these areas. The increase in Zn concentration is indicative of substrate exposure, meaning that there was very little coating present in these blistered areas.

The blistered areas were, without question, the weak-points of the coating and the observations made with the film breakdown during NSS testing add further credence to this. Why these areas appeared, however, was unclear. They may have been due to imperfections on the coating surface caused by areas of damage or due to inhomogeneity in the topography of the substrate surface. Mechanical or chemical damage would produce an area where substrate was exposed. Topographic inhomogeneity could cause localised stresses in the coating, which would cause weakness in the coating. When exposed to corrosive media, these areas would corrode

preferentially and, due to Mo being a poor oxidising agent, there would be little coating self-repair. This would mean that the mechanism of further corrosion would be pitting corrosion, which, as discussed previously is a localised form of corrosion that occurs in areas of coating weakness.

6.3.5 Initiation of Corrosion in MoPSi Coatings

The addition of nano-sized silica produced a dense, slightly cracked coating which has already been discussed in detail in Section 6.2.9.1. After 4 h of 5% NaCl exposure, the MoPSi coating appeared uncorroded; the main visual difference was that the surface appeared duller. FEG-SEM analysis showed the surface to have a structure similar to an uncorroded surface of this type, with only the prominence of pores of around 5 – 10 µm in diameter showing any difference (Figure 5-36). The pores were a factor of ten smaller than those seen on the corroded MoP treated surface and were not visible to the naked eye.

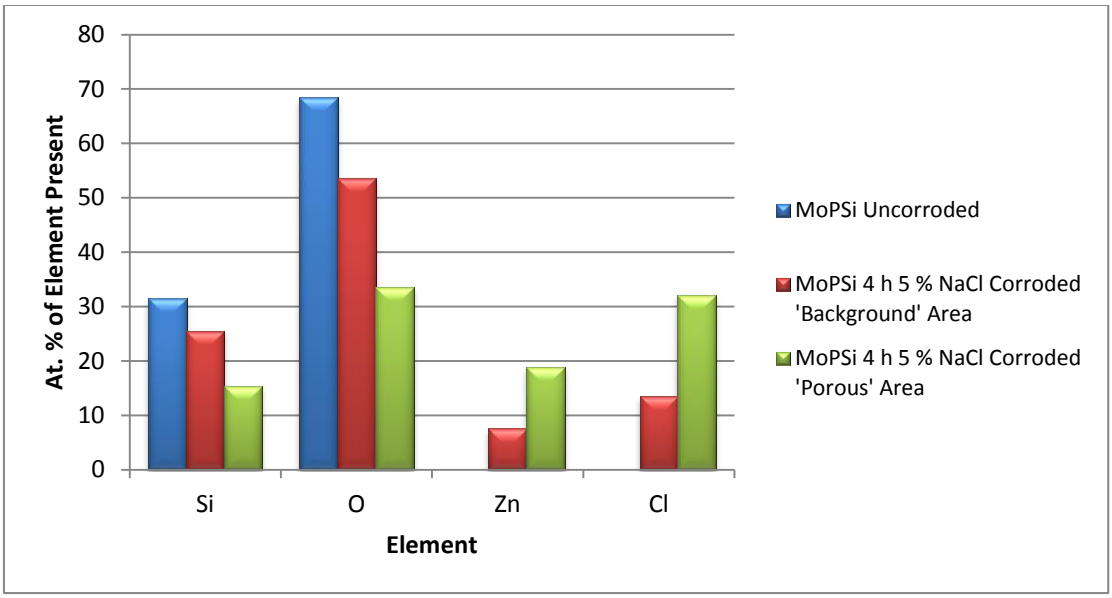

Figure 6-2: *Data obtained from AES measurements of the MoPSi coating in un-corroded and slightly corroded states.*

The coating composition for the intact and porous areas of the coating as well as an un-corroded coating of the same type can be found in Figure 6-2. It is important to note that there was a lack of Mo present; this was consistent with the findings with AES investigations of un-corroded coatings of this type, as mentioned in Section 6.2.9.1. The general area of the coating can be thought to have been made up of SiO_2 and some $ZnCl_2$. The appearance of $ZnCl_2$ was probably due to some substrate corrosion in the cracked and porous areas, with the main body of the coating having a surface rich in SiO_2, analogous to the un-corroded MoPSi treated sample. In the porous area tested, the concentrations of Si and O were lower than the more intact, 'background' areas and there were proportional increases in the Zn and Cl concentrations, suggesting that substrate corrosion occurred preferentially in these areas. In contrast to the MoP coatings, there was still a significant amount of original coating constituents present in the porous areas of the coating; this was possibly due to the small size of the pores, as

they were around ten times smaller than the blisters seen on the corroded MoP coatings and were more difficult to gain spectra from, meaning that the spectra were taken from areas that covered a few of these pores.

Coating breakdown for coatings of this type was probably due to pitting corrosion which occurred in these porous areas. As with the MoP coatings, it was not clear whether the pores were a product of the substrate or from areas of weakness that were caused by the coating formation process. It may have been that corrosion occurred in a cracked area, forcing a 'platelet' of coating to become detached because of the volume expansion of the substrate as it corroded.

7 Conclusions

7.1 Techniques Used

1. Linear Polarisation Resistance testing was shown to be a suitable technique to assess comparative corrosion resistances of the coatings studied.

    1.1. The quantitative nature and reasonably short testing time (30 mins) allowed for representative data to be obtained.

    1.2. This enabled any slight enhancements gained from coating modification to be quantitatively assessed.

2. NSS corrosion testing was a much more aggressive technique; it was used when coatings had been found to perform relatively well in LPR tests. The most enhanced coatings were selected for this and had their corrosion resistances compared with industry standard chromate coatings.

    2.1. Performance in the NSS tests were found to correlate experimentally with LPR tests for most coating variations studied.

    2.2. The main exception to this rule was the REM molybdate dual-layer coatings, that performed relatively well in LPR tests and very poorly in NSS tests.

3. Electron microscopy was shown to be a powerful technique for viewing the surface morphology of the samples studied and allowed for conclusions to be made about the coating structure with respect to its corrosion resistance. These were:

3.1. Simple molybdate coatings were cracked, also with the appearance of dimples at some of the crack junctions. The zinc substrate was inevitably exposed by these cracks, meaning that corrosion resistance was poor.

3.2. MoP type nhanced molybdate coatings were porous, with 100 nm pores apparent on the surface. Although the the pores looked as if to expose the substrate, the cryofracture technique showed there to be a small amount of coating at the base of the pores. This coating, provided barrier protection to the substrate, preventing the ingress of corrosive species.

3.3. MoPSi type enhanced molybdate silica coatings were cracked, but not as so as to create the crack junctions that the simple molybdate coatings did, furthermore the cracks were much thinner than the simple molybdate coatings. Coatings were also dense with a particulate type structure that had excellent barrier properties which lead to the good corrosion resistance seen.

3.4. Chromate coatings were also cracked, and appeared to expose the substrate in between the cracks. EDXA showed the areas that appeared to exposed substrate to be made up of a chromate coating.

7.2 The Development of an Enhanced Molybdate Conversion Coating

1. Simple acid molybdate coatings performed relatively poorly in LPR tests in comparison to a commercially available chromate system. A typical simple molybdate coating would yield an LPR value of ~ 3 000 Ω.cm^2, whereas a chromate coating would be close to 12 000 Ω.cm^2. Furthermore, times to 5 % white rust were

even poorer in comparison, with simple acid molybdate coatings generally showing corrosion after two hours and chromate coatings typically after 120 h.

1.1. The molybdate coatings were improved in stages, by investigating and optimising process parameters such as molybdate concentration, immersion time, temperature, acid used to adjust pH, pH, oxidising additives, complexants, cobalt additives, rare earth metal additive and dual layer systems, silica nanoparticle additives and silicate sealants.

1.2. Optimisation of the above process parameters by LPR performance testing led to an enhanced molybdate conversion coating system.

1.3. The enhanced molybdate system contained: 60 g dm^{-3} sodium molybdate, 90 dm^{-3} sodium orthophosphate and 10 dm^{-3} sodium nitrate adjusted to pH 5.0 with orthophosphoric acid at 60 °C and an immersion time of 120 s.

1.4. This enhanced coating offered a LPR resistance that was ~ 75 % of the chromate reference samples; 9 000 Ω.cm^2 against 12 000 Ω.cm^2. This coating was relatively thin at around 300 nm, decreasing to < 50 nm at the bottom of pores (Figure 5-19), present on the surface, despite attempts to thicken the coatings with nanoparticle additions, these porous coatings exhibited the highest corrosion resistance of the any of the molybdate type coatings studies.

2. Silica nano-particle containing coatings were investigated. These were of a modified structure and composition, with the coating being significantly thicker and more dense in structure.

2.1. These ‘MoPSi’ coatings did not perform as well in LPR tests, having average LPR values of approximately 5 000 Ω.cm^2, possibly due to slight cracking, allowing the ingress of corrosive chloride species.

3. Attempts were made to create multilayer coatings using REM nitrates and MoP or MoPSi as a second stage treatment.

3.1. Although some of these coatings showed encouraging LPR values, they performed poorly in NSS tests.

3.2. Multilayer coatings were also created using silicate sealants; these were found to deposit a layer of silicate of up to 9 µm thick.

3.3. Adhesion was problematic with the multi-layer coatings, possibly because of the high water content of the coatings contracting when under vacuum, as was the appearance of pores that probably led to the poor corrosion resistance seen, where 5 % white rust was seen within 10 hours in natural salt spray corrosion tests.

7.3 Corrosion Resistance

1. The enhanced molybdate and molybdate-silica coatings were found to perform very well in NSS tests compared to molybdate coatings studied in the literature, with average times to 5 % white rust of 24 h and 20 h respectively. This was an encouraging result and demonstrates the potential that these coatings have of being the basis of a truly ‘non-chromium’ replacement. It must be remembered that the initial Cr(III) based coatings (studied previously by researchers in the 1980s) resisted

white rust for up to 24 h in NSS tests, but the second generation coatings have been reported to resist for more than 300 h.

1.1. This gives rise to the possibility that the molybdate coatings studied here could be subsequently improved by adaptation of the treatment solution, to produce a coating with increased integrity and decreased solubility.

2. Less successful was the investigation into the use of top-coats to further improve the corrosion resistance of the enhanced molybdate based coatings. It appeared that the commercially available silicate sealants produced a layer that was relatively thick (> 5 µm) and heterogeneous.

2.1. Failure of silicate sealed coatings was probably due to the apparent etching of the conversion coating from the surface, giving rise to substrate exposure in localised areas.

7.4 Partially Corroded Coatings

1. There were clear differences in how the coatings studied degraded in flooded chloride media immersion tests:

1.1. The untreated, electroplated Zn surface produced voluminous corrosion products quickly, that covered the surface evenly after as little as 20 minutes exposure.

1.2. The hexavalent chromium coating lost adhesion, with parts of the coating 'spalling' off. The exposed areas were found to maintain a significant amount of chromium oxide in a relatively thin layer.

1.2.1. The onset of corrosion occurred eventually at these areas of exposure; however, they continued to protect the surface for a good period of time after this initial stage was observed.

1.3. Simple molybdate coatings showed initial signs of corrosion at the crack junctions in the coating, being areas of low Mo concentration, this, in all probability, lead to the rapid corrosion of these samples. Crack junctions expose much more of the substrate than cracks do, and furthermore, in the case of simple molybdate coatings, dimple like structures were apparent at the crack junctions.

1.4. Enhanced molybdate coatings corroded by blistering in areas of Mo depletion, eventually exposing the substrate and leading to corrosion after the 24 h.

1.5. Enhanced molybdate-silica coatings corroded by pitting, resulting in pits that were so large, they were apparent to the naked eye.

1.5.1. This weakness was due to a loss of adhesion at the coating-substrate interface, probably due to the inherent solubility of Mo oxides in chloride media.

1.5.2. Ingress at the crack junctions could weaken the structure, causing a blister to occur; pitting corrosion would then take place until adhesion of that part of the coating was lost. Little direct evidence was found regarding these pits at the substrate coating interface. But the lack of adhesion of the coating due to the lifting of platelets of the coating in chloride media is

likely because of this because of the inherent solubility of molybdenum compounds.

1.6. Viewing the weaknesses in the coatings was valuable because it furthers the knowledge into the way coatings physically behave when they are exposed to chloride media; research that was not readily available to the author when performing the literature survey.

1.7. Overall, the results correlated well with those found in the corrosion trials, with the highest performing coatings remaining the most intact, and the poorest performing coatings showing the weaknesses that the corrosion testing results suggested. See Table 7-1 for a summary of the failure mechanisms of the coatings tested. Furthermore, the results, in terms of ranking, agree with those found in other tests.

Table 7-1: Summary of the Key Differences of Failure Mechanisms of the Named Coatings.

Sample Name	Failure Mechanism	Uncorroded: Species Present (At. %)	Corroded: Species Present (At. %)	Surface Appearance After Corrosion	Time to Onset Of Corrosion
Zn	Gross oxide precipitation.	O (52 %), Zn (46 %), Cl (2 %)	O (45 %), Zn (46 %), Cl (11 %)	Voluminous crystalline corrosion product, 5 µm crystals.	20 min, voluminous after 2 h (visual).
Cr10	Spalling off of outer coating, under layer of Cr_2O_3 exposed.	Cr (8 %), O (82 %), Zn (7 %), Cl (3 %)	Cr (5 %), O (58 %), Zn (23 %), Cl (14 %)	Coating changed from iridescent to clear.	4 h (visible by SEM).
Simple Molybdate	Corrosion nucleated at crack junctions.	Mo (12 %), O (76 %), Zn (10 %)	Mo (1 %), O (65 %), Zn (23 %), Cl (11 %)	Barely visible white powder on surface.	4 h (visual).
MoP	Substrate exposure due	Mo (<2 %), O (57 %), Zn (27	O (45 %), Zn (35 %), P (4 %),	Infrequent, barely visible	4 h (visual).

	to blisters of around 70 µm in diameter.	%), P (6 %), Cl (8 %)	Cl (16 %)	white spots on surface.	
MoPSi	5-10 µm pores, leading to substrate exposure.	Si (32 %), O (68 %)	Porous/ Background: Si (15/ 26 %), O (34/ 53 %), Zn (19/ 8 %), Cl (32/ 13 %)	Surface darkening.	4 h (visual)

7.5 Further Investigations

1. In light of the work carried out in the present thesis the outlook for the use of molybdate as a potential replacement for chromate for the conversion coating of electrodeposited zinc surfaces is a positive one.
2. The author recommends that subsequent research should be focussed upon the further development of these coatings and that, in light of the progress made in the current study; research into top coats would be likely to produce a coating with superior corrosion resistance to chromate coatings, this would be in a similar way to sealants being used to enhance the corrosion resistance of early trivalent chromium coatings.
   2.1. The surface porosity of the enhanced 'MoP' type coatings appear to be an ideal candidate for the addition of a topcoat, allowing enhanced adhesion due to mechanical interlocking. Insoluble, nano-particle type coatings would be an ideal candidate, as the size of the particles would allow physical compatibility with the pores, possibly improving adhesion. Research would focus on producing a sealant that is sufficiently homogeneous to provide a continuous barrier to corrosion, in an immersion type process. This would allow the top coat process to be carried out on the same production line as the electroplating

and conversion coating steps, an important consideration for industrial viability. In the present study, success was not gained in this area, but with a more extensive investigation, and in light of the research carried out into topcoats for trivalent chromium systems in the mid to late 1980s.

3. The corrosion initiation studies provided little evidence of molybdate coatings being capable of the self-repair that chromate coatings are said to exhibit. Therefore a study of the enhanced molybdate coatings using the SVET technique, to monitor the changing electrochemical environment of a scratched surface (Lewis *et al.* 2006), would be useful to evaluate whether they exhibit any self-repair would serve as a conclusive argument.
4. Coating adhesion performance could be investigated with a simple adhesion test such as ASTM D3359, where a pressure sensitive tape is applied to the coating, cut into sections through the coating and substrate and removed. A qualitative assessment of substrate adhesion can then be made.
5. Another area of investigation that could potentially lead to coating improvement would be to gain further chemical data using XPS. This would allow a fuller understanding of the oxidation states of the molybdate species present on the surface.

8 References

Abd El Aal, E.E., Abd El Aal, A. and Abd El Haleem, S.M., *Initiation of Pitting Corrosion on Zinc in Neutral Inhibited Conditions*, Anti-Corrosion Methods and Materials, 1994, 41, 4-11.

Almeida, E., Diamantino, T.C., Figueiredo, M.O. and Sá, C., *Oxidising Alternative Species to Chromium VI in Zinc Galvanised Steel Surface Treatment. Part 1—A Morphological and Chemical Study*, Surface and Coatings Technology, 1998, 106 (1), 8-17.

American Society for Testing and Materials (ASTM), Standard B 117-07a, 2007.

American Society for Testing and Materials (ASTM), Standard B 368-09, 2009.

American Society for Testing and Materials (ASTM), Standard D3359 - 09e2, 2009.

Aramaki, K., *A Self-healing Protective Film Prepared on Zinc by Treatment in a $Ce(NO_3)_3$ Solution and Modification with $Ce(NO_3)_3$*, Corrosion Science,2005, 47, 1285-1298.

Barnes, C., Ward, J.J.B, Sembhi, T.S. and Carter V.E., *Non-Chromate Passivation Treatments for Zinc*, Transactions of the Institute of Metal Finishing, 1982, 60, 45-48.

Bibber, J. W., *Chromium-free Conversion Coatings for Zinc and its alloys,* Journal of Applied Surface Finishing, 2007, 2, 273-275.

Bibber, J. W., *Non-chrome-containing Conversion Coatings for Zinc and Zinc Alloys: Environmentally Friendly Alternatives Provide Equal or Better Adhesion and Corrosion Resistance as Conventional Methods*, Metal Finishing, 2008, 106 (4), 41-46.

Biestek, T. and Weber, J., *Electrolytic and Chemical Conversion Coatings a Concise Survey of their Production, Properties and Testing*, 1st English edition, 1976, Surrey, Portcullis Press.

Bi-lan Lin, B-L., Lu, J-T.and Kong, G., *Synergistic corrosion protection for galvanized steel by phosphating and sodium silicate post-sealing,* Surface and Coatings Technology 202 (2008) 1831–1838

Bishop, C.V., Foley, T.S. and Frank, J.M., 1979, US Patent 4171231.

Boose, C. A., and Stancu, R., *Chromate Free Passive Layers on Zinc and Zinc Alloy Coatings,* UPB Buletin Stiintific, Series B: Chemistry and Materials Science (Romania), 2001, vol. 63, no. 3, pp. 105-110.

Briggs, D., and Sheah, M.P., *Practical Surface Analysis: Volume 1: Auger and X-ray Photoelectron Spectroscopy*, 2nd Edition, 1990, Chichester, John Wiley & Sons.

Chapaneri, R., *'Investigation into Hexavalent and Trivalent Chromium Conversion Coatings on Zinc Electrodeposited Steel'*, 2010, PhD Thesis, Loughborough University, Leicestershire UK.

Chautauqua Metal Finishing Supply, Ashville, N.Y., *It Is Easier Being Greener,* Metal Finishing, 2008 106 (4), 62-65.

Cobalt poisoning. U.S. National Library of Medicine and U.S. National Institutes of Health. Available at:.http://www.nlnxnih.gov/medlineplus/ency/artide/002495.htnx, accessed July 2007.

Conde, A., Arenas, M. A., de Frutos, A. and de Damborenea, J. *Effective corrosion protection of 8090 alloy by cerium conversion coatings,* Electrochimica Acta, 2008, 53, 7760-7768.

Coslett, T. W., 1907, US Patent 870937.

Coslett, W.T., 1906, UK Patent 8663,

Cotton, F.A., Wilkinson, G., Murillo, C.A. and Bochmann, M.: in Advanced Inorganic Chemsistry, Sixth edn, '18. C. Molybdenum and Tungsten'; 1999, New York, John Wiley and Sons inc.

Crotty, D.E, 1981, US Patent 417123.

Da Silva, C.G., Correia, A.N., de Lima-Neto, P., Maragarit, I.C.P., and Mattos, O.R., *Study of Conversion Coatings Obtained from Tungste-Phosphoric Acid Solutions,* Corrosion Science, 2005, 47, 709-722.

Dalbin, S., Maurin, G., Noguiera, R. P., Persello, J. and Pommier, N., *Silica-based Coating for Corrosion Protection of Electrogalvanized Steel*, Surface and Coatings Technology, 2005, 194, 363-371.

Davó, B., and Damborenea, J.J. de., *Use of Rare Earth Salts as Electrochemical Corrosion Inhibitors for an Al–Li–Cu (8090) Alloy in 3.56% NaCl*, Electrochimica Acta, 2004, 48 (27), 4957-4965.

Dingwerth B. and Bishop C., *The black barrier: Characteristics of high-performance black passivates for zinc substrates*, Metal Finishing, 2008, 106 (10), 37-44.

Eichinger, E., Osborne, J. and Van Cleave, T., *Hexavalent Chromium Elimination: An Aerospace Industry Progress Report*, Metal Finishing, 1997, 95 (3), 36-41.

European Parliament and Council. Directive 2000/53/EC of the European Parliament and of the Council of 18th September 2000 on End-of Life Vehicles. Official Journal of the European Communities, 18/09/2000, 2000, vol. L269, no. 34.

European Parliament and Council. Directive 2002/96/EC of the European Parlaiment and of the Council of 27 January 2003 on Waste Electrical and Electronic Equipment (WEEE). Official Journal of the European Union, 13/02/2003, 2003, vol. L37, no. 24.

European Parliament and Council. Directive 67/548/EEC of 27 June 1967 on the Approximation of Laws, Regulations and Administrative Provisions Relating to the Classification, Packaging and Labelling of Dangerous Substances. Official Journal of the European Union, 1967, vol. 196.

European Parliament and Council: 'Directive 2008/35/EC of the European Parliament and Council of 11th March2008 on ‘the use of certain hazardous substances in electrical and electronic equipment (RoHS)’, 2008, L81/67.

Ferreira, M.G.S ., Duarte, R.G., Montemor, M.F. and Simões, A.M.P., *Silanes and Rare Earth Salts as Chromate Replacers for Pre-treatments on Galvanised Steel*, Electrochimica Acta, 49 (17-18), 2927-2935.

Gabe, D. R. and Gould S. E., *Black molybdate conversion coatings*, Surface and Coatings Technology, 1988, 35, 79-91.

Gabe, D.R., The Principles of Surface Treatment and Protection, 2nd edition, Pergamon Press Oxford, 1978.

Greenwood, N.N. and Earnshaw, A.: in Chemistry of the Elements, Second edn, 'Chromium, Molybdenum and Tungsten'; 1998, Oxford, Butterworth-Heinemann.

Han, K. and Fang, J., *Colour Conversion Coatings on Zinc*. Transactions of the Institute of Metal Finishing, 1996, 74 (1), 36-38.

Hara, M., Ichino, R., Okido, M. and Wada, N. *Corrosion Protection Property of Colloidal Silicate Film on Galvanized Steel,* Surface and Coatings Technology, 2003, 169-170, 679-681.

Heavens, O. S. Thin Film Physics. 1st ed. London: Methuen and Co ltd, 1970.

Hosseini, M., Ashassi-Sorkhabi, H., Allah Yaghobkhani Ghiasvand, H.A.Y., *Corrosion Protection of Electro-Galvanized Steel by Green Conversion Coatings*, Journal of Rare Earths, 2007, 25 (5), 537-543.

Http://www.Fisher.Co.Uk/ accessed 5/5/2009.

Hulser, P. *Manuscript of the presentation on the MKS-Meeting in Dortmund*

Manual DÖRKEN AG, 1999 from http://www.surtec.com/Publikationen/DeltacollE.pdf Accessed 20/7/2007.

Hughes, A.E., Gorman, J.D., Harvey, T.G., Galassi, A. and McAdam G., *Development of Permanganate-based Coatings on Aluminum Alloy 2024-T3,* Corrosion, 2006, 62, 773-780.

Jahan, F. and Smith, B. E., *Characterization of Molybdenum Black Coatings on Zinc Substrates*, Journal of Materials Science, 1997, 32, 3869-3874

Jesionowski, T., *Preparation of Colloidal Silica from Sodium Metalsilicate Solution and Sulphuric Acid in Emulsion Medium*, Colloids and Surfaces A: Physicochemical and Engineering Aspects, 2001, 190, 153-165.

Keeler, L.J., 1926, US Patent 1574289.

Kobe Steel Ltd. UK Patent 2,070,073.

Konno, H., Narumi, K. and Habazaki, H., *Molybdate/Al(III) Composite Films on Steel and Zinc-Plated Steel by Chemical Conversion,* Corrosion Science, 2002, 44, 1889-1900.

Kulinich, S. A., Farzaneh, M. and Du, X. W., *Growth of Corrosion-resistant Manganese Oxide Coatings on an Aluminum Alloy,* Inorganic Materials, 2007, 43, 956–963.

Kurosawa, K., and Fukusima, *Effects of pH of an Na2MoO4-H3PO4 Type Aqueous Solution on the Formation of Chemical Conversion Coatings on Steels,* Corrosion Science, 29 (9), 1989, 1103-1114

Lee, D-J., Kang, T., Sohn, H-J. and Kim, H-J., *Structural and Electrochmical Properties of Al Added Molybdate Conversion Coatings on Zinc*, Corrosion Science and Technology, 2002, 31 (2), 185-188

Lewis, O. D.; Greenfield, D.; Akid, R.; Dahm, R. H. and Wilcox, G. D., *SVET Investigation into use of Simple Molybdate Passivation Treatments on Electrodeposited Zinc Coatings,* Transactions of the Institute of Metal Finishing, 2006, 86 (4), 188-195.

Liu, L., Hu, J-M., Zhang, J-Q. and Cao, C-N., *Improving the Formation and Protective Properties of Silane Films by the Combined Use of Electrodeposition and Nanoparticles Incorporation*, Electrochimca Acta, 52 (2), 538-545.

Loar, G. W. and Page, B.J. Chromium Compounds : Kirk Othmer Encyclopedia of Chemical Technology : Wiley InterScience. , Available from: <http://www.mrw.interscience.wiley.com/emrw/9780471238966/kirk/article/chropage.a01/current/html?hd=All,chromium>.

Lu, J. T, Kong, G., Chen, J.H., Xu, Q. Y. and Sui , R. Z., *Growth and Corrosion Behaviour of Molybdate Passivation Film on Hot Dip Galvanized Steel.* Transactions of the Nonferrous Metals Society of China, 2003, 13(1), 145-148.

Lu, J., Kong, G., Chen, J., Xu, Q. and Song, J., *Passivation of Galvanized Steel by Molybdate.* Corrosion Science and Protection Technology, 2001, 13(1), 1, 46-48.

Magalhaes, A.A.O., Margarit, I.C.P. and Mattos, O.R., *Molybdate Conversion Coatings on Zinc Surfaces*, Journal of Electroanalytical Chemistry., 2003 572, 443-440.

Mansfeld F., Wang, Y. and Shih, H., *The Ce・Mo Process for the Development of a Stainless Aluminum*, Electrochima Acta, 1992, 37, 2277-2282.

Martyak, N.M., *Internal Stresses in Zinc-Chromate Coatings*, Surface and Coatings Technology, 1996, 88, 139-146.

Material Safety Data Sheet., Available from: <http://66.102.9.104/search?q=cache:x3vAvTua6tQJ:www.aerospace.henkel.com/Images/Datasheet_PDF/msds_alodine1600.pdf+sodium+dichromate+acute+toxicity+LD50+ratandhl=enandct=clnkandcd=2andgl=uk>. Accessed 21 June 2009.

Matsushima, Y., 1972, US Patent 3632452.

Meyers, B.R., Lynn, S.C. and Lang, E., *Case Study – Alternatives to the Use of Chromium in Plating and Conversion Coating at the McClellan Air Force Base, California*, 1994, 9th Annual Aerospace Hazardous Materials Management Conference.

Montagu, H. and Nicholson, A., 1953, US Patent 2657156.

Page, B. J. and Loar, G. W., in Kirk-Othmer Encyclopaedia of Chemical Technology (Electronic), Vol. 6, 'Chromium Compounds'; 2004, John Wiley and Sons Inc. Available at: http://mrw.interscience.wiley.com/emrw/9780471238966/kirk/article/chropage.a01/current/pdf, Accessed 16th June 2009.

Palanivel, V., Zhu, D. and Van Ooij, W. J., *Nanoparticle-filled Silane Films as Chromate Replacements for Aluminum Alloys*, Progress in Organic Coatings, 2003, 47, 384-392.

Pourbaix, M. Atlas of Electrochemical Equilibria in Aqueous Solution. Oxford: Pergamon Press, 1966.

Robertson, W.D., *Molybdate and Tungstate as Corrosion Inhibitors and the Mechanism of Inhibition,* Journal of the Electrochemical Society, 1951, 98, 94-100.

Ross, W.A., 1869, UK Patent 3119.

Rout, T. K. and Bandyopadhyay, N., *Effect of Molybdate Coating for White Rusting Resistance on Galvanized Steel*, Anti-Corrosion Methods and Materials, 2007, 54, 16-20.

Rudd, A. L., Breslin, C. B. and Mansfeld, F., *The Corrosion Protection Afforded by Rare Earth Conversion Coatings Applied to Magnesium*, Corrosion Science, 2000, 42, 275-288.

Schrott, A. G., Frankel, G.S, Davenport, A.J., Isaacs, H.S., Jahnes, C.V. and Russak, M.A., *CrLVV Auger Emission and Photoreduction of Hexavalent Cr Oxides*, Surface Science, 1991, 250 (1-3), 139-146.

Schweikher, E. W., 1944, UK Patent 2351639.

Sienkowski, M. L., 1999, US Patent 5885373.

Slunder, C. J.; and Boyd, W. K. Zinc: Its Corrosion Resistance. 1st Edition London: Zinc Development Association, 1971.

Song, Y. K., and Mansfeld, F., *Development of a Molybdate-Phosphate-Silane-Silicate (MPSS) Coating Process for Electrogalvanized Steel*, Corrosion Science, 2006, 48 (1), 154-164.

Stauffer, R. E., *Determination of Arsenic and Phosphous Compounds in Groundwater with Reduced Molybdenum Blue*, Analytical Chemistry, 1983, 55, 1205-1210

Stern, M., and Geary, A.L, *Electrochemical Polarization I . A Theoretical Analysis of the Shape of Polarization Curves*, Journal of the Electrochemical Society, 1957, 104 (4), 56-63.

Stiefel, E. I., in Kirk-Othmer Encyclopaedia of Chemical Technology (Electronic), Vol. 16, 'Molybdenum Compounds'; 2001, John Wiley and Sons Inc. Available at: http://mrw.interscience.wiley.com/emrw/9780471238966/kirk/article/molystie.a01/current/pdf Accessed 16th June 2009.

Takenaka, T., Ono, T., Narazaki, Y., Naka, Y and Kawakami, M., *Improvement of Corrosion Resistance of Magnesium Metal by Rare Earth Elements*, Electrochimica Acta, 2007, 53 (1), 117-121.

Tang, P. T., Bech-Nielsen, G. and Moller, P., *Molybdate-based Alternatives to Chromating as a Passivation Treatment for Zinc*, Plating and Surface Finishing, 1994, 81 (11), 20-23.

Thiery, L., and Pommier, N., Hexavalent Chromium-free Passivation Treatments in the Automotive Industry, 2004, Coventya SAS, available at:

http://www.sintef.no/static/mt/norlight/ICEPAM/P10-Pommier_Coventya.pdf

Accessed 05/02/2009.

Trabelsi, W., Cecilio, P., Ferreira, M.G.S and Montemor M.F., *Electrochemical Assessment of the Self-healing Properties of Ce-doped Silane Solutions for the Pre-treatment of Galvanised Steel Substrates*, Progress in Organic Coatings, 2005, 54, 276-284.

Treacy, G. M., Wilcox, G. D. and Richardson, M. O. W., *Behaviour of Molybdate-Passivated Zinc Coated Steel Exposed to Corrosive Chloride Environments*, Journal of Applied Electrochemistry, 1999, 29 (5), 647-654.

Wharton, J. A., Ross, D. H., Treacy, G. M., Wilcox, G. D. and Baldwin, K. R., *An EXAFS Investigation of Molybdate-based Conversion Coatings*, Journal of Applied Electrochemistry, 2003, 33, 553-561.

Wharton, J. A., Wilcox, G. D., and Baldwin, K. R., *An Electrochemical Evaluation of Possible Non-chromate Conversion Coating Treatments for Electrodeposited Zinc-nickel Alloys*, Transactions of the Institute of Metal Finishing, 1999, 77 (4), 152-158.

Wiederholt, W., The Chemical Surface Treatment of Metals, Translated by W. E. Cattley, 1965, R. Draper (Translated).

Wilcox, G. D. and Gabe, D. R., *Chemical Molybdate Conversion Treatments for Zinc*, Metal Finishing, 1988, 86, 71-74.

Wilcox, G. D., *Replacing Chromates for the Passivation of Zinc Surfaces*, Transactions of the Institute of Metal Finishing, 2003, 81, B13-B15.

Wilcox, G. D., *The Development of Passivation Coatings by Cathodic Reduction in Sodium Molybdate Solutions,* Corrosion Science, 1989, 28 (6), 577-587.

Wilcox, G. D.; and Gabe, D. R., *Passivation Studies Using Group VIA Anions – Part IV: Cathodic Redox Reactions and Film Formation*, British Corrosion Journal, 1984, 19 (4), 196-200.

Winn, D. and Dalton, W., *Chromium-Free Corrosion Solutions*, Metal Finishing, 2008, 106 (6), 70-74.

Wynn, P.C. and Bishop, C.V., *Replacing Hexavalent Chromium*, Transactions of the Institute of Metal Finishing, 2001, 79, B27-B29.

Yu, X., Yan, C and Cao, C., *Study on the rare earth sealing procedure of the porous film of anodized Al6061/SiCp*, Materials Chemistry and Physics, 2002, 76 (3), 228-235.

Zaki, N., Met. Fin., *Trivalent Chrome Conversion Coating for Zinc and Zinc Alloys*, 2007, 105, 425-435.